海洋観測船・中性子回折・放射光科学・・・

名古屋大学工学研究科マテリアル理工学専攻応用物理分野
構造物性物理学講座構造物性工学研究グループ　教授　　坂田　誠

海洋観測船　　溶存酸素の鉛直分布

中性子回折　　非調和熱振動・リートヴェルト解析の検証・非晶質合金

放射光科学　　3元系合金散漫散乱・MEM

MEM（Si, フラーレン化合物、軌道整列、PbTiO3、---

最近の研究（GA. 蛋白質結晶、---

・・・

三宅研究室関連

1968 B4 ～ 1970 D1

教授　　三宅泰男

奥様　すず（画家）　長女　榛名（ピアニスト）----柴田翔（作家）

弟（東大物性研教授　三宅静雄）

気象庁気象研究所　猿橋勝子

助教授　松尾貞士

中性子回折

1970 D1 ～ 1974 学位取得

1975 助手 ～ 1976 助手

1976 AERE Harwell ～ 1980 帰国------1983 PF共同利用実験開始

物性研中性子部門

所員	教授 平川金四郎	助手	池田宏信（元KEK・KENS施設長）
	教授 星埜貞男	助手	藤井保彦（JAEA量子ビーム応用研究部門長）
		院生	新村信雄（茨城大学教授） 私
	助教授 伊藤雄而	助手	秋光純 （青山学院大学教授）
	・・・		
		助手	下村 理（KEK・物質構造科学研究所長）

KEK：高エネルギー加速器研究機構

JAEA：日本原子力研究機構

ダイレクトビームの観察

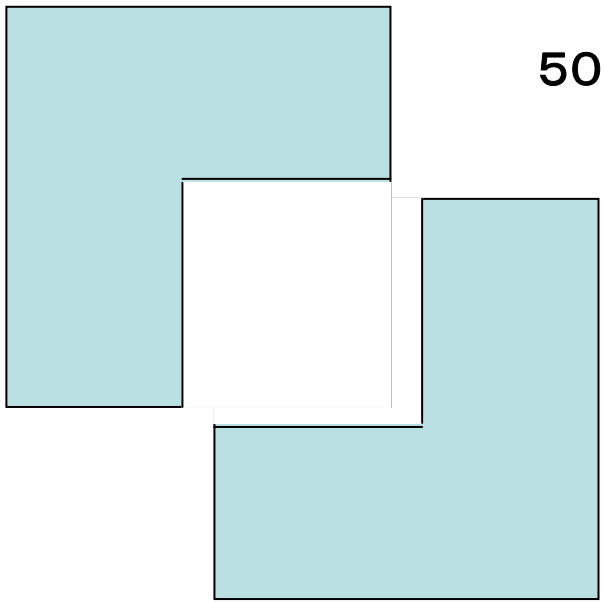

Cdの板

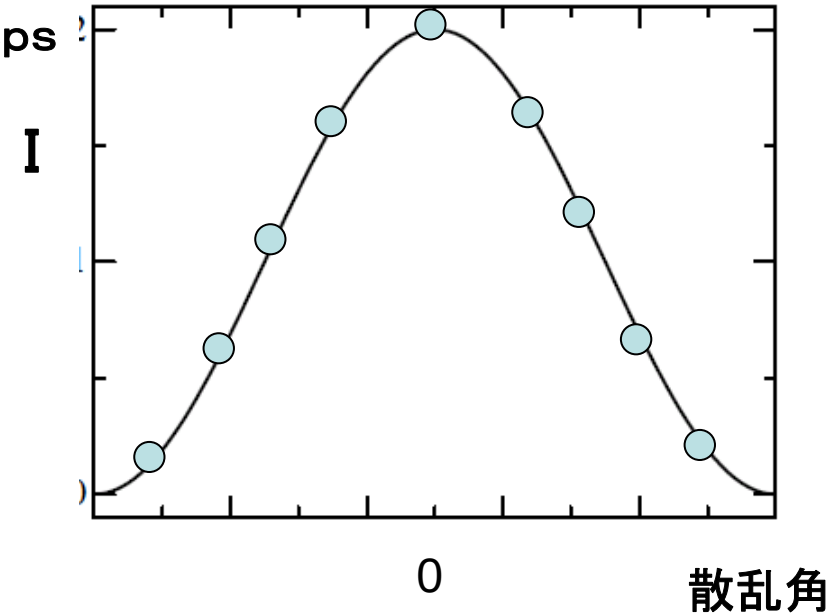

最初の実験の論文

Acta Cryst. (1974). A**30**, 655

Neutron Diffraction Study of Asymmetric Anharmonic Vibration of the Copper Atom in Cuprous Chloride

BY MAKOTO SAKATA* AND SADAO HOSHINO

Institute for Solid State Physics, The University of Tokyo, Minatoku, Tokyo, Japan

AND JIMPEI HARADA

Department of Applied Physics, Nagoya University, Chikusa-ku, Nagoya, Japan

(*Received* 6 *April* 1974; *accepted* 2 *May* 1974)

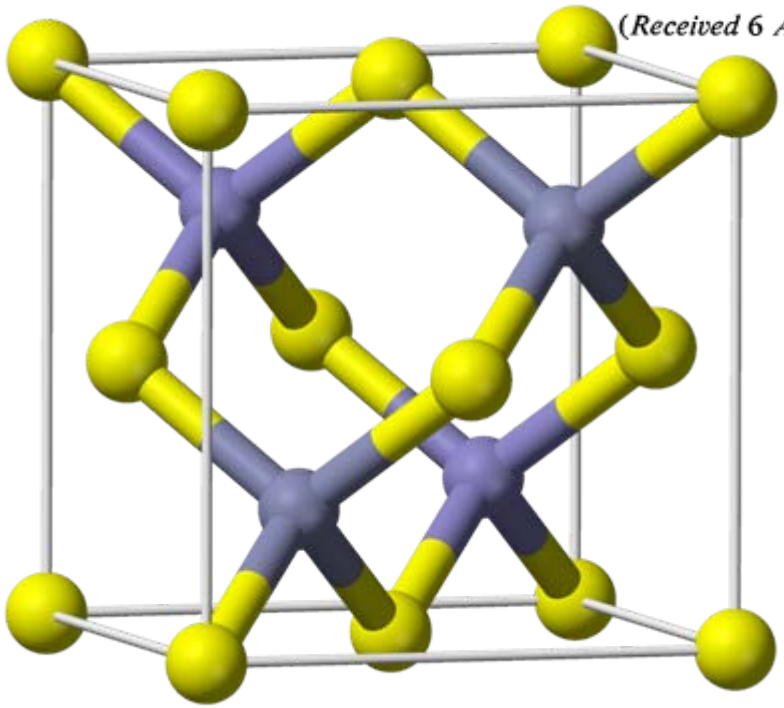

CuClの構造

CuClの非調和熱振動

atomic-potential fields for the zincblende structure

$$V_j(\mathbf{r}) = V_{0j} + \tfrac{1}{2}\alpha_j(u_1^2 + u_2^2 + u_3^2) + \beta_j u_1 u_2 u_3 + \cdots$$

were obtained as $\alpha_{Cu} = 0{\cdot}74 \pm 0{\cdot}01$, $\alpha_{Cl} = 1{\cdot}35 \pm 0{\cdot}02 \times 10^{-12}$erg Å^{-2}, and $\beta_{Cu} = 1{\cdot}15 \pm 0{\cdot}66$, $\beta_{Cl} = 0{\cdot}0 \pm 1{\cdot}6 \times 10^{-12}$erg Å^{-3}. It is also shown that the temperature dependence of the Bragg reflexion observed from room temperature to 523 °K can be explained very well with the use of the above parameters.

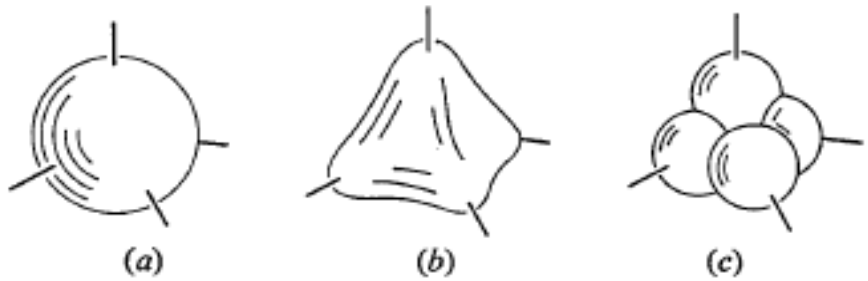

Fig. 1. The schematic models for thermal vibrations of copper atoms in cuprous halides, (*a*) harmonic thermal vibration, (*b*) asymmetric anharmonic vibration and (*c*) atoms located statistically at four displaced positions with moderate thermal vibration.

Fourier Transform of crystal

$$I \propto |F|^2$$

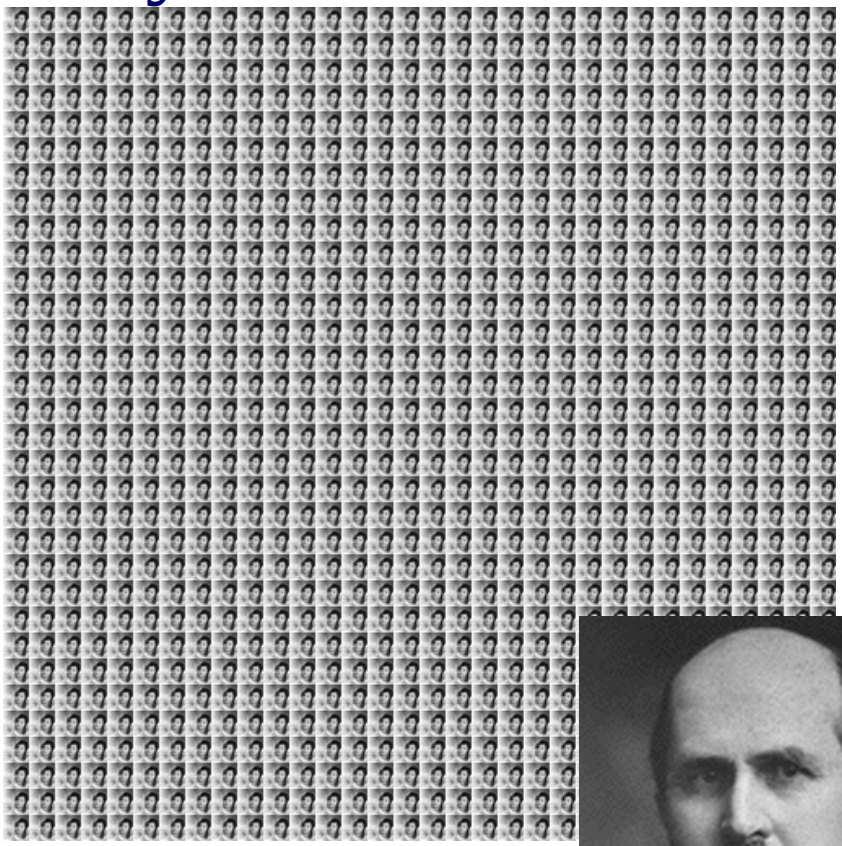

$\mathcal{F}$

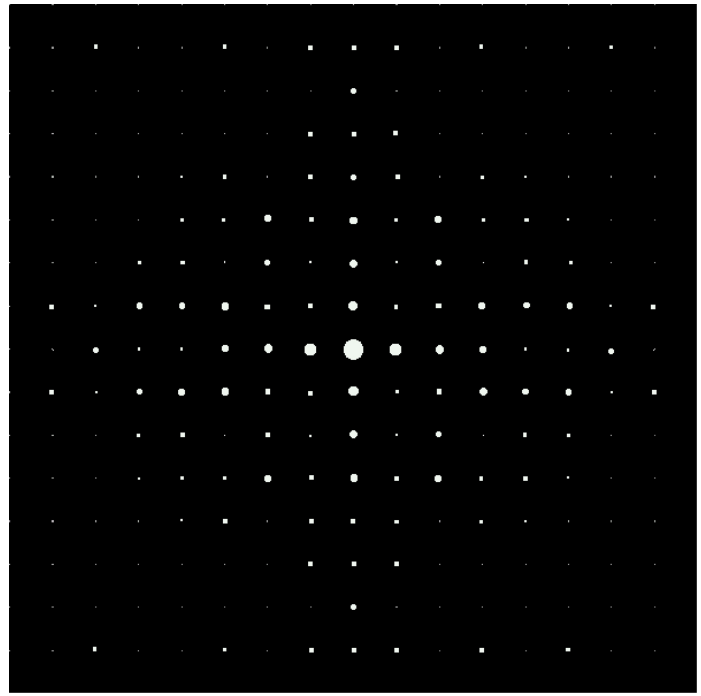

Real Space

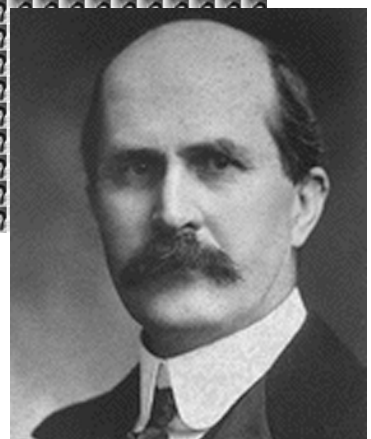

Reciprocal Space

X-ray diffraction experiment

$$F(k)=\int \rho(r)\exp(-2\pi i r\cdot k)dr$$

$$=\sum_j f_j(\boldsymbol{K})\exp(-i\boldsymbol{K}\cdot\boldsymbol{r}_j)$$

r_j ; *単位胞の原点から原子* j *までの距離*

$\mathcal{F}$

$\rho(r)$ ⇒ $F(k)$

Fourier Transform

Real Space **Reciprocal Space**

Crystal Structure Determination

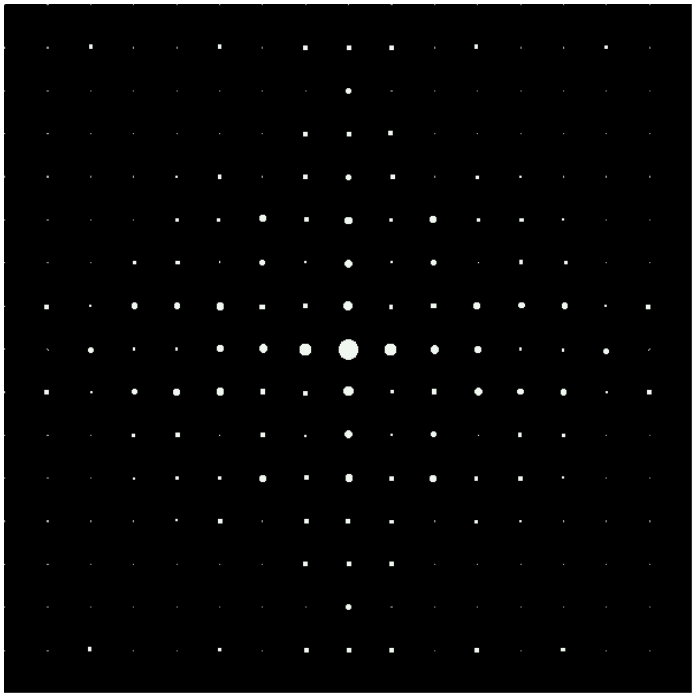

$\mathcal{F}^{-1}$

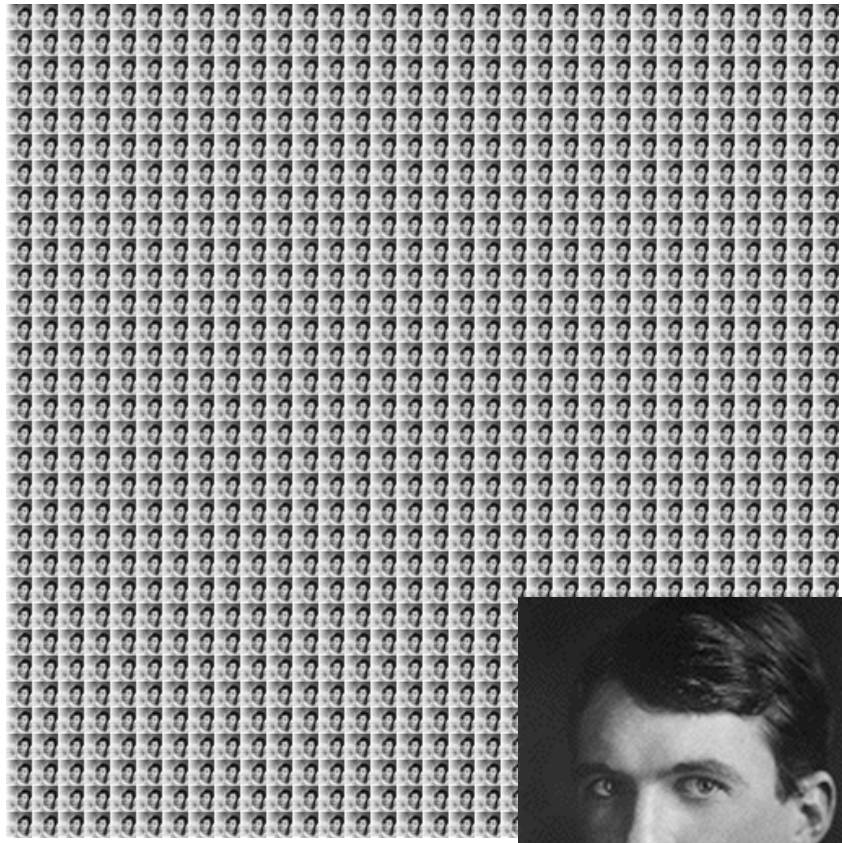

Reciprocal Space

Real Space

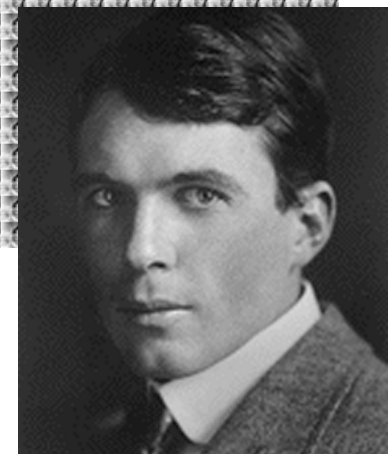

Structure Determination

$$\rho(\mathbf{r}) = \sum_{\mathbf{k}} F(\mathbf{k}) \exp(2\pi i \mathbf{k} \bullet \mathbf{r})$$

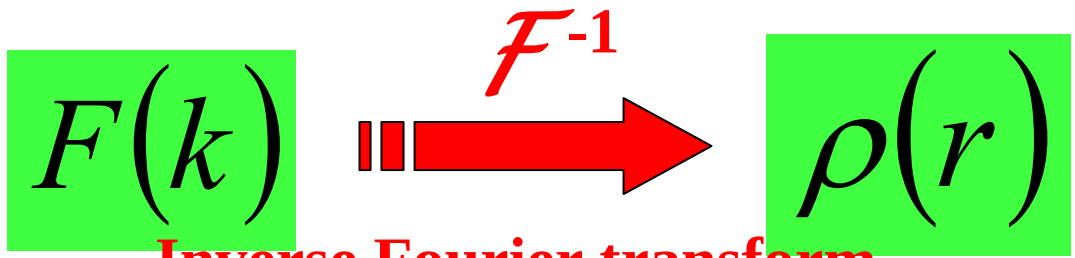

Reciprocal Space **Real Space**

調和近似の式

$$F(\mathbf{Q}) = \sum_j b_j T_j(\mathbf{Q}) \exp(i\mathbf{Q}\mathbf{r}_j) , \qquad (1)$$

$$T_j(\mathbf{Q}) = \exp\{-B_j(\sin\theta/\lambda)^2\} , \qquad (9)$$

$$B_j = 8\pi^2 \langle \mathbf{u}_j^2 \rangle \qquad (10)$$

$$B_j = 8\pi^2 k_B T/\alpha_j . \qquad (11)$$

(i) $h+k+l=4n$

$$F(\mathbf{Q})F^*(\mathbf{Q}) = [b_{Cu}T_{Cu}(\mathbf{Q}) + b_{Cl}T_{Cl}(\mathbf{Q})]^2 \qquad (6)$$

(ii) $h+k+l=4n+2$

$$F(\mathbf{Q})F^*(\mathbf{Q}) = [b_{Cu}T_{Cu}(\mathbf{Q}) - b_{Cl}T_{Cl}(\mathbf{Q})]^2 \qquad (7)$$

(iii) $h+k+l=4n\pm 1$

$$F(\mathbf{Q})F^*(\mathbf{Q}) = [b_{Cu}T_{Cu}(\mathbf{Q})]^2 + [b_{Cl}T_{Cl}(\mathbf{Q})]^2 . \qquad (8)$$

非調和の式

$$V_j = V_{0j} + \tfrac{1}{2}\alpha_j(u_1^2 + u_2^2 + u_3^2) + \beta_j u_1 u_2 u_3 + (\text{higher-order terms}) , \quad (5)$$

$$T_j(\mathbf{Q}) = T_{cj}(\mathbf{Q}) + iT_{aj}(\mathbf{Q}) . \quad (12)$$

(i) $h+k+l=4n$

$$F(\mathbf{Q})F^*(\mathbf{Q}) = [b_{\mathrm{Cu}} T_{c\mathrm{Cu}}(\mathbf{Q}) + b_{\mathrm{Cl}} T_{c\mathrm{Cl}}(\mathbf{Q})]^2 + [b_{\mathrm{Cu}} T_{a\mathrm{Cu}}(\mathbf{Q}) + b_{\mathrm{Cl}} T_{a\mathrm{Cl}}(\mathbf{Q})]^2 \quad (15)$$

(ii) $h+k+l=4n+2$

$$F(\mathbf{Q})F^*(\mathbf{Q}) = [b_{\mathrm{Cu}} T_{c\mathrm{Cu}}(\mathbf{Q}) - b_{\mathrm{Cl}} T_{c\mathrm{Cl}}(\mathbf{Q})]^2 + [b_{\mathrm{Cu}} T_{a\mathrm{Cu}}(\mathbf{Q}) - b_{\mathrm{Cl}} T_{a\mathrm{Cl}}(\mathbf{Q})]^2 \quad (16)$$

(iii) $h+k+l=4n\pm 1$

$$\begin{aligned} F(\mathbf{Q})F^*(\mathbf{Q}) = {} & [b_{\mathrm{Cu}} T_{c\mathrm{Cu}}(\mathbf{Q})]^2 + [b_{\mathrm{Cl}} T_{c\mathrm{Cl}}(\mathbf{Q})]^2 \\ & \pm 2 b_{\mathrm{Cu}} b_{\mathrm{Cl}} [T_{a\mathrm{Cu}}(\mathbf{Q}) T_{c\mathrm{Cl}}(\mathbf{Q}) \\ & - T_{c\mathrm{Cu}}(\mathbf{Q}) T_{a\mathrm{Cl}}(\mathbf{Q})] \\ & + [b_{\mathrm{Cu}} T_{a\mathrm{Cu}}(\mathbf{Q})]^2 + [b_{\mathrm{Cl}} T_{a\mathrm{Cl}}(\mathbf{Q})]^2 . \end{aligned} \quad (17)$$

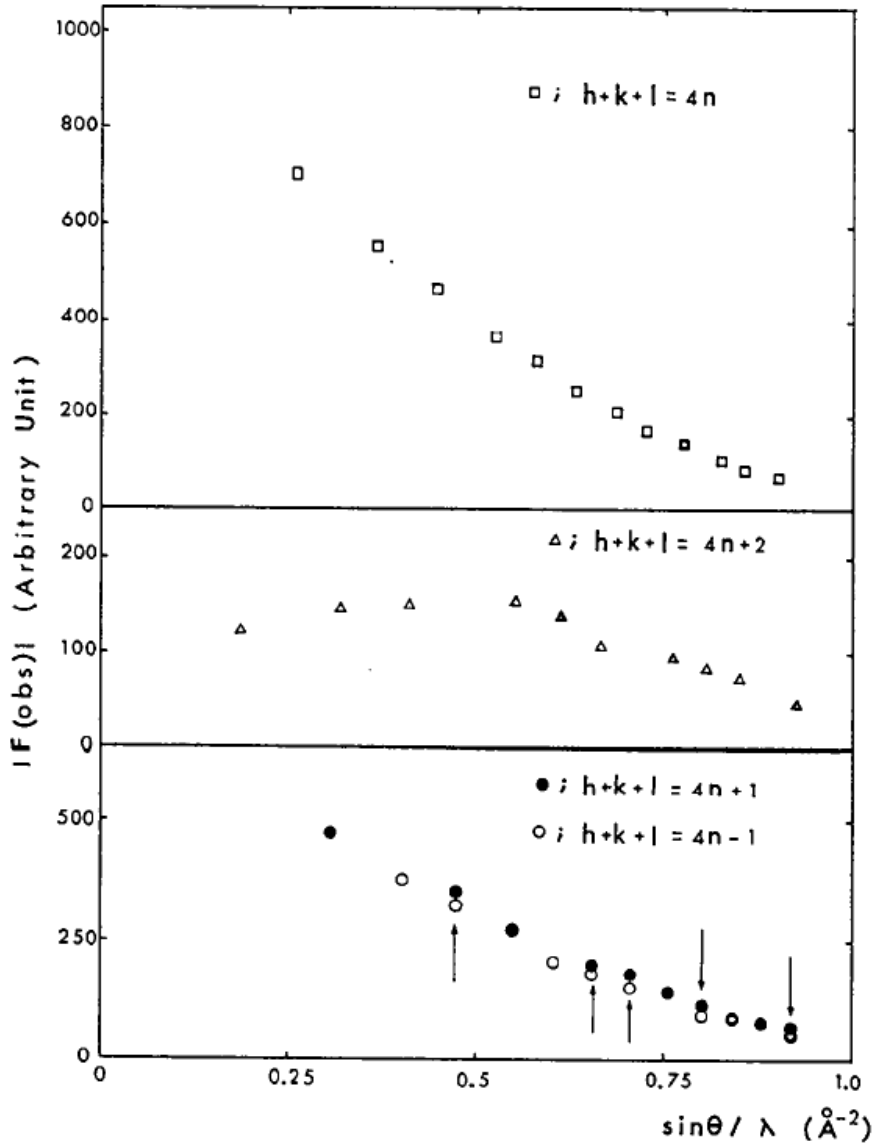

Fig. 2. Observed structure factors for the three types of reflexions as a function of sin θ/λ. □, △, ○ represent two reflexions with different indices.

最初の日本語の論文

日本結晶学会誌 22, 387 (1980)

〔総合報告〕

温度因子と非調和熱振動

シェフィールド大(英)・物理　坂　田　　誠*
名大工・応用物理　原　田　仁　平

Makoto SAKATA and Jimpei HARADA : Temperature Factor and Anharmonic Thermal Vibrations.

$$P(u)=\frac{\exp\left\{-\frac{V(u)}{k_BT}\right\}}{\int\exp\left\{-\frac{V(u)}{k_BT}\right\}du} \qquad (5)$$

$$V=V_0+\frac{1}{2}\alpha u^2+\beta u_1u_2u_3+\gamma u^4+\delta\left(u_1^4+u_2^4+u_3^4-\frac{3}{5}u^4\right) \qquad (6)$$

$$\exp(-V/k_BT)=\exp(-V_0/k_BT)\exp\left(-\frac{\alpha}{2}u^2/k_BT\right)$$
$$\times\left\{1-\frac{\beta}{k_BT}u_1u_2u_3+\frac{1}{2}\left(\frac{\beta}{k_BT}\right)^2u_1^2u_2^2u_3^2-\frac{\gamma}{k_BT}u^4\right.$$
$$\left.-\frac{\delta}{k_BT}\left(u_1^4+u_2^4+u_3^4-\frac{3}{5}u^4\right)\right\} \qquad (7)$$

$$T(Q)=T_c(Q)+iT_a(Q)$$

ただし

$$T_c(Q)=N\exp\left(-\frac{k_BT}{2\alpha}Q^2\right)\left[1\right.$$
$$-k_BT\left(\frac{15\gamma}{\alpha^2}-\frac{\beta^2}{2\alpha^3}\right)$$
$$+(k_BT)^2\left(\frac{10\gamma}{\alpha^3}-\frac{\beta^2}{2\alpha^4}\right)Q^2$$
$$-(k_BT)^3\left[\frac{\gamma}{\alpha^4}Q^4+\frac{2}{5}\frac{\delta}{\alpha^4}\{(Q_1^4+Q_2^4+Q_3^4)\right.$$
$$-3(Q_1^2Q_2^2+Q_2^2Q_3^2+Q_3^2Q_1^2)\}$$
$$\left.\left.-\frac{\beta^2}{\alpha^5}(Q_1^2Q_2^2+Q_2^2Q_3^2+Q_3^2Q_1^2)\right]\right],$$
$$T_a=N\exp\left(-\frac{k_BT}{2\alpha}Q^2\right)\cdot\frac{\beta}{\alpha^3}(k_BT)^2Q_1Q_2Q_3,$$
$$N=\left[1-k_BT\left(\frac{15\gamma}{\alpha^2}-\frac{\beta^2}{2\alpha^3}\right)\right]^{-1} \qquad (8)$$

第2表　種々の物質中にある $\bar{4}3m$ 原子位置のポテンシャル係数の比較

構造	物質	非調和原子	実験法	B値(A^{-2})	α (10^{-12}ergA^{-2})	β (10^{-12}ergA^{-3})	β^2/α^3	*Ref.*
F	UO_2	O	N	0.426	7.49	9.0	0.19	34)
F	CaF_2	F	N	0.697	4.58	5.66	0.28	35)
F	BaF_2	F	N	1.048	3.04	3.06	0.33	51)
F	SrF_2	F	N	0.846	3.77	3.95	0.29	8, 34)
F	Mg_2Si	Mg	X	0.767	4.18	2.39	0.08	36)
Z	CuCl	Cu	N	4.4	0.74	1.15	3.26	31)
Z	CuBr	Cu	N	3.67	0.937	1.0	1.21	14)
Z	ZnS	Zn	N	0.879	3.633	4.2	0.36	30)
		S		0.724	4.408		0.21	
Z	ZnTe	Zn	N	1.296	2.463	3.8	0.97	30)
		Te		0.758	4.213		0.19	

F：ほたる石構造，Z：閃亜鉛鉱構造，N：中性子回折，X：X線回折

CaF_2・CuClの非調和ポテンシャル

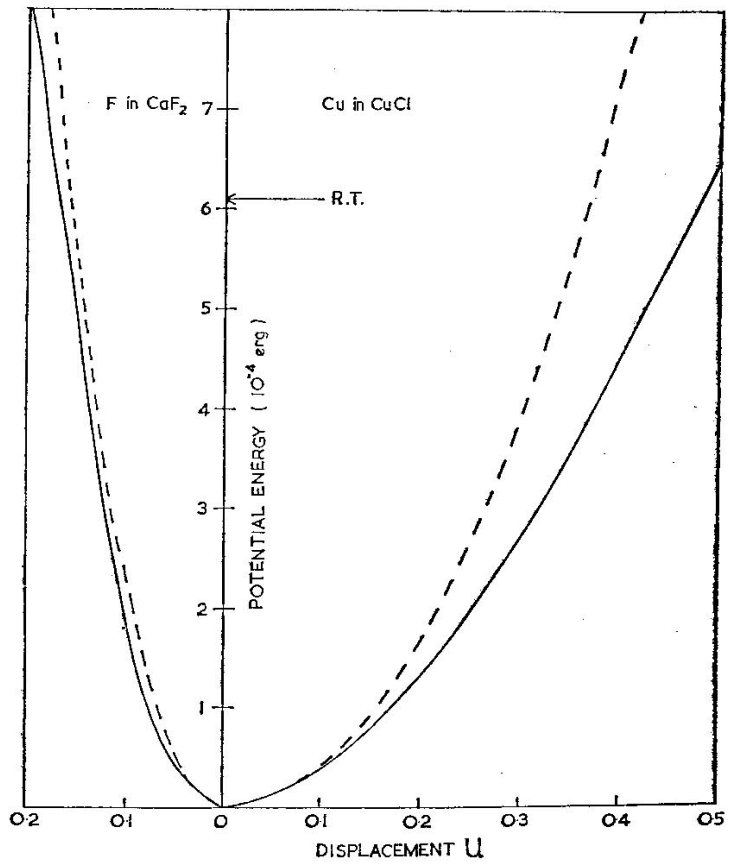

第8図 CaF_2 の F および CuCl 中の Cu の非調和ポテンシャル．点線は〔111〕方向，実線が〔$\bar{1}\bar{1}\bar{1}$〕方向

から β^2/α^3 をとることも出来る．第2表にこの値ていかに非調和効果が大きいかがこれでわかる．

リートヴェルト解析の検討

J. Appl. Cryst. (1979). **12**, 554–563

An Analysis of the Rietveld Profile Refinement Method

BY M. SAKATA* AND M. J. COOPER

*Materials Physics Division, AERE, Harwell, Oxfordshire, OX*11 0*RA, England*

(*Received* 24 *August* 1978; *accepted* 25 *June* 1979)

Abstract

An analysis of the Rietveld profile refinement method used in the interpretation of neutron or X-ray powder diffraction patterns has been carried out. It is shown that the values obtained for the structural parameters are not exactly the same as those obtained from an integrated intensity refinement of the same data and that the standard deviations of the parameters are determined incorrectly. Whilst the differences in the values of the parameters may not be statistically significant, the fact that their standard deviations are estimated incorrectly severely limits their usefulness. These conclusions are confirmed by refinement of a number of data sets using both methods and in most of these cases the standard deviations are found to be underestimated by the profile refinement method by a factor of at least two. Discussions based on the results of profile refinement must therefore be reconsidered and the relative value of powder diffraction techniques must be reviewed.

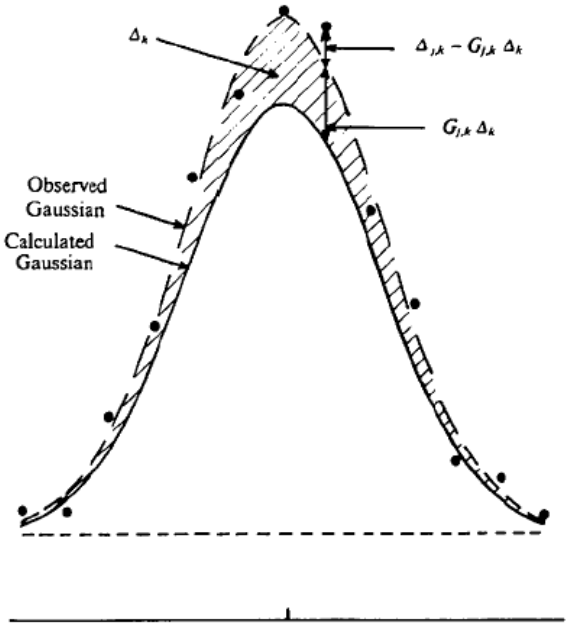

Fig. 1. Illustration of the correlation between $\Delta_{j,k}$ values for the same Bragg peak. The observed points are distributed randomly about the observed peak rather than the calculated peak, so that the differences which must be considered statistically are Δ_k and $\Delta_{j,k} - G_{j,k}\Delta_k$ rather than $\Delta_{j,k}$.

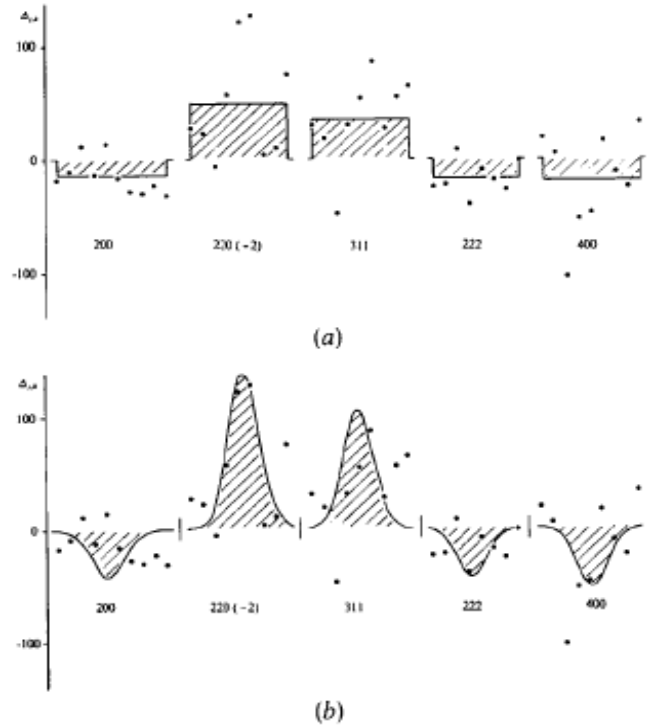

Fig. 2. Values of $\Delta_{j,k}$ for five peaks in the profile for UO_2, showing their correlation for the same Bragg peak. The shaded areas correspond to the values of Δ_k. (*a*) The solid lines give the average values of $\Delta_{j,k}$ for each peak. (*b*) The solid lines correspond to the values of $G_{j,k}\Delta_k$.

$(x+y+z+\cdots)^2 - x^2+y^2+z^2+\cdots = 2xy+2xz+\cdots\cdots$

単結晶　　リートヴェルト解析

Zeitschrift für Kristallographie 149, 337–338 (1979)
© by Akademische Verlagsgesellschaft 1979

Short Communication

The Neutron scattering amplitude of Uranium

M. J. Cooper and M. Sakata*

Materials Physics Division, AERE Harwell, Oxon., OX11 0RA, England

Received: November 28, 1978

Abstract. Reanalysis of six different sets of neutron diffraction data for UO_2 leads to a value of the neutron scattering amplitude ratio of $b_u/b_0 = 1.451(2)$ and hence a value for the neutron scattering amplitude of uranium of b_u between 0.842(2) and $0.846(2) \times 10^{-12}$ cm.

J. Phys. F: Metal Phys., 11(1981)L157–62. Printed in Great Britain

LETTER TO THE EDITOR

Chemical short-range order in liquid and amorphous $Cu_{66}Ti_{34}$ alloys

M Sakata†§, N Cowlam† and H A Davies‡

† Department of Physics, University of Sheffield, Sheffield, S3 7RH, England, UK

‡ Department of Metallurgy, University of Sheffield, Sheffield, S1 3JD, England, UK

Received 6 March 1981, in final form 26 March 1981

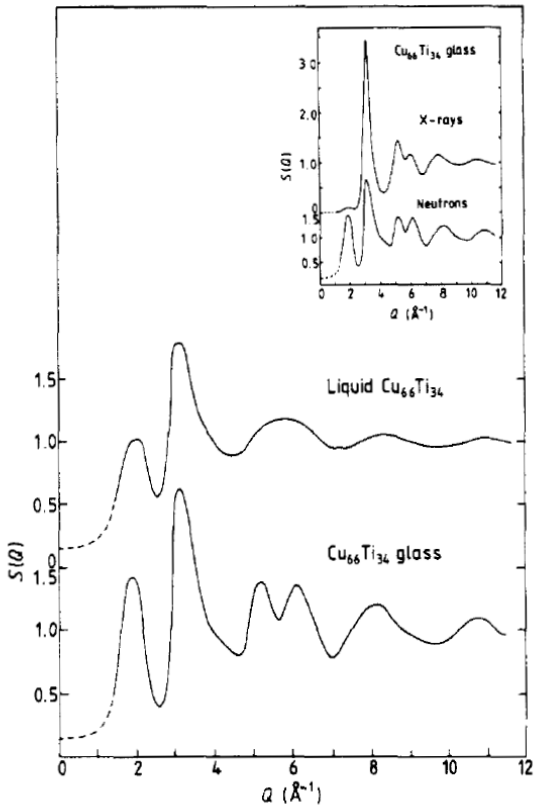

Figure 1. The structure factor $S(Q)$ for liquid $Cu_{66}Ti_{34}$ is shown together with $S(Q)$ for $Cu_{66}Ti_{34}$ glass, both curves being obtained from neutron diffraction. The inset shows a comparison of the structure factors of $Cu_{66}Ti_{34}$ glass obtained by neutron and x-ray diffraction.

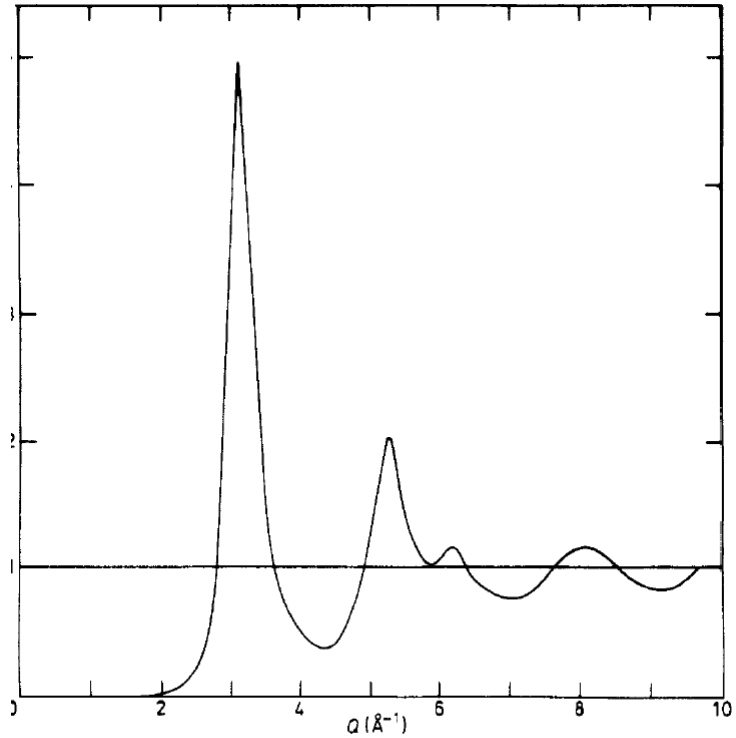

ure 1. The structure factor $S(Q)$ for $Fe_{83}B_{17}$ metallic glass with $Q_{max} = 9{\cdot}78$ Å^{-1}, ived from a neutron diffraction measurement.

$$\langle f^2\rangle S(Q) = \langle f^2\rangle S_{NN}(Q) + 2\,\Delta f\langle f\rangle S_{NC}(Q) + \Delta f^2 S_{CC}(Q). \qquad (2)$$

For a binary alloy $A_{C_A}B_{C_B}$, the atomic scattering factors have the following values

$$\langle f\rangle = C_A f_A + C_B f_B,$$
$$\langle f^2\rangle = C_A f_A^2 + C_B f_B^2,$$
$$\Delta f = f_A - f_B.$$

Journal of Non-Crystalline Solids 46 (1981) 329–341
North-Holland Publishing Company

DIFFUSE SCATTERING AND CHEMICAL SHORT RANGE ORDER IN BINARY METALLIC GLASSES

M. SAKATA *, N. COWLAM and H.A. DAVIES **

Department of Physics, University of Sheffield, Sheffield, S3 7RH, UK

Received 12 June 1981
Revised manuscript received 24 September 1981

NiNbのChemical Short Range Order

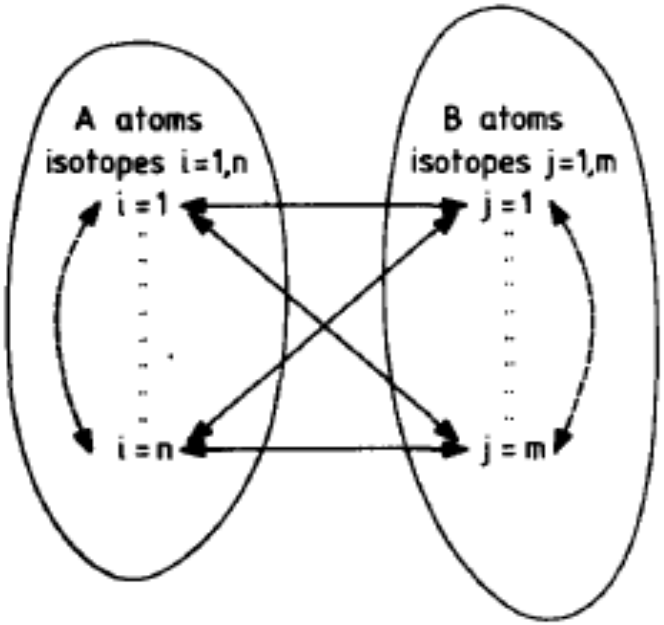

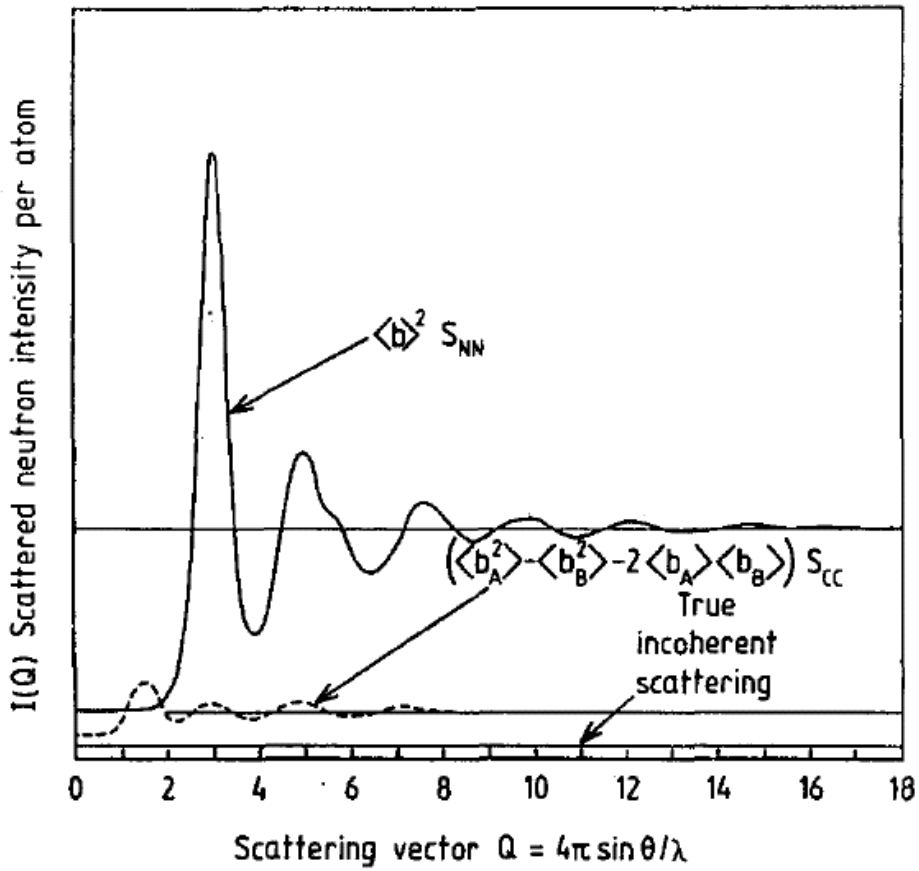

	今までの式	新しい式
$Ni_{60}Nb_{40}$	0. 029	0. 113

応用物理学科

第1講座　志水教授	羽賀助教授	井上研
第2講座　吉原教授	近助教授	中村研
第3講座　原田教授	坂田助教授	坂田研
第4講座　美浜教授	一宮助教授	齋藤研
第5講座　岩間教授	野口助教授	生田研
第6講座　阿部教授	八田助教授	美宅研
工業数学　桑原教授	田村講師	金田研
工業数学　加藤（義）教授	吉原助教授	張研
工業力学　中野教授	木村助教授	笹井研
人口結晶　石橋教授	沢田助教授	田中研
結晶材料　加藤（範）教授	内川助教授	財満研
		黒田研

放射光科学

1980　帰国------1983　PF共同利用実験開始　～1997　SPring -8の供用開始

～1998　BL02B2立ち上げ～現在

Journal of the Physical Society of Japan
Vol. 54, No. 10, October, 1985, pp. 3796–3807

Study of Local Atomic Order in a Ternary $Cu_{0.47}Ni_{0.29}Zn_{0.24}$ Alloy Using Anomalous Scattering of Synchrotron Radiation

Shinya HASHIMOTO, Hiroshi IWASAKI,* Ken-ichi OHSHIMA,†
Jimpei HARADA,† Makoto SAKATA† and Hikaru TERAUCHI††

The Research Institute for Iron, Steel and Other Metals,
Tohoku University, Sendai 980
†*Department of Applied Physics, Nagoya University, Nagoya 464*
††*Faculty of Science, Kwansei Gakuin University, Nishinomiya 662*

(Received May 7, 1985)

$$I_{\mathrm{SRO}}(\boldsymbol{q})=x_A x_B|f_A-f_B|^2\alpha^{AB}(\boldsymbol{q})+x_B x_C|f_B-f_C|^2\alpha^{BC}(\boldsymbol{q})+x_C x_A|f_C-f_A|^2\alpha^{CA}(\boldsymbol{q}), \qquad (1)$$

Table II. Warren-Cowley SRO parameters α_{lmn}^{ij} determined for the three pairs of atoms in $Cu_{0.47}Ni_{0.29}Zn_{0.24}$ alloy.

l m n	Ni–Zn	Zn–Cu	Cu–Ni
0 0 0	0.8	0.6	0.3
1 1 0	-0.042 ± 0.005	-0.019 ± 0.004	0.015 ± 0.006
2 0 0	0.130 ± 0.005	0.058 ± 0.004	-0.046 ± 0.006
2 1 1	-0.036 ± 0.005	-0.017 ± 0.004	0.013 ± 0.006
2 2 0	0.110 ± 0.005	0.049 ± 0.004	-0.038 ± 0.006

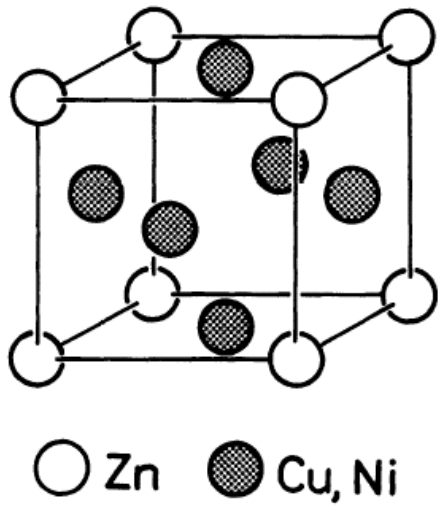

Fig. 7. A model for the local atomic arrangements in the quenched $Cu_{0.47}Ni_{0.29}Zn_{0.24}$ alloy.

MEMの最初の論文

精密結晶構造解析に対する一考察

－ Maximum Entropy による結晶構造解析 －

日本結晶学会誌 30、135－143 （1988）

シリコンの1次元電子密度を求めた。

Acta Cryst. (1990). A46, 263-270

Accurate Structure Analysis by the Maximum-Entropy Method

BY MAKOTO SAKATA AND MASUMI SATO

Department of Applied Physics, Nagoya University, Furo-cho, Chikusa-ku, Nagoya, Japan 464-01

(*Received* 4 *August* 1989; *accepted* 3 *November* 1989)

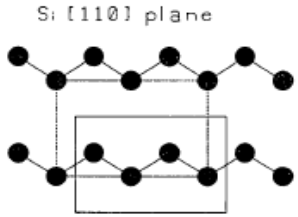

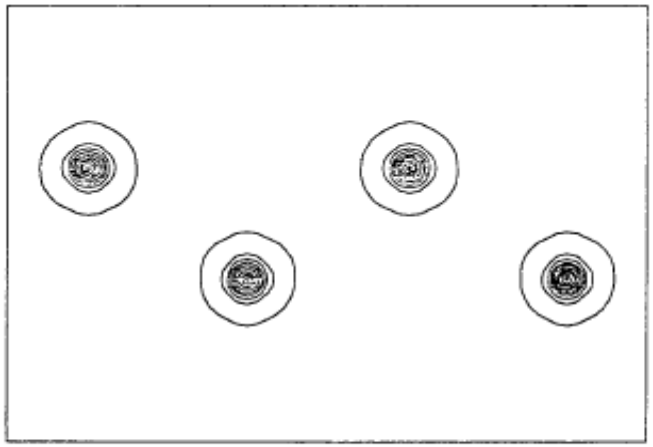

(*a*)

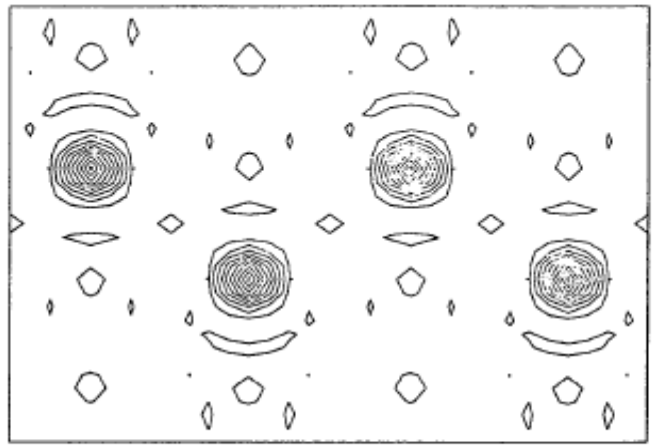

(*a*)

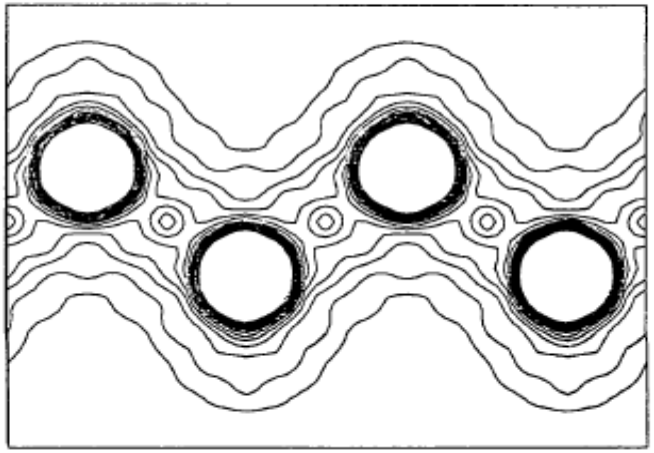

(*b*)

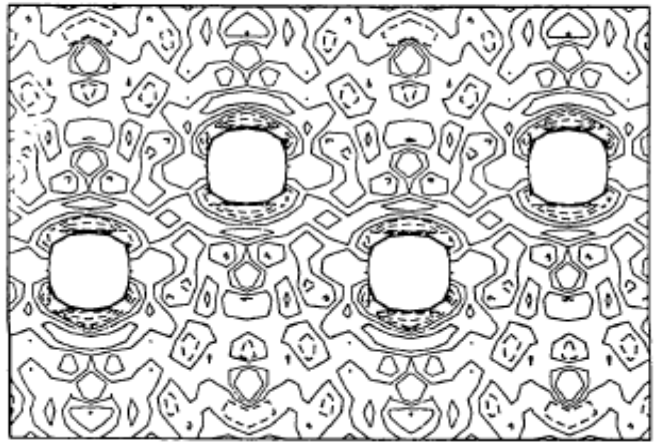

(*b*)

電子密度分布のピーク値

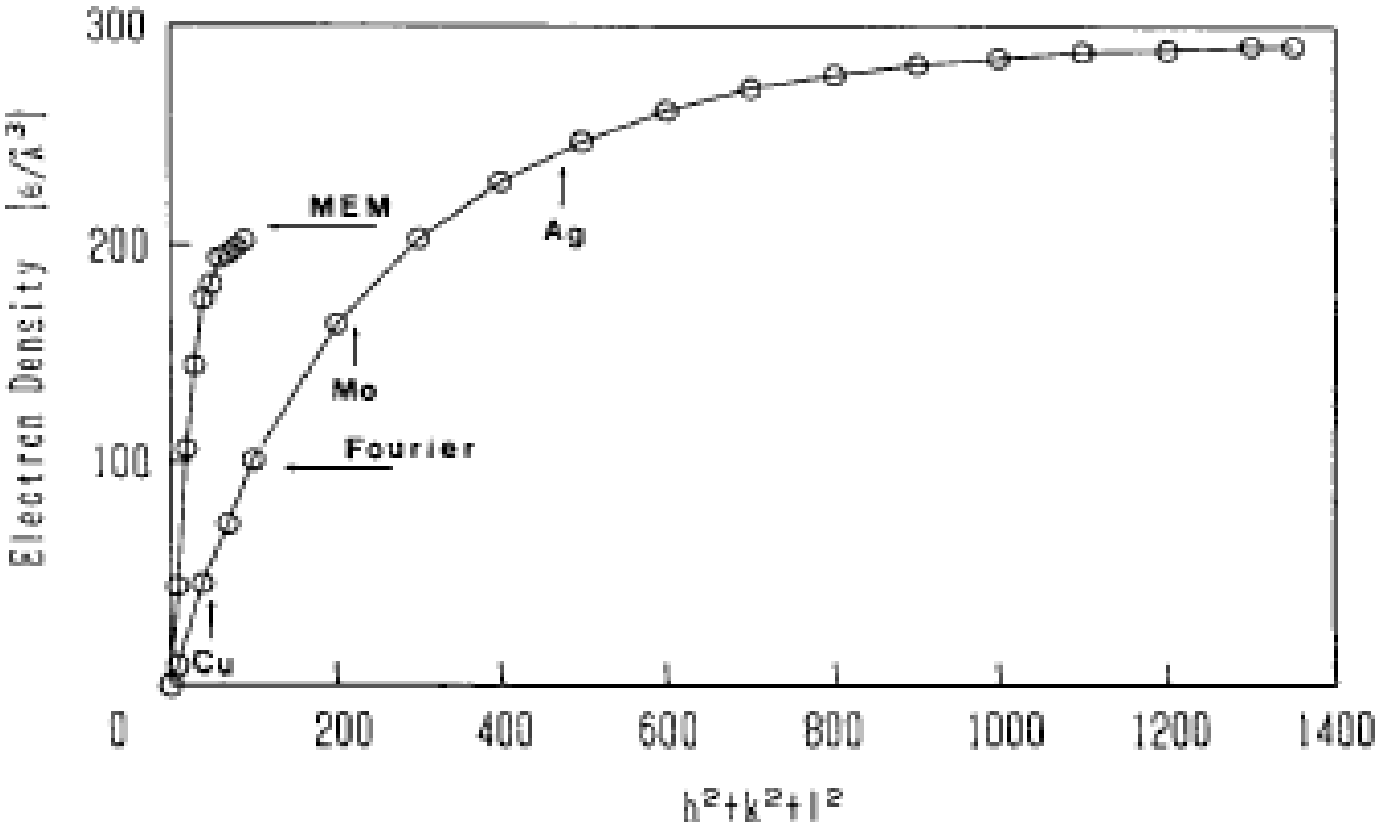

禁制反射

Table 3. *Values of the structure factor F(222) for silicon at room temperature*

Reference	*F*(222)
Hewat, Prager, Stephenson & Wagenfeld (1969)	0·88
Aldred & Hart (1973)	1·35 ± 0·04
DeMarco & Weiss (1965)	1·44 ± 0·08
Alkire, Yelon & Schneider (1982)	1·456 ± 0·008
Roberto & Batterman (1970)	1·46 ± 0·04
Jennings (1969)	1·48 ± 0·03
Fujimoto (1974)	1·50 ± 0·015
Present work (calculated value)	1·527
Colella & Merlini (1966)	1·54
Renninger (1960)	1·55
Fehlman & Fujimoto (1975)	1·65 ± 0·03
Göttlicher, Kuphal, Nagorsen & Wölfel (1959)	1·78

MEM for Charge density study.

Collins's formalism is based on the entropy expression, *S,* obtained by Jaynes(1968):

Information Entropy $$S = -\sum_{\mathbf{r}} \rho'(\mathbf{r}) \ell n \frac{\rho'(\mathbf{r})}{\tau'(\mathbf{r})}$$

The probability of $\rho'(\mathbf{r})$ and prior probability $\tau'(\mathbf{r})$ are connected with the actual density by

$$\rho'(\mathbf{r}) = \rho(\mathbf{r}) \Big/ \sum_{\mathbf{r}} \rho(\mathbf{r}), \quad \tau'(\mathbf{r}) = \tau(\mathbf{r}) \Big/ \sum_{\mathbf{r}} \tau(\mathbf{r})$$

We introduce a constrain as given information. $$C = \frac{1}{N} \sum_{\mathbf{k}} \frac{\left| F_{cal}(\mathbf{k}) - F_{obs}(\mathbf{k}) \right|^2}{\sigma^2(\mathbf{k})}$$

Where, $$F_{cal}(\mathbf{k}) = V \sum_{\mathbf{r}} \rho(\mathbf{r}) \exp\left[-2\pi i \mathbf{k} \cdot \mathbf{r}\right]$$

We use Lagrange's method of undetermined multipliers to constrain *C* to be unity while we maximize the entropy.

$$Q(\lambda) = -\sum_{\mathbf{r}} \rho'(\mathbf{r}) \ell n \frac{\rho'(\mathbf{r})}{\tau'(\mathbf{r})} - \frac{\lambda}{2}(C-1)$$

By setting $\frac{\partial Q(\lambda)}{\partial \rho'(\mathbf{r})} = 0$, we have $$\rho(\mathbf{r}) = \tau(\mathbf{r}) \cdot \exp\left[\frac{\lambda F_0}{N} \sum_{\mathbf{k}} \frac{\{F_{obs}(\mathbf{k}) - F_{cal}(\mathbf{k})\}}{\sigma^2(\mathbf{k})} \exp(-2\pi i \cdot \mathbf{k} \cdot \mathbf{r}) \right]$$

$$F_{cal}(\mathbf{k}) = V \sum_{\mathbf{r}} \tau(\mathbf{r}) \exp\left[-2\pi i \mathbf{k} \cdot \mathbf{r}\right]$$

The Flow Chart of MEM Analysis

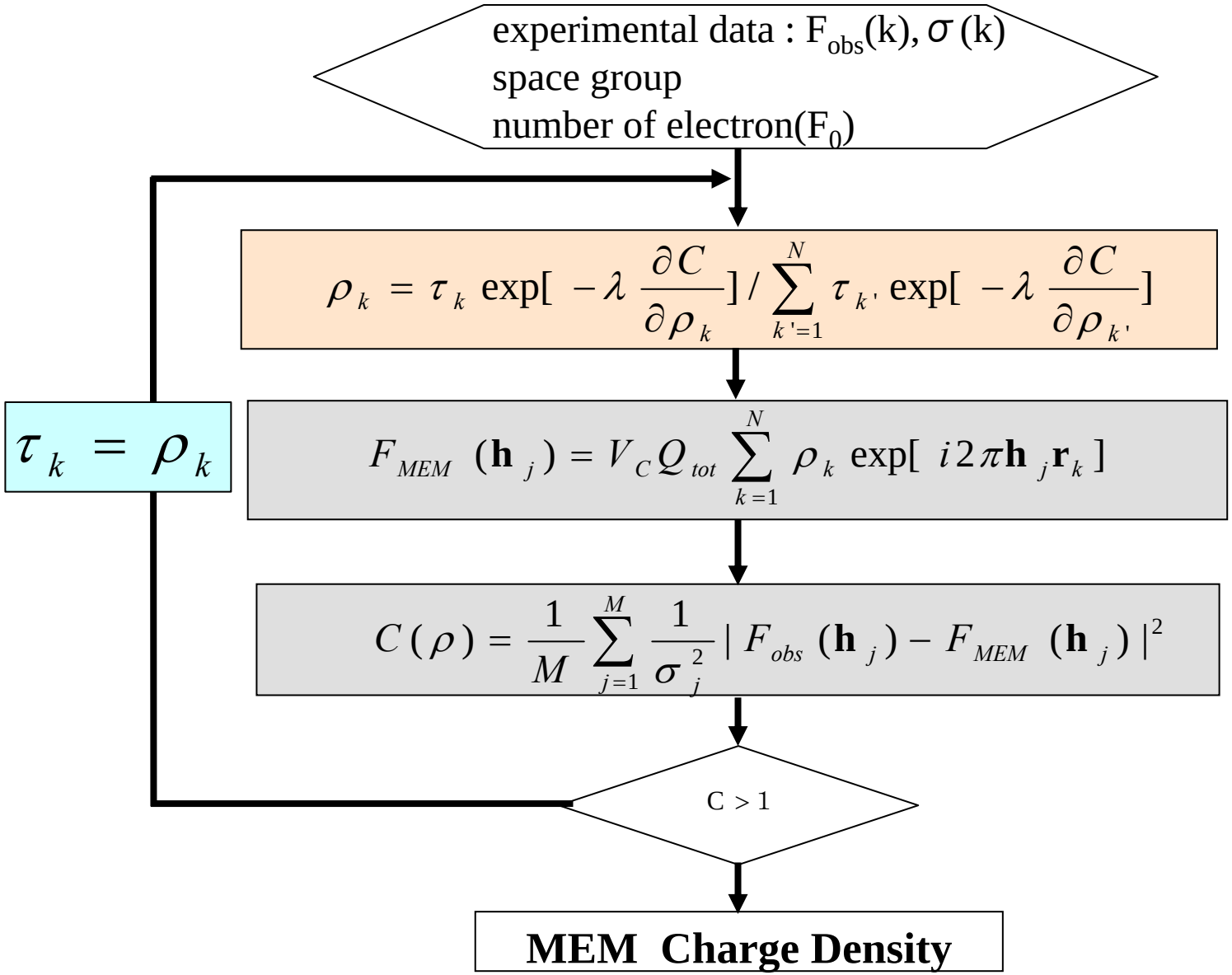

The process of obtaining the MEM solution

Initial solution

After 2nd iteration

Charge density of Silicon for (110) plane

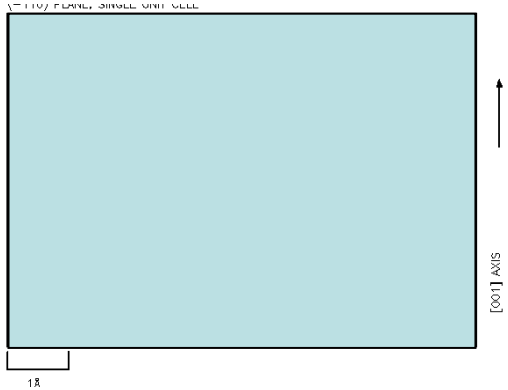

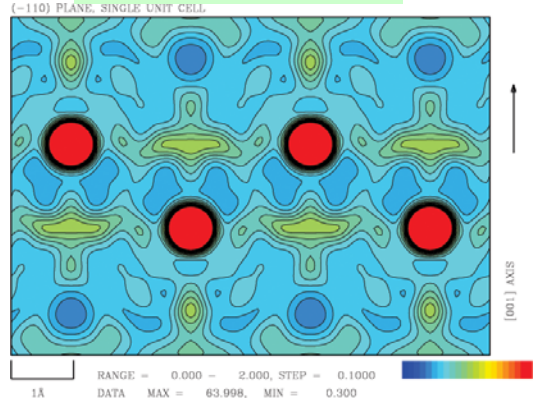

1D Charge densites of (111) direction

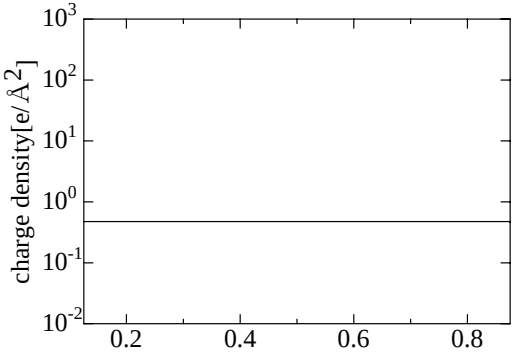

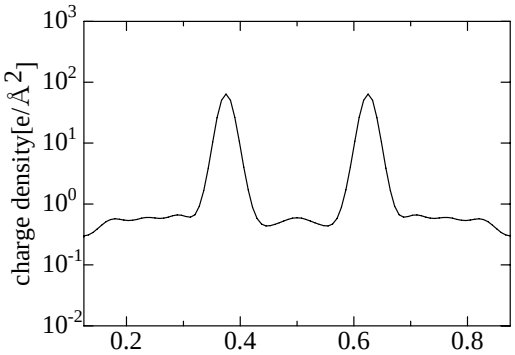

Amplitude of atomic scattering factor

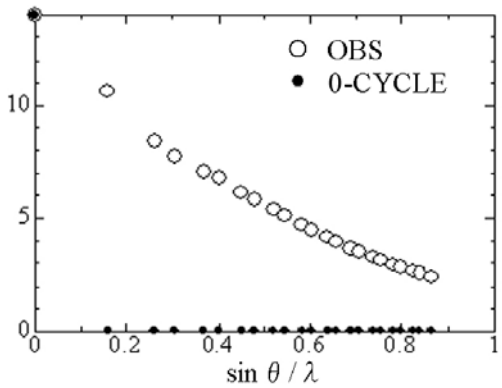

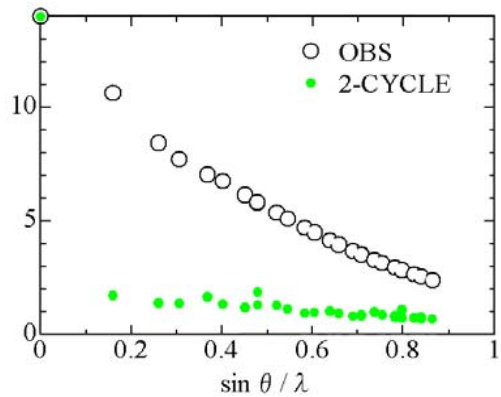

The process of obtaining the MEM solution

After 10th iteration

Final results (775 iterations)

Charge density of Silicon for (110) plane

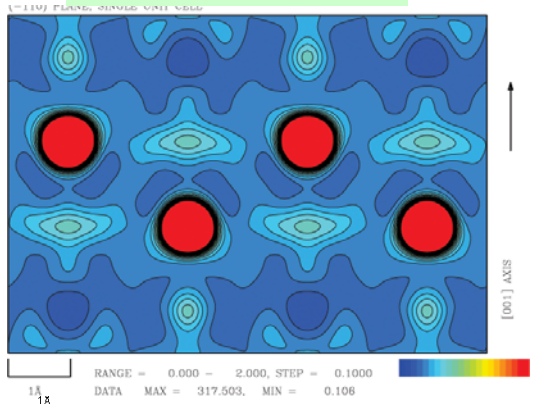

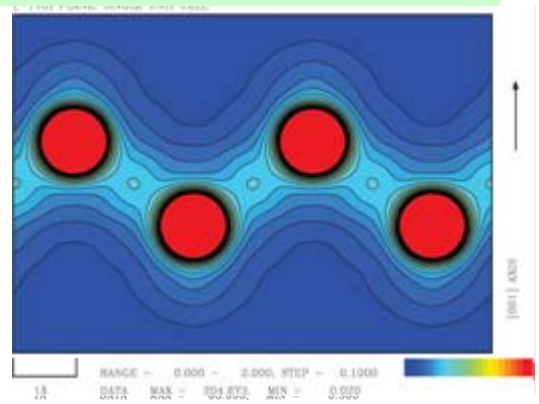

1D Charge densites of (111) direction

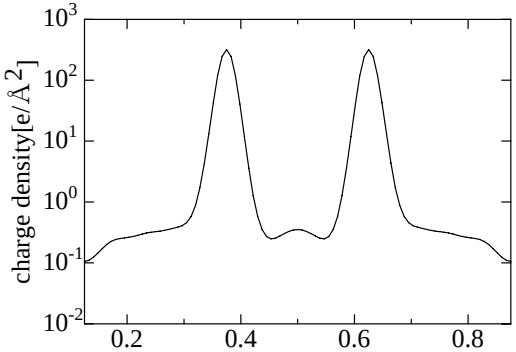

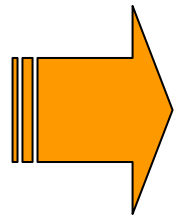

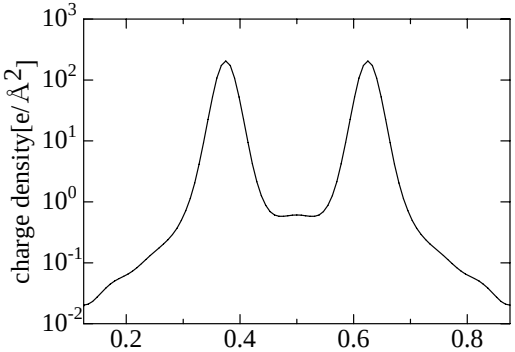

Amplitude of atomic scattering factor

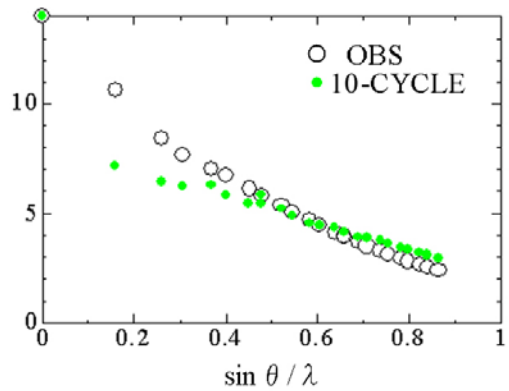

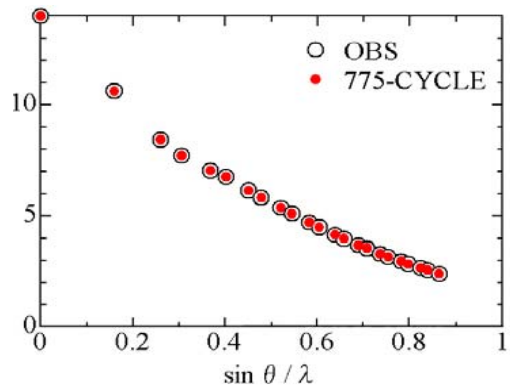

Estimated structure factors by MEM

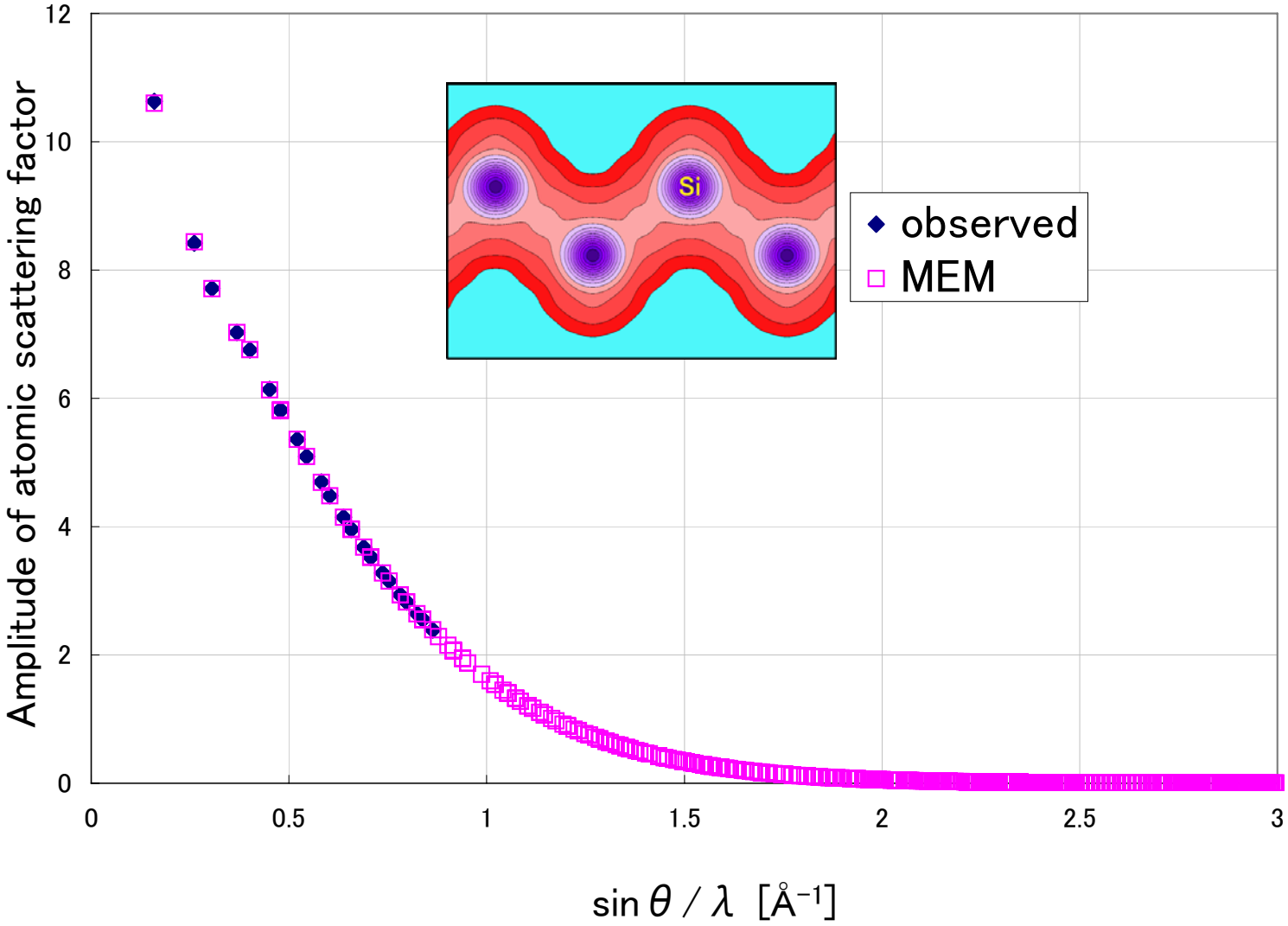

Charge densities of Silicon (110) plane

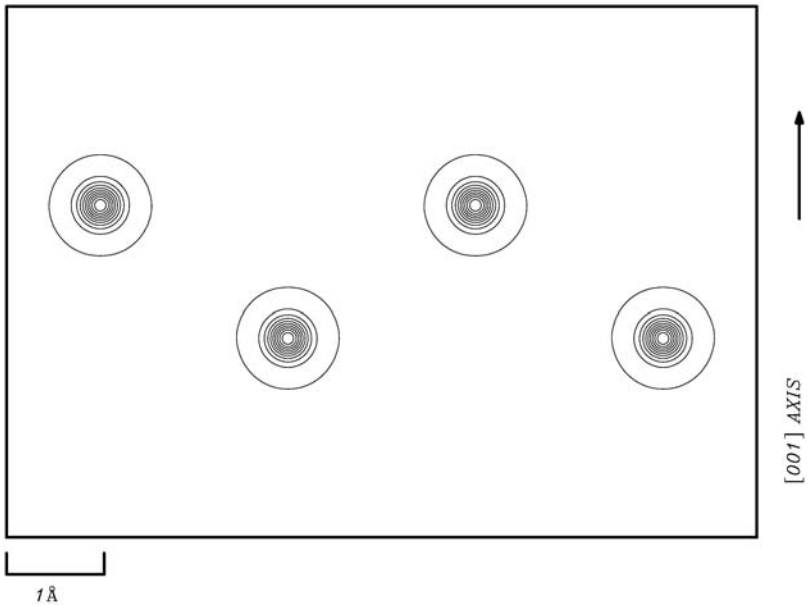

MEM

2 ～200, 20[e/Å^3] step

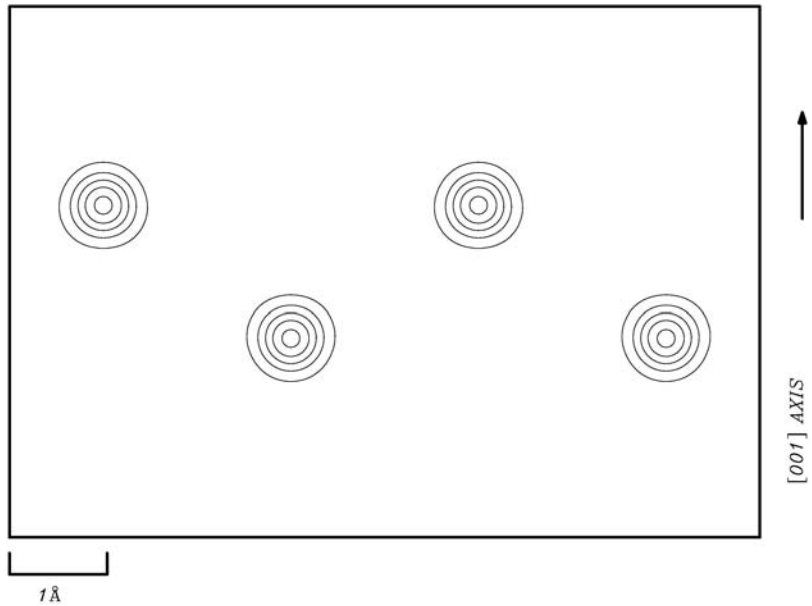

Fourier synthesis

5 ～100, 20[e/Å^3] step

Charge Densities of Silicon (110) Plane

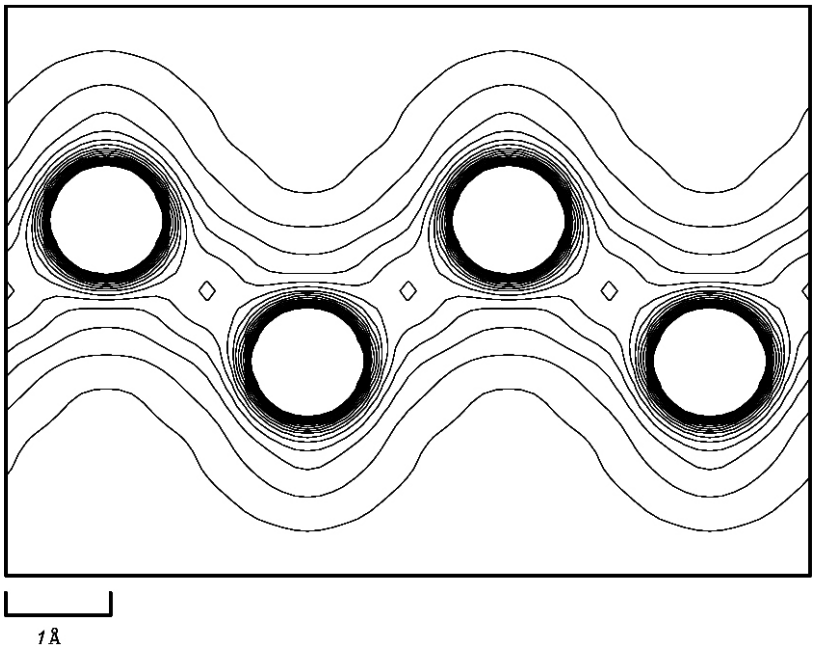

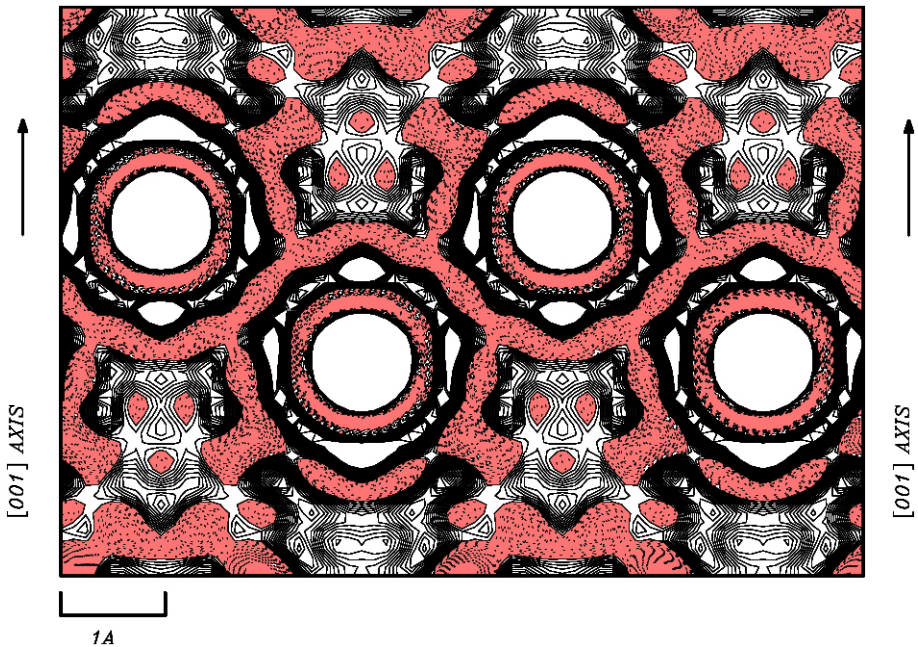

MEM

Fourier synthesis

-2.0 ～2.0,0.1[e/Å^3] step

MEM for Nuclear density study.

Entropy of the density from Positive Scattering length b_+ : $S_+ = -\sum_{\mathbf{r}} \rho'_+(\mathbf{r}) \ell n \frac{\rho'_+(\mathbf{r})}{\tau'_+(\mathbf{r})}$

Entropy of the density from Negative Scattering length b_- : $S_- = -\sum_{\mathbf{r}} \rho'_-(\mathbf{r}) \ell n \frac{\rho'_-(\mathbf{r})}{\tau'_-(\mathbf{r})}$

Total Entropy of the system $S = S_+ + S_-$

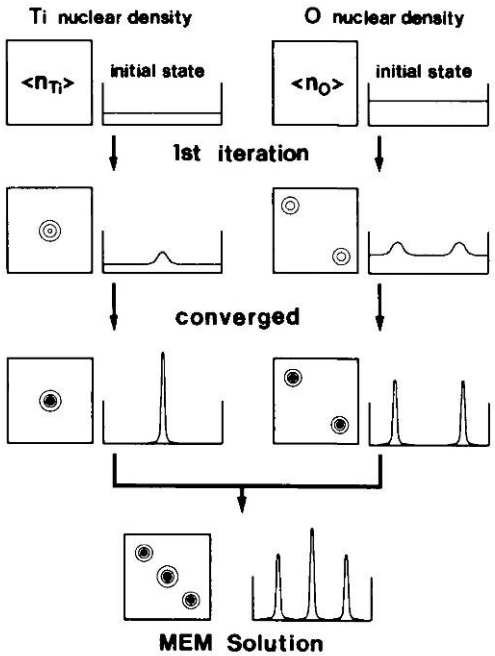

Fig. 1. Third approach: schematic illustration of the iterative procedure used to solve the two MEM equations.

$$F_{cal}(\mathbf{k}) = V \sum_{\mathbf{r}} [\rho_+(\mathbf{r}) b_+ + \rho_-(\mathbf{r}) b_-] \exp[-2\pi i \mathbf{k} \cdot \mathbf{r}]$$

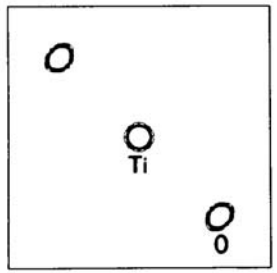

(*a*)

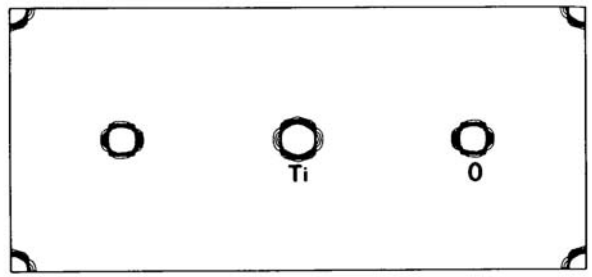

(*b*)

Fig. 4. The MEM maps of the nuclear-density distribution of rutile obtained by the third approach; (*a*) and (*b*) show maps on the (002) and (110) planes, respectively. The contour range is from 0 to 10 with intervals of 1.0 (neutrons $Å^{-3}$). These figures are judged to provide realistic representations of the nuclear density in rutile and it has been concluded that the third approach to dealing with negative scattering lengths is very satisfactory.

An Example of MEM Charge Density: Silicc

Structure Factor for Si by *Pendellösung* Method

h	k	l	F_{obs}
1	1	1	60.13 (5)
2	2	0	67.34 (5)
3	1	1	43.63 (3)
4	0	0	56.23 (4)
3	3	1	38.22 (3)
4	2	2	49.11 (3)
5	1	1	32.94 (2)
3	3	3	32.83 (2)
4	4	0	42.88 (3)
5	3	1	28.81 (2)
6	2	0	37.59 (6)
5	3	3	25.36 (4)
4	4	4	33.18 (5)
7	1	1	22.37 (3)
5	5	1	22.42 (3)
6	4	2	29.42 (4)
5	5	3	19.98 (3)
7	3	1	19.90 (3)
8	0	0	26.23 (4)
7	3	3	17.83 (3)
8	2	2	23.48 (4)
6	6	0	23.48 (4)
7	5	1	15.98 (2)
5	5	5	15.98 (2)
8	4	0	21.15 (3)
9	1	1	14.46 (2)
7	5	3	14.43 (2)
6	6	4	19.13 (3)
9	3	1	
8	4	4	17.44 (3)
7	7	1	
9	3	3	
7	5	5	
10	2	0	
8	6	2	
9	5	1	
7	7	3	
9	5	3	
10	4	2	
7	7	5	
8	8	0	12.41 (2)

MEM

Acta Cryst. (1990). A**46**, 263–270

Accurate Structure Analysis by the Maximum-Entropy Method

BY MAKOTO SAKATA AND MASUMI SATO

Department of Applied Physics, Nagoya University, Furo-cho, Chikusa-ku, Nagoya, Japan 464-01

(*Received* 4 *August* 1989; *accepted* 3 *November* 1989)

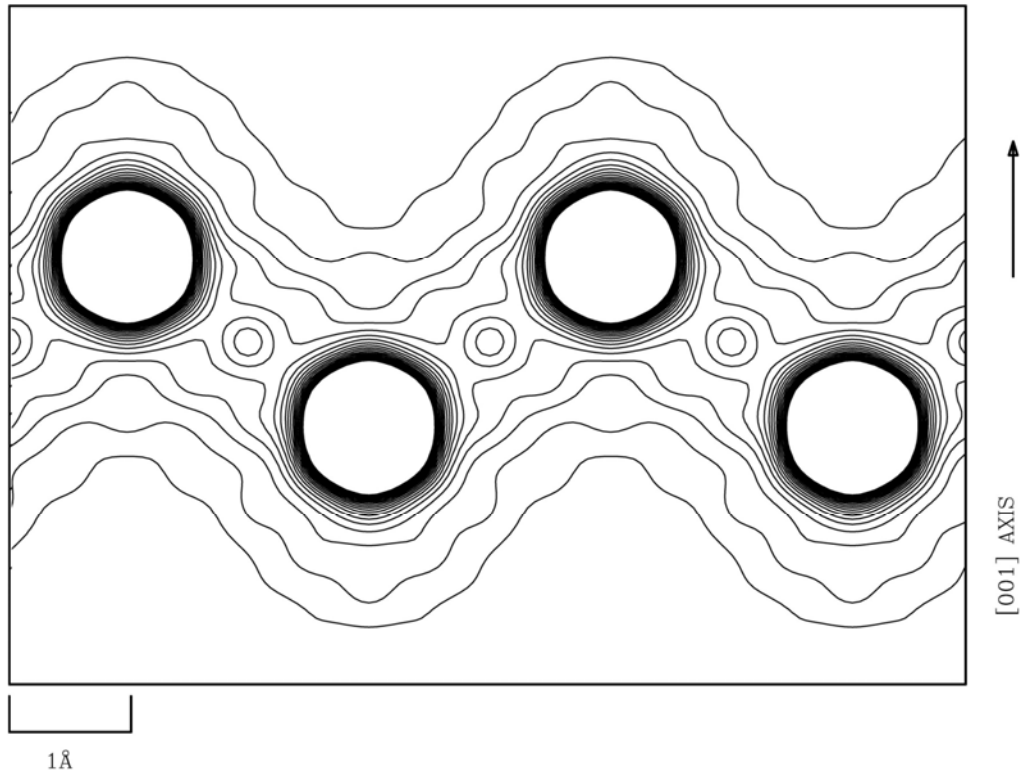

T. Saka and N. Kato
Acta. Cryst. **A42**(1986)

Structure Factor for Si by *Pendellösung* Method

h	k	l	F_{obs}
1	1	1	60.13 (5)
2	2	0	67.34 (5)
3	1	1	43.63 (3)
4	0	0	56.23 (4)
3	3	1	38.22 (3)
4	2	2	49.11 (3)
5	1	1	32.94 (2)
3	3	3	32.83 (2)
4	4	0	42.88 (3)
5	3	1	28.81 (2)
6	2	0	37.59 (6)
5	3	3	25.36 (4)
4	4	4	33.18 (5)
7	1	1	22.37 (3)
5	5	1	22.42 (3)
6	4	2	29.42 (4)
5	5	3	19.98 (3)
7	3	1	19.90 (3)
8	0	0	26.23 (4)
7	3	3	17.83 (3)
8	2	2	23.48 (4)
6	6	0	23.48 (4)
7	5	1	15.98 (2)
5	5	5	15.98 (2)
8	4	0	21.15 (3)
9	1	1	14.46 (2)
7	5	3	14.43 (2)
6	6	4	19.13 (3)
9	3	1	
8	4	4	17.44 (3)
7	7	1	
9	3	3	
7	5	5	
10	2	0	
8	6	2	
9	5	1	
7	7	3	
9	5	3	
10	4	2	
7	7	5	
8	8	0	12.41 (2)

MEM

Acta Cryst. (1996). A**52**, 287–290

The Influence of the Completeness of the Data Set on the Charge Density Obtained with the Maximum-Entropy Method. A Re-examination of the Electron-Density Distribution in Si

MASAKI TAKATA AND MAKOTO SAKATA

Department of Applied Physics, Nagoya University, Nagoya 464-01, Japan

(*Received 17 July 1995; accepted 30 October 1995*)

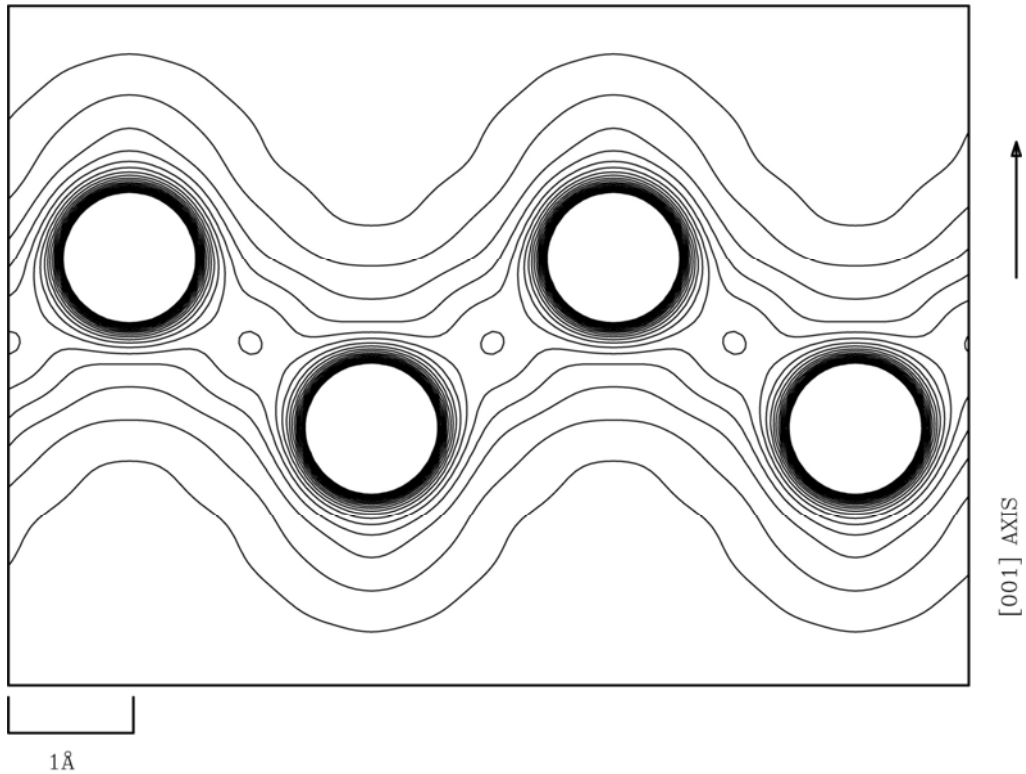

T. Saka and N. Kato
Acta. Cryst. **A42**(1986)

Powder Data@SPring-8

Acta Crystallographica Section A
Foundations of Crystallography
ISSN 0108-7673

Received 24 July 2006
Accepted 8 November 2006

Accurate structure factors and experimental charge densities from synchrotron X-ray powder diffraction data at SPring-8

Eiji Nishibori,[a]* Eiji Sunaoshi,[a] Akihiro Yoshida,[a] Shinobu Aoyagi,[a] Kenichi Kato,[b,c,d] Masaki Takata[b,c,d] and Makoto Sakata[a]

Acta Cryst. **A63**(2007)

		$F(h\,k\,l)$		
		Powder	Powder	Saka Kato
		100K	300K	294K
h	*k*	*l*			
1	1	-60.4 (1)	-60.0 (1)	-60.13 (5)
2	0	-68.3 (1)	-67.2 (1)	-67.34 (5)
1	1	-44.3 (1)	-43.4 (1)	-43.63 (3)
2	2	1.6 (3)	1.6 (3)	
0	0	-57.7 (2)	-56.0 (2)	-56.23 (4)
3	1	39.7 (1)	38.5 (1)	38.22 (3)
2	2	51.3 (1)	49.3 (1)	49.11 (4)
3	3	34.5 (2)	32.9 (2)	32.83 (2)
1	1	34.5 (1)	32.9 (1)	32.94 (2)
4	0	45.5 (2)	43.1 (2)	42.88 (3)
3	1	30.7 (1)	28.9 (1)	28.81 (2)
2	0	40.3 (2)	37.4 (2)	37.59 (6)
3	3	-27.5 (2)	-25.5 (2)	-25.36 (4)
4	4	-36.5 (3)	-33.4 (3)	-33.18 (5)
5	1	-24.6 (2)	-22.5 (2)	-22.42 (3)
1	1	24.6 (2)	22.5 (2)	22.37 (3)
4	2	-32.7 (1)	-29.5 (1)	-29.42 (4)
3	1	-22.2 (1)	-19.9 (1)	-19.90 (3)
5	3	-22.2 (2)	-19.9 (2)	-19.98 (3)
0	0	29.1 (4)	25.8 (4)	26.23 (4)
3	3	-20.1 (2)	-17.6 (2)	-17.83 (3)
2	2	-26.9 (2)	-23.6 (3)	-23.48 (4)
6	0	-26.9 (3)	-23.6 (2)	-23.48 (4)
5	1	-18.4 (1)	-16.1 (2)	-15.98 (2)
5	5	18.3 (4)	16.0 (4)	15.98 (2)
4	0	-24.5 (2)	-21.4 (2)	-21.15 (3)
5	3	16.8 (2)	14.5 (2)	14.43 (2)
1	1	-16.8 (2)	-14.5 (2)	-14.46 (2)
6	4	22.8 (2)	19.4 (2)	19.13 (3)
3	1	-15.5 (2)	-13.1 (2)	
4	4	20.9 (2)	17.5 (3)	
5	5	14.3 (2)	11.9 (3)	
7	1	14.3 (2)	11.9 (3)	
3	3	14.3 (2)	11.9 (3)	
6	2	19.2 (2)	16.0 (2)	
2	0	-19.2 (2)	-15.9 (3)	
5	1	13.4 (2)	11.0 (2)	
7	3	13.3 (2)	10.9 (3)	
5	3	12.4 (2)	9.9 (2)	
4	2	16.7 (2)	13.6 (2)	
7	5	-11.5 (3)	-9.1 (3)	
1	1	-11.5 (3)	-9.1 (3)	
8	0	16.2 (4)	12.8 (4)	
3	1	10.9 (2)	8.6 (2)	
7	1	10.9 (2)	8.6 (2)	
5	5	-10.9 (3)	-8.5 (3)	
6	6	-14.8 (3)	-11.5 (3)	

		$F(h\,k\,l)$		
		Powder	Powder	Saka Kato
		100K	300K	294K
h	*k*	*l*			
10	6	0	14.8 (3)	11.5 (3)	
11	3	3	10.0 (3)	7.8 (3)	
9	7	3	-10.1 (2)	-7.8 (2)	
12	0	0	-13.8 (6)	-10.6 (6)	
8	8	4	-14.0 (3)	-10.9 (3)	
7	7	7	-9.4 (5)	-7.2 (5)	
11	5	1	9.6 (2)	7.4 (2)	
10	6	4	-13.2 (2)	-10.0 (2)	
12	2	2	13.1 (3)	9.9 (3)	
11	5	3	-9.2 (2)	-6.9 (2)	
9	7	5	-9.2 (2)	-6.9 (2)	
12	4	0	12.3 (3)	9.3 (3)	
9	9	1	-8.3 (3)	-6.5 (3)	
10	8	2	-12.1 (2)	-8.8 (2)	
13	1	1	8.2 (3)	6.0 (3)	
9	9	3	-8.2 (3)	6.0 (3)	
11	7	1	-8.3 (2)		
11	5	5			
12	4	4			
9	7	7			
13	3	1			
11	7	3			
12	6	2			
9	9	5	7.2 (3)		
13	3	3	-7.2 (3)	-5.2 (3)	
8	8	8	10.3 (5)	7.0 (6)	
13	5	1	-7.3 (2)	-4.9 (2)	
11	7	5	7.3 (2)	4.9 (2)	
10	8	6	10.1 (2)	7.0 (2)	
10	10	0	-9.9 (4)	-6.8 (5)	
14	2	0	10.0 (3)	6.9 (3)	
11	9	1	-7.0 (2)	-4.7 (2)	
13	5	3	-7.0 (2)	-4.7 (2)	
12	8	0	-9.2 (3)	-6.8 (4)	
11	9	3	6.6 (2)	4.3 (3)	
9	9	7	6.5 (3)	4.2 (4)	
14	4	2	-9.2 (2)	-6.2 (3)	
12	6	6	9.1 (3)	6.0 (4)	
10	10	4	9.1 (3)	6.0 (4)	
13	5	5	6.4 (3)	4.2 (4)	
11	7	7	6.4 (3)	4.2 (4)	
13	7	1	-6.6 (2)	-4.3 (3)	
12	8	4	9.2 (2)	6.0 (3)	
15	1	1	6.2 (3)	3.9 (4)	
11	9	5	6.3 (2)	4.0 (3)	
13	7	3	6.3 (2)	4.0 (3)	
14	6	0	-8.5 (3)	-5.1 (4)	

MEM

			$F(h\,k\,l)$
			Powder
			100K
h	*k*	*l*	
15	3	1	-5.8 (2)
9	9	9	-5.5 (6)
13	7	5	5.8 (2)
15	3	3	-5.6 (3)
11	11	1	5.6 (3)
14	6	4	8.1 (2)
12	10	2	8.1 (2)
11	9	7	-5.5 (2)
15	5	1	-5.5 (2)
11	11	3	5.5 (3)
13	9	1	5.5 (2)
16	0	0	8.2 (7)
13	9	3	5.5 (2)
15	5	3	5.5 (2)
10	1	8	-7.3 (4)
14			7.5 (2)
16			-7.3 (4)
			-5.2 (4)
			(4)
			(4)
			(4)
			-5.2 (3)
15			5.2 (3)
12	1	8	-7.0 (3)
15	3	3	4.9 (3)
11	9	9	-4.8 (4)
16	4	4	6.6 (4)
12	12	0	6.5 (5)
17	1	1	-4.5 (4)
11	11	7	-4.5 (4)
13	11	1	4.6 (3)
14	10	0	6.4 (4)
14	8	6	-6.5 (3)
16	6	2	6.5 (3)
13	9	7	-4.5 (3)
17	3	1	-4.5 (3)
13	11	3	-4.5 (3)
15	7	5	-4.5 (3)

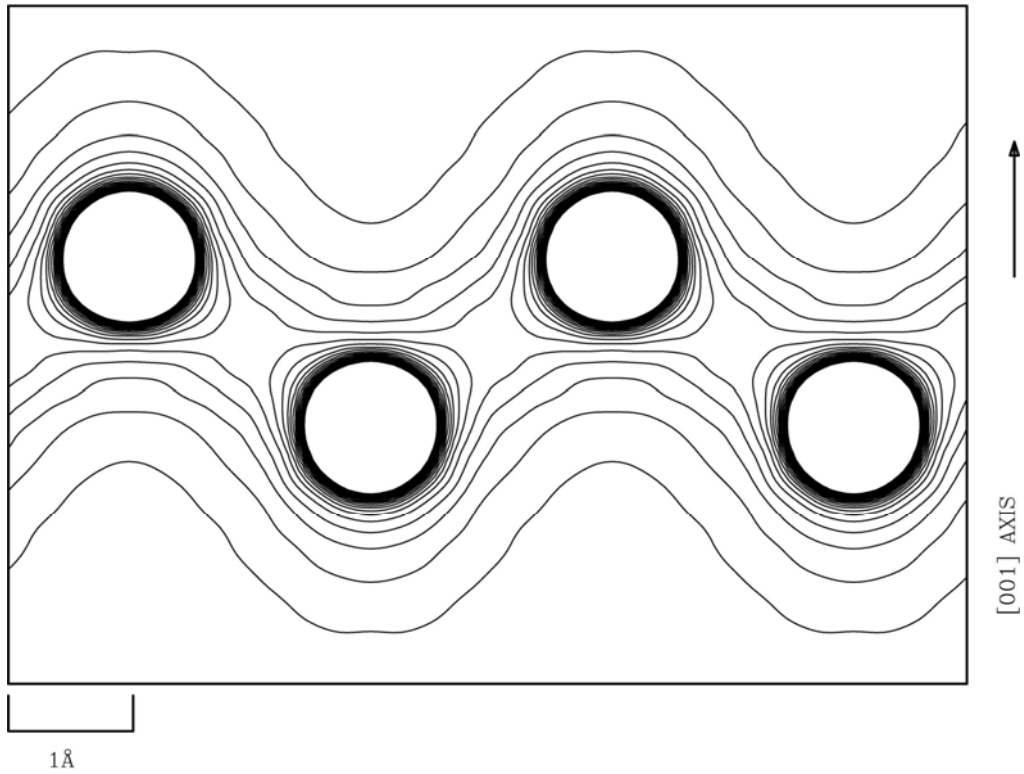

Charge Densities at Bond midpoint

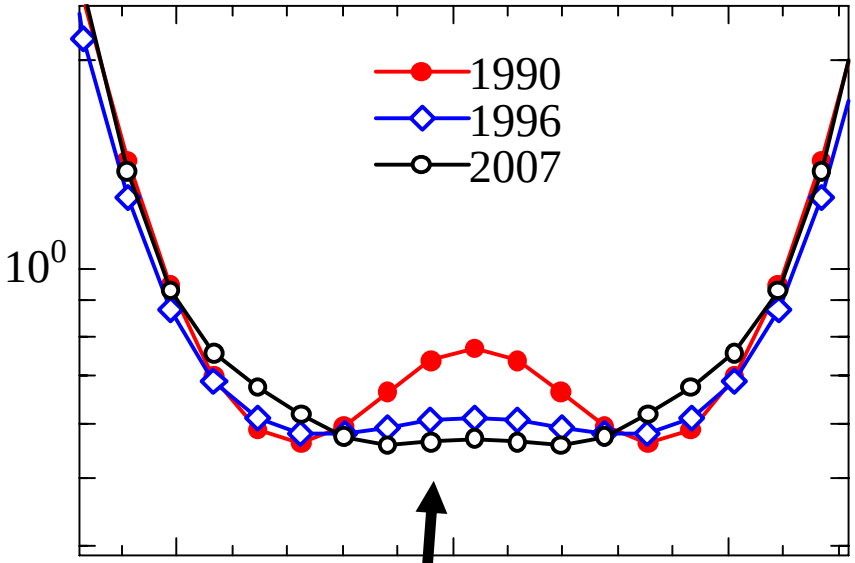

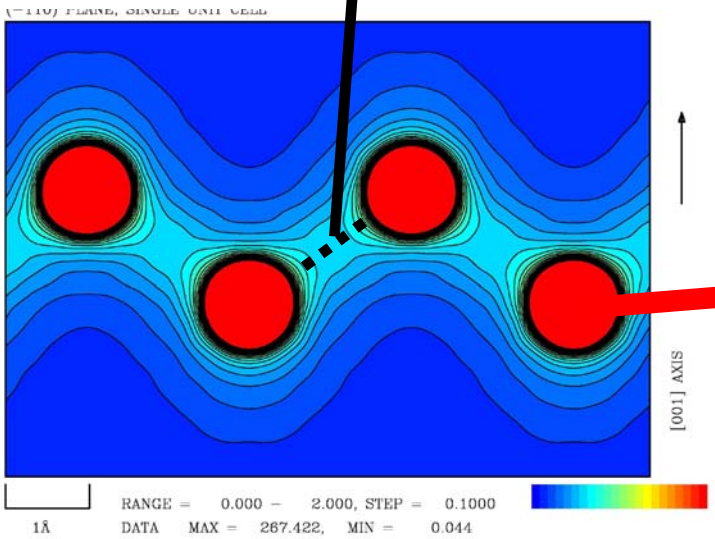

Charge Density at Peak

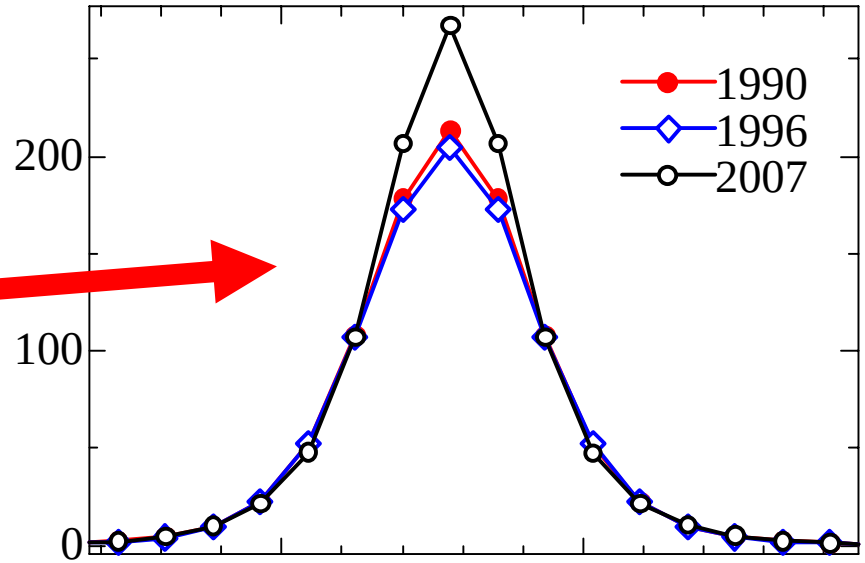

MDM
(Minimum Distance Mthod)

$$S = -\sum_{\mathbf{r}} \{ \rho'(\mathbf{r}) - \tau'(\mathbf{r}) \}^2$$

$$\rho(\mathbf{r}) = \tau(\mathbf{r}) + \frac{\lambda F_0}{N} \sum_{\mathbf{k}} \frac{1}{\sigma^2(\mathbf{k})} \{ F_{obs}(\mathbf{k}) - F_{cal}(\mathbf{k}) \} \exp(-2\pi i \mathbf{k} \cdot \mathbf{r})$$

MEM
(Maximum Entropy Method)

$$S = -\sum_{\mathbf{r}} \rho'(\mathbf{r}) \ln \frac{\rho'(\mathbf{r})}{\tau'(\mathbf{r})}$$

$$\rho(\mathbf{r}) = \exp[\ln \tau(\mathbf{r}) + \frac{\lambda F_0}{N} \sum_{\mathbf{k}} \frac{1}{\sigma^2(\mathbf{k})} \{ F_{obs}(\mathbf{k}) - F_{cal}(\mathbf{k}) \} \exp(-2\pi i \mathbf{k} \cdot \mathbf{r})]$$

Charge Density by MDM and Fourier

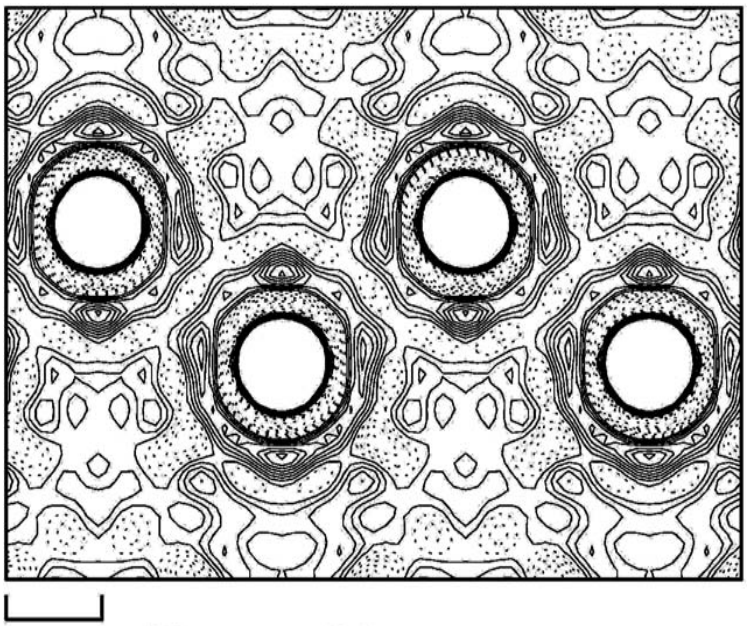

Fig.2 The (110) **MDM** electron density distributions of **Si** based on the data measured by Saka and Kato

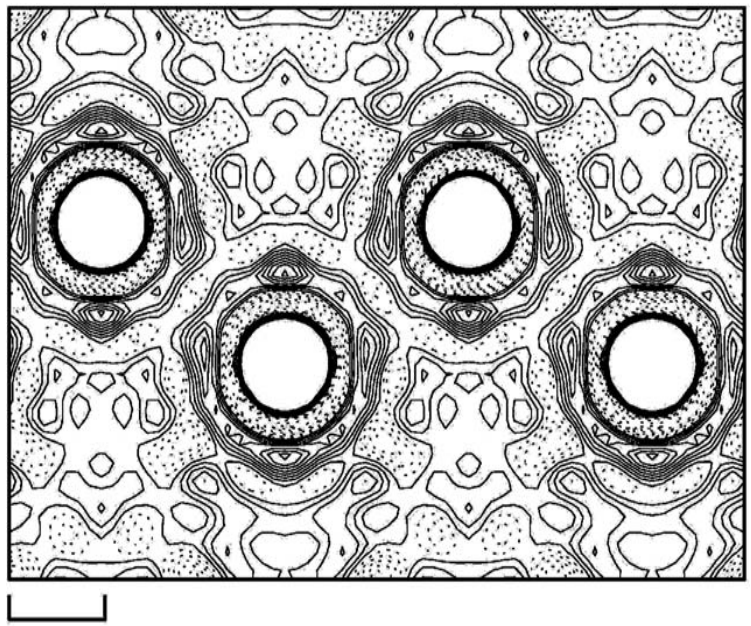

Fig.1 The (110) **Fourier** electron density distributions of **Si** based on the data measured by Saka and Kato

Difference MDM and Fourier

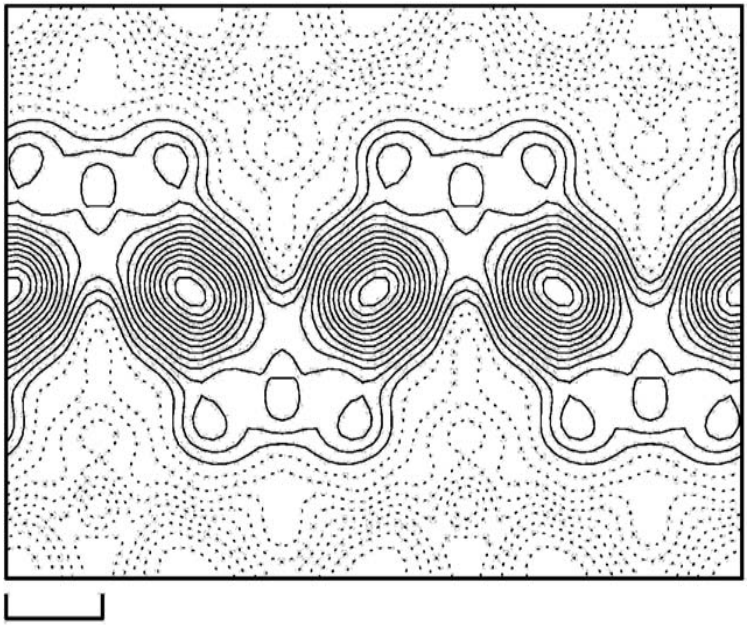

Fig.1 The (110) **Difference MDM** electron density distributions of **Si**

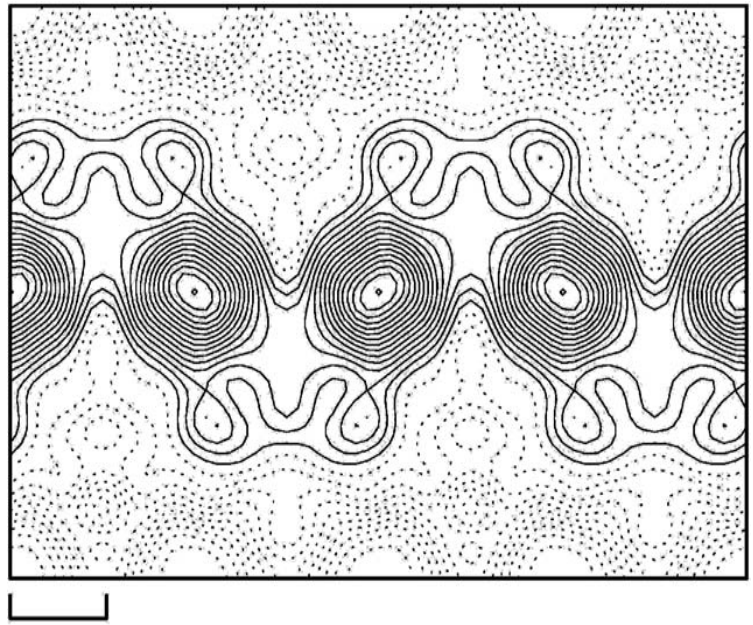

Fig.2 The (110) **Difference Fourier** electron density distributions of **Si**

MEM (Maximum Entropy Method)

Information theory

$\{ P_i \}$

Probability distribution

$-\ln P_i$

Information

$$S = -\sum_i P_i \ln \frac{P_i}{M_i}$$

Information Entropy

Crystallography

$\{ \rho(\mathbf{r}) \}$

Electron density distribution

$-\ln \rho'(\mathbf{r})$

Geometrical distribution

$$S = -\sum_{\mathbf{r}} \rho'(\mathbf{r}) \ln \frac{\rho'(\mathbf{r})}{\tau'(\mathbf{r})}$$

Geometrical Entropy

Imaging of Diffraction Data by the MEM

Fine Structure Prediction

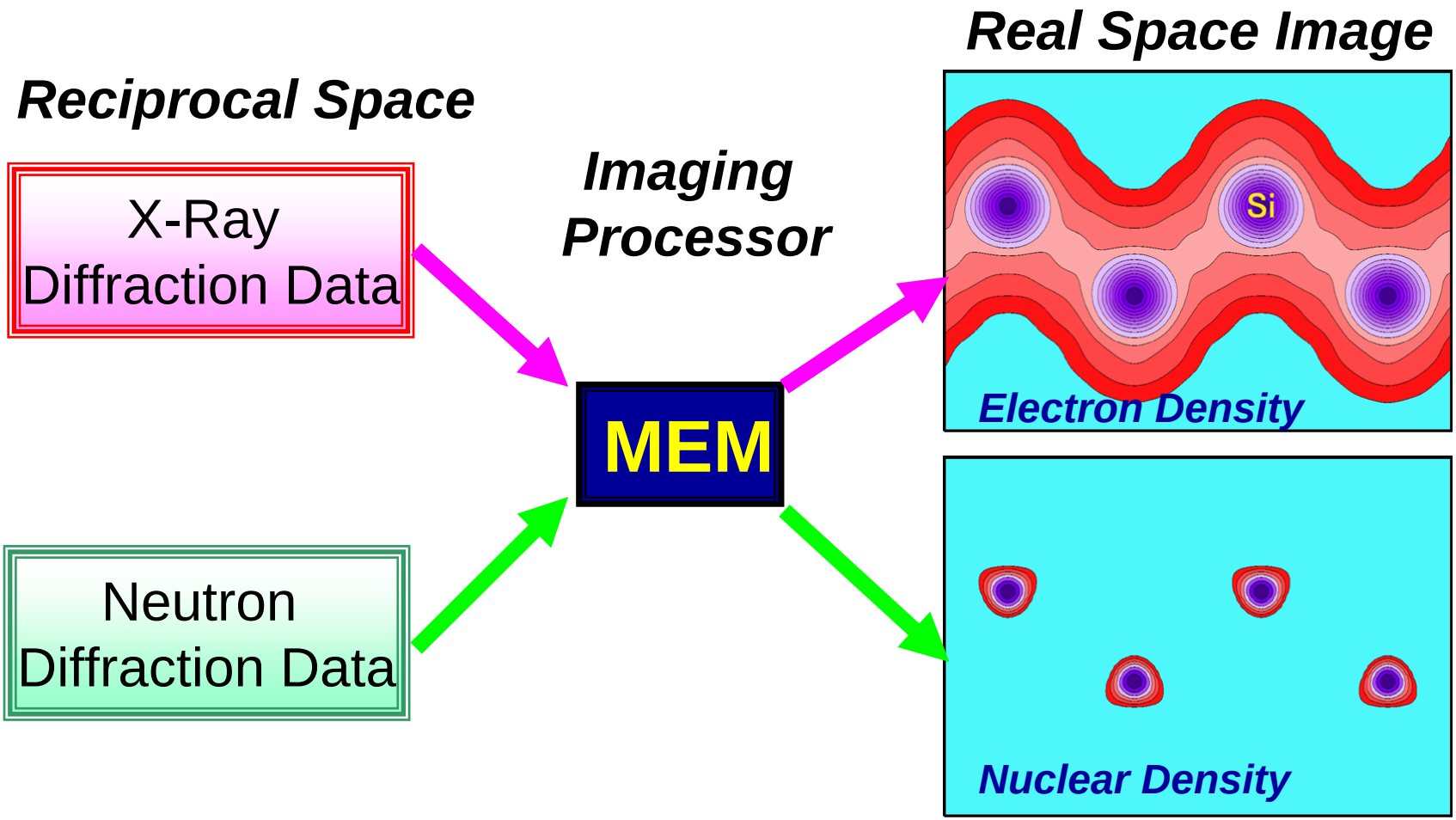

MEM

Virtual Crystallographic X-ray Microscopy

Electron Microscopy

Diffraction Pattern *Electromagnetic Lens* *Electron Micrograph*

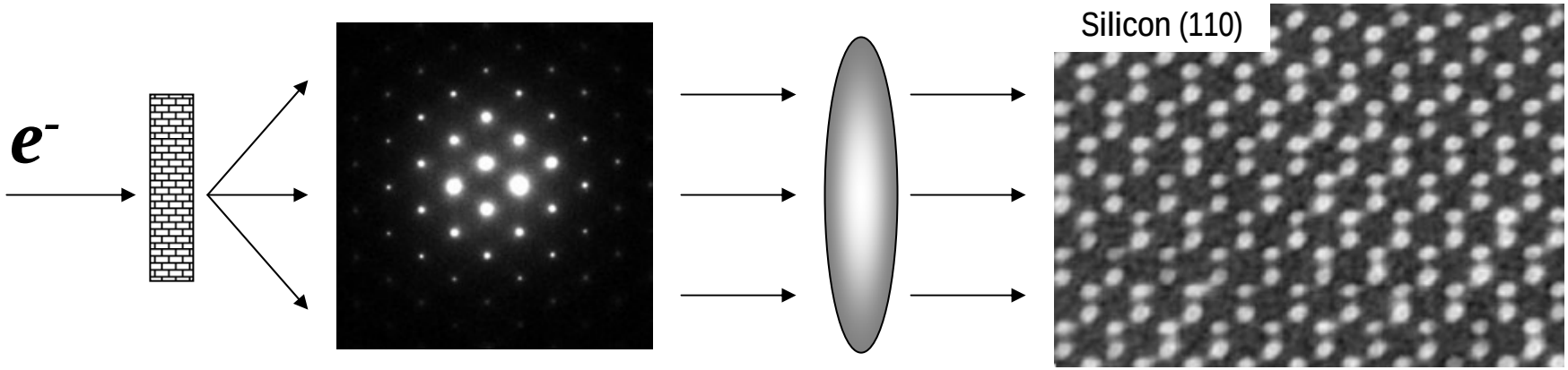

Imaging of X-ray Diffraction Data

Diffraction Data *MEM* *Charge, Nuclear Density*

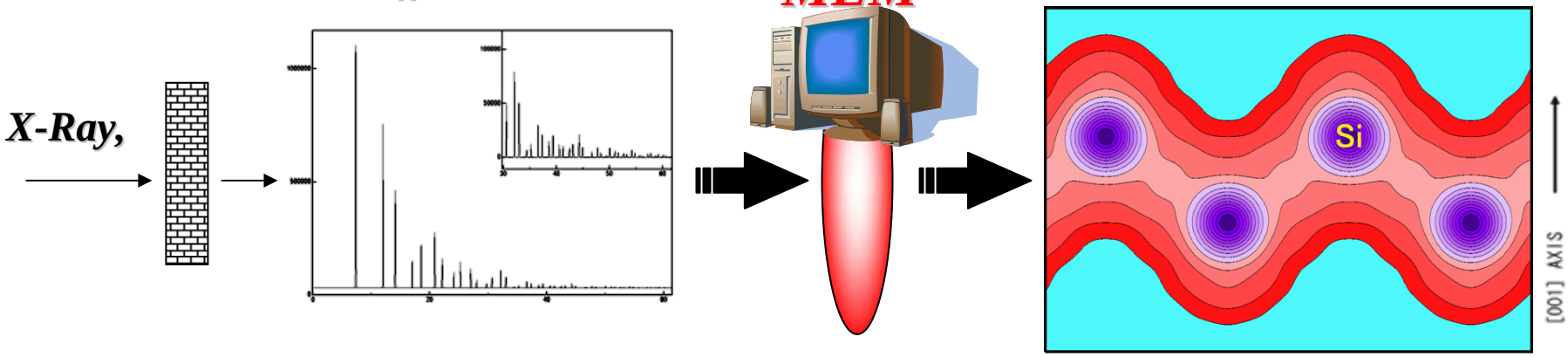

SR Powder Method at Photon Factory

PF BL-6A$_2$

Translation Geometry
Right Materials
(Fullerenes, Borons, etc.)

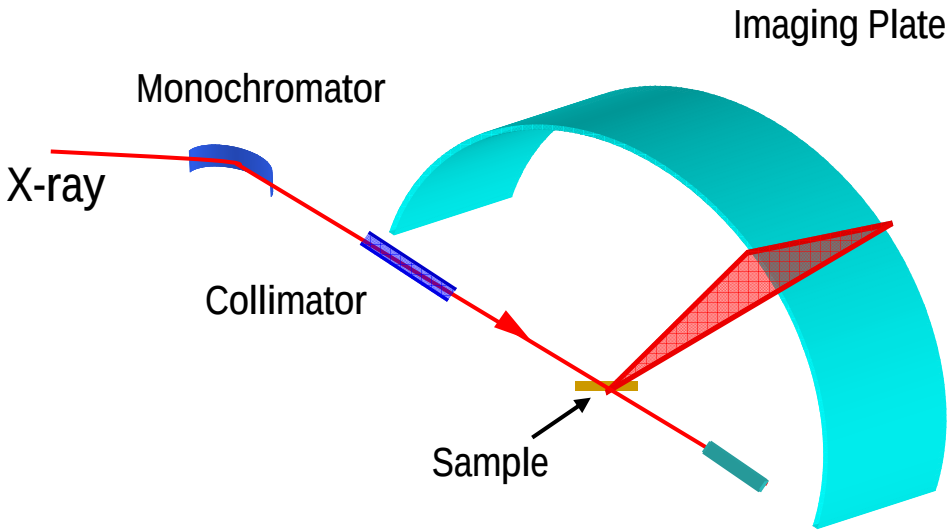

PF BL-3A

Reflection Geometry
Heavy Materials
Manganites, High-Tc Superconductors, etc.

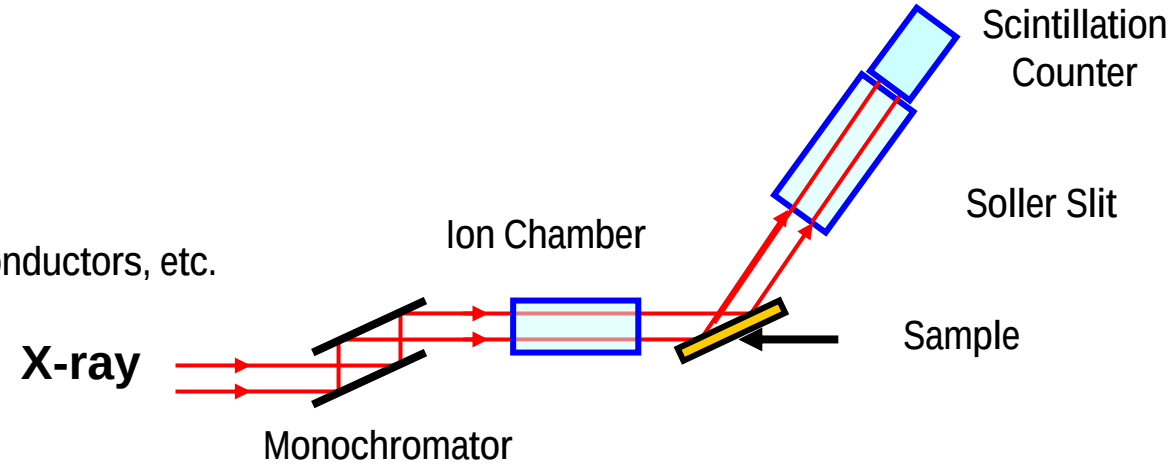

Experimental Arrangement at BL-3A(PF)

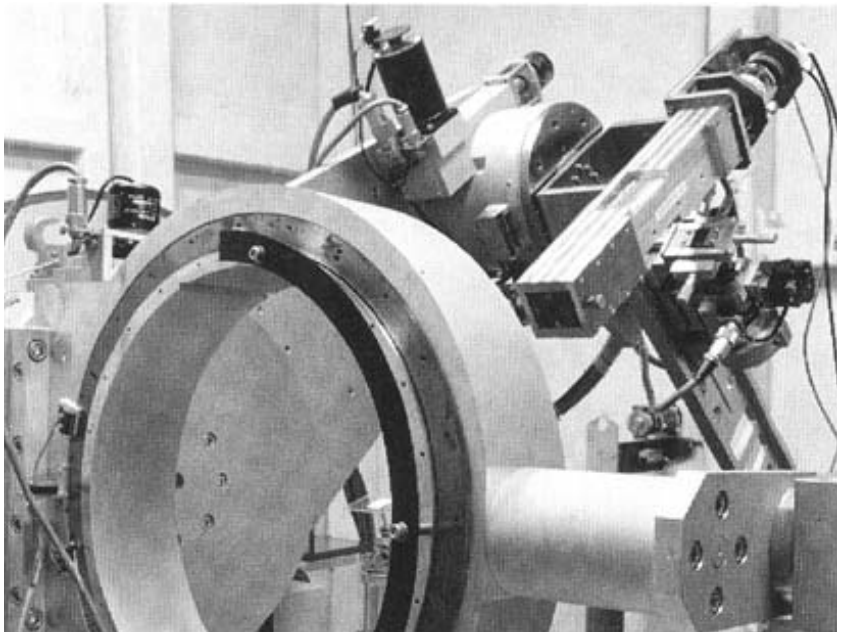

Sample : $NdSr_2Mn_2O_7$
Temperature : R.T. & 19K
Wave Length : 1.0Å
Step in 2θ : 0.01°
Collection Time : 20s
Resolution of Data : 0.78Å

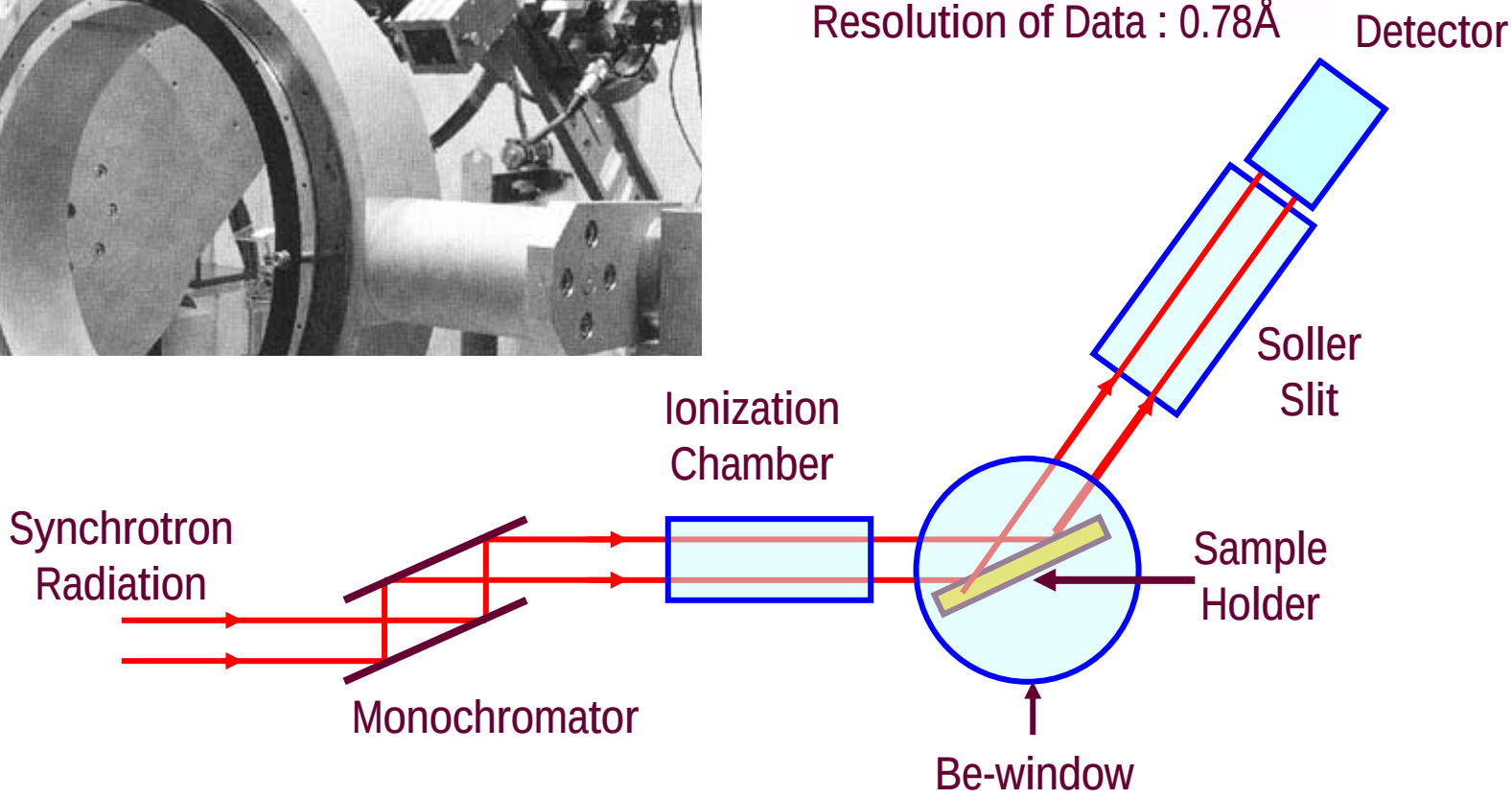

自作カメラ

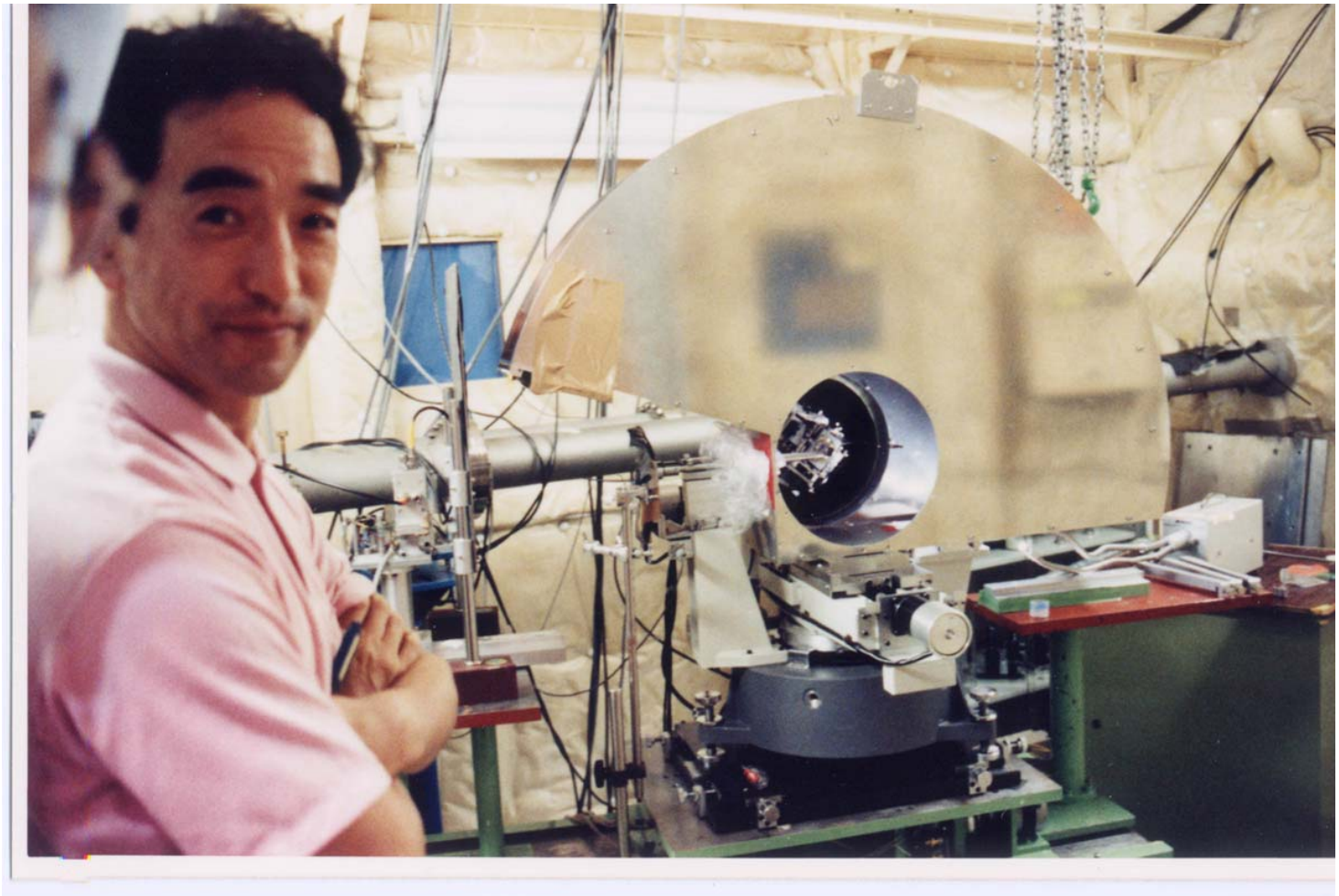

超高輝度X線発生源SPring-8

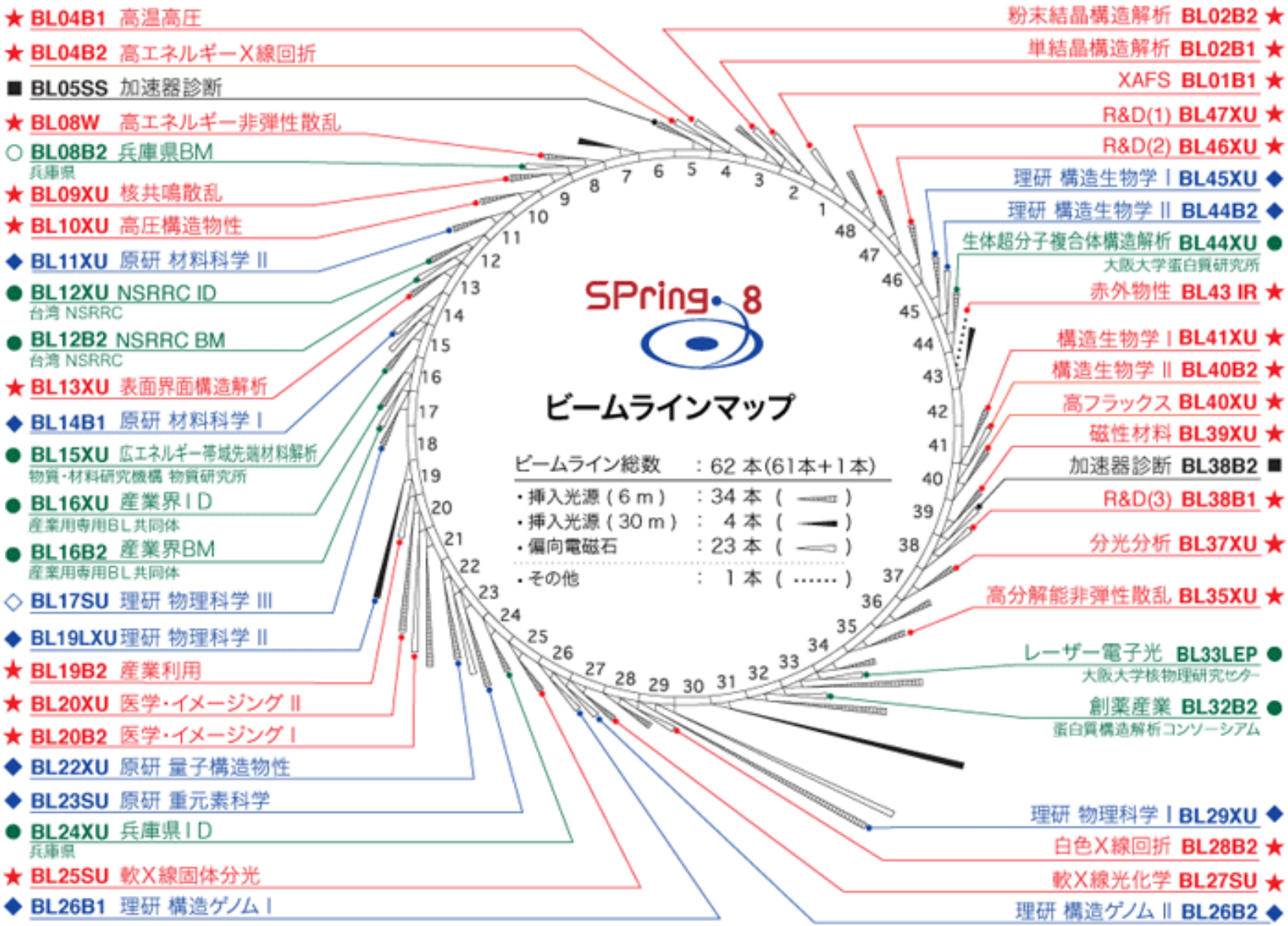

The Large Debye-Scherrer Camera at SPring-8 BL02B2

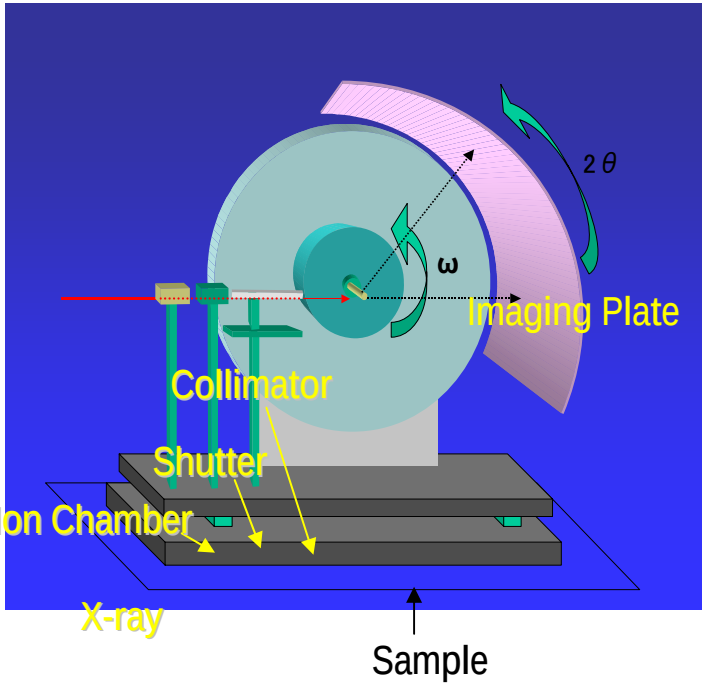

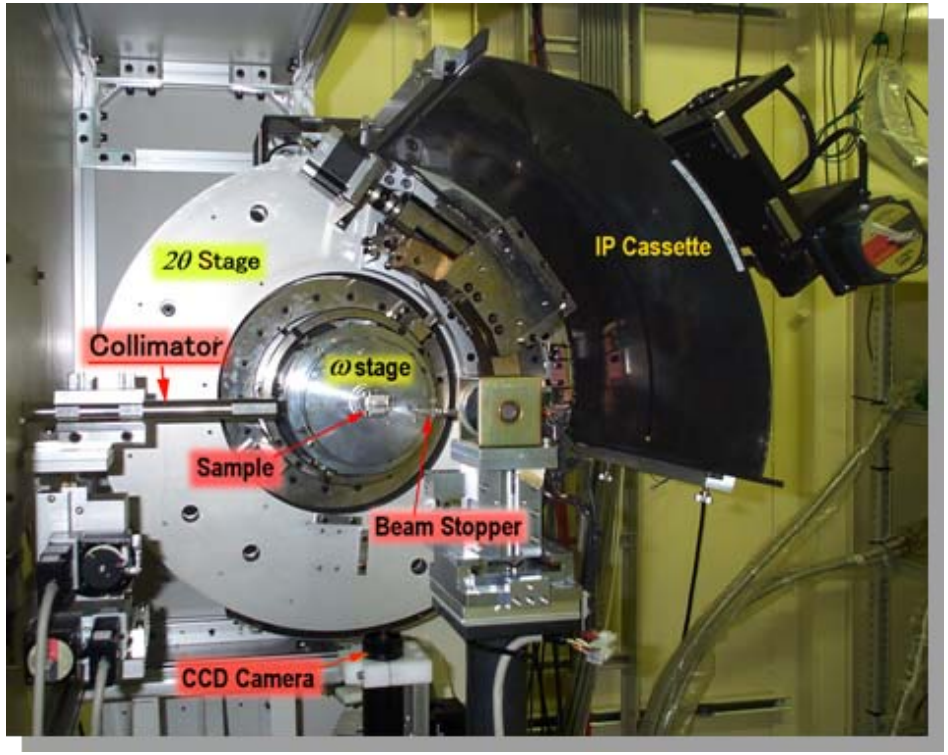

Low and High Temperature Powder Diffraction

15K～300K
Displex System

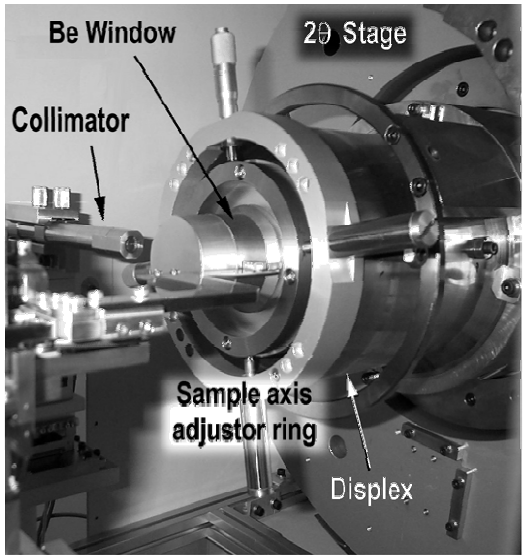

80K～300K
Dry N_2 Gas Flow System

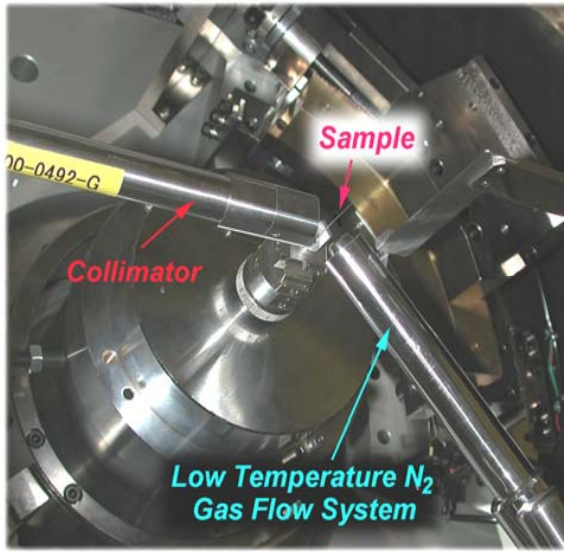

300K～1000K
Dry N_2 Gas Flow System

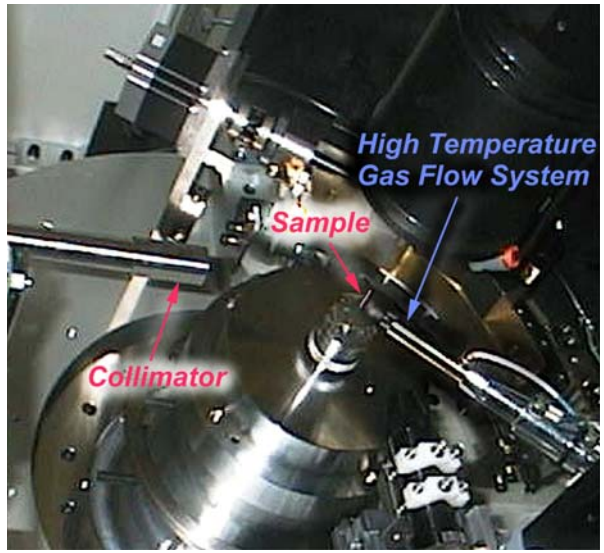

Displex

Powder Sample Sealed in Silica Glass Capillary

(0.2mm int. diam.)

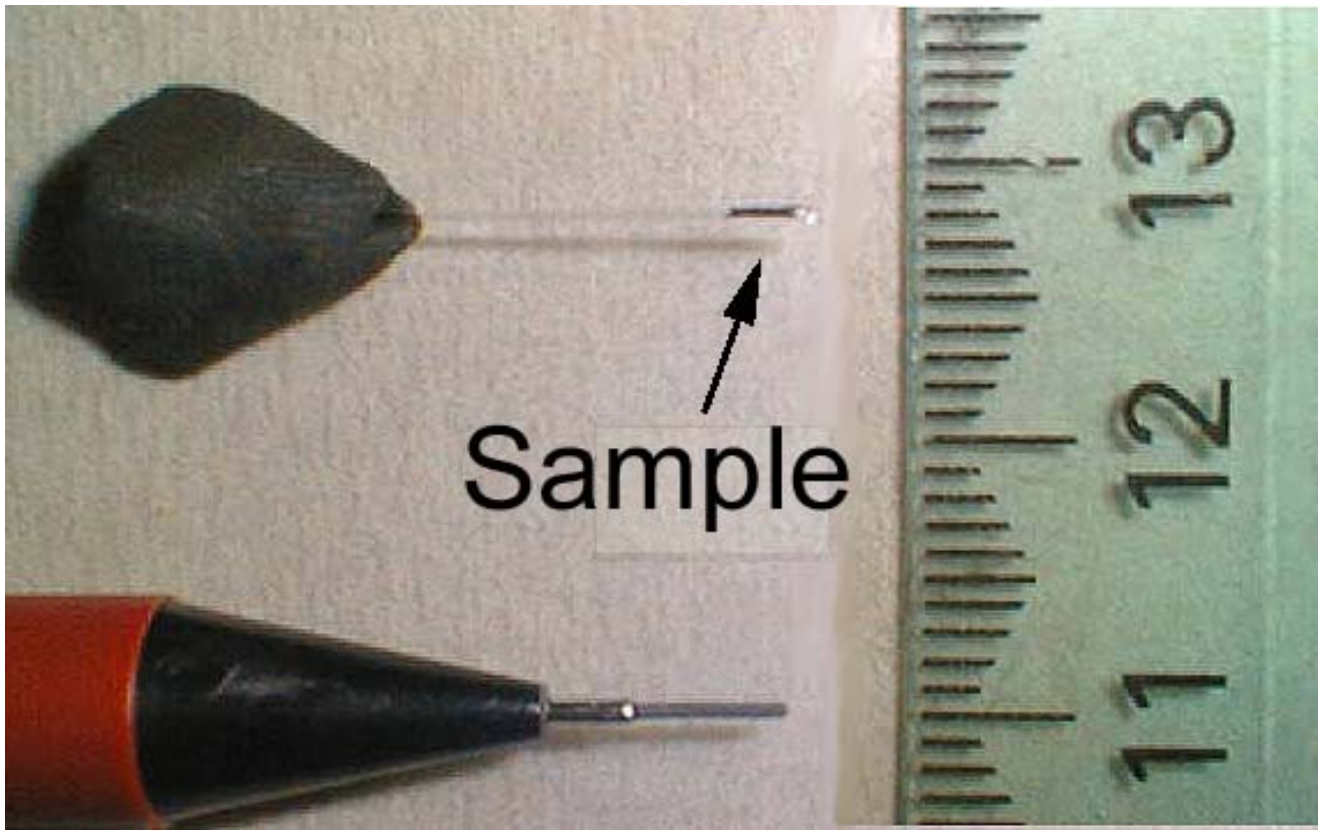

装置の論文

ELSEVIER

Journal of Physics and Chemistry of Solids 62 (2001) 2095–2098

JOURNAL OF PHYSICS AND CHEMISTRY OF SOLIDS

www.elsevier.com/locate/jpcs

The large Debye–Scherrer camera installed at SPring-8 BL02B2 for charge density studies

E. Nishibori[a], M. Takata[a], K. Kato[a], M. Sakata[a,*], Y. Kubota[b], S. Aoyagi[c], Y. Kuroiwa[c], M. Yamakata[d], N. Ikeda[d]

[a]*Department of Applied Physics, Nagoya University, Nagoya 464-8603, Japan*
[b]*Osaka Women's University, Osaka 590-0035, Japan*
[c]*Department of Physics, Okayama University, Okayama 700-8530, Japan*
[d]*JASRI, Hyogo, Sayo-gun, Mikazuki, Kouto, 679-5198, Japan*

Congratulations, M. Sakata

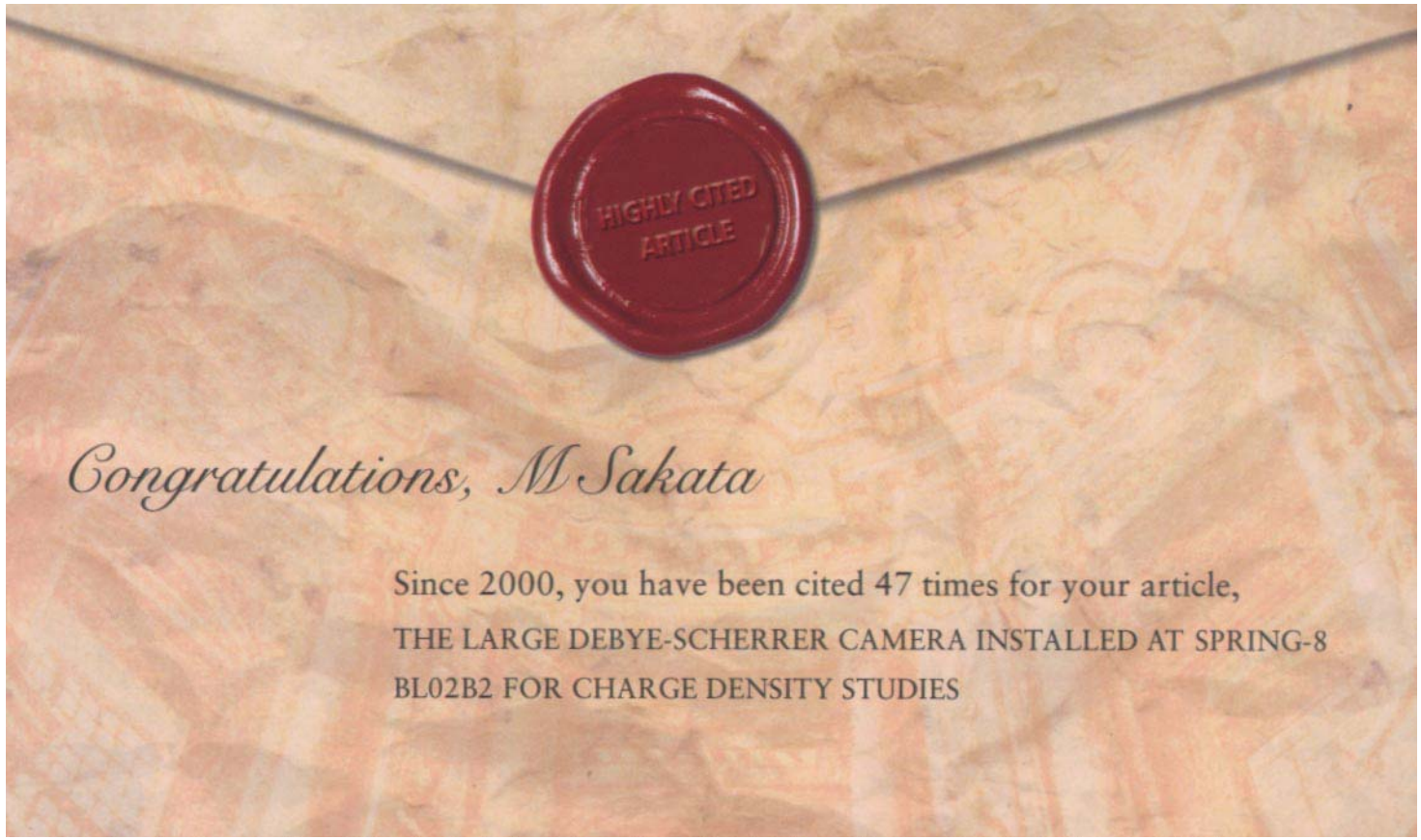

Essential Science Indicators

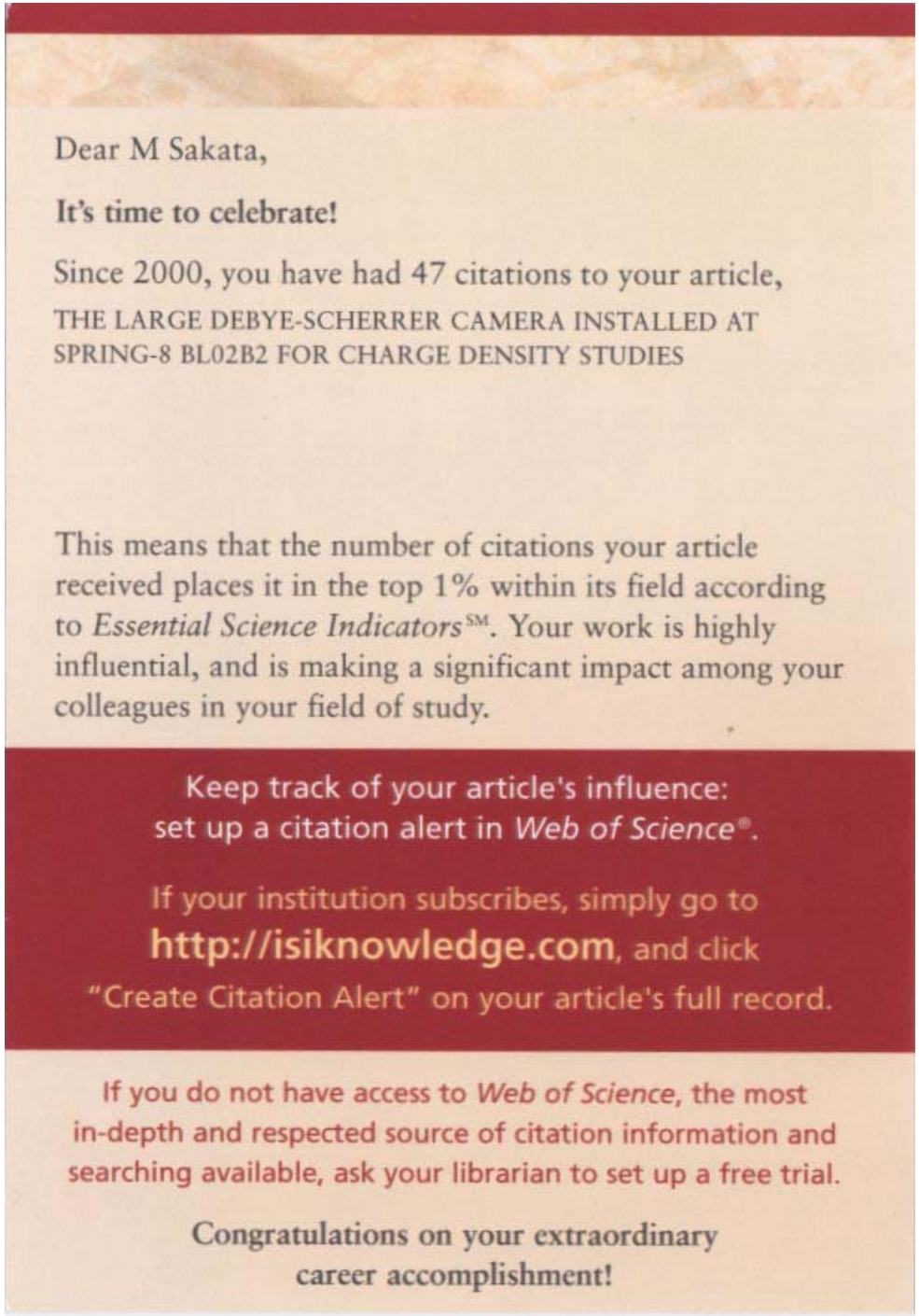

Dear M Sakata,

It's time to celebrate!

Since 2000, you have had 47 citations to your article,

THE LARGE DEBYE-SCHERRER CAMERA INSTALLED AT SPRING-8 BL02B2 FOR CHARGE DENSITY STUDIES

This means that the number of citations your article received places it in the top 1% within its field according to *Essential Science Indicators*℠. Your work is highly influential, and is making a significant impact among your colleagues in your field of study.

Keep track of your article's influence:
set up a citation alert in *Web of Science*®.

If your institution subscribes, simply go to
http://isiknowledge.com, and click
"Create Citation Alert" on your article's full record.

If you do not have access to *Web of Science*, the most in-depth and respected source of citation information and searching available, ask your librarian to set up a free trial.

Congratulations on your extraordinary career accomplishment!

MEM/Rietveld for Endohedral metallofullerene

Confirmation by X-ray diffraction of the endohedral nature of the metallofullerene Y@C_{82}

Masaki Takata*, Buntaro Umeda*, Eiji Nishibori*, Makoto Sakata*, Yahachi Saito†, Makoto Ohno‡ & Hisanori Shinohara‡

* Department of Applied Physics, Nagoya University, Nagoya 464-01, Japan
† Department of Electrical and Electronic Engineering, Mie University, Tsu 514, Japan
‡ Department of Chemistry, Nagoya University, Nagoya 464-01, Japan

THE synthesis of fullerenes encapsulating various metal atoms within the carbon cage (endohedral metallofullerenes) has stimulated wide interest[1,2] because of their unusual structural and electronic properties. Most of the metallofullerenes prepared so far have been based on C_{82}, and have incorporated lanthanum[1,3-5], yttrium[6,7], scandium[8-10] and most of the lanthanide elements[11,12]. Although there has been some debate about the endohedral nature of these compounds[2,13,14], observations using scanning tunnelling microscopy[15,16], extended X-ray absorption fine structure[17,18], transmission electron microscopy[19] and electron spin resonance[3,6-8,10] have strongly suggested that the metal atoms are indeed inside the fullerene cages; theoretical calculations[20,21] also indicate that this is the case. But until now, no structural model has been derived experimentally to confirm the endohedral nature of the metallofullerenes. Here we report the results of a synchrotron X-ray powder diffraction study of Y@C_{82} that confirms that the yttrium atom is located within the carbon cage. The yttrium atom is displaced from the centre of the C_{82} molecule and is strongly bound to the carbon cage.

Soot containing Y@C_{82} was produced in direct-current (500 A) spark mode under He flow at 50 Torr and collected under totally anaerobic conditions to avoid degradation of the metallofullerene during collection and handling[15,16,22]. The Y@C_{82} fullerene was separated and isolated from various hollow fullerenes (C_{60}–C_{110}) by two-stage high-performance liquid chromatography (HPLC)[22]. The isolation of Y@C_{82} was confirmed by mass spectrometry for the corresponding HPLC fraction. The purity of the fullerene was >99.9%. Y@C_{82} powder samples grown from toluene solvent[22] were sealed in 0.3 mm int. diam. silica glass capillary. To obtain an X-ray powder pattern with good counting statistics, the Synchrotron Radiation X-ray powder experiment with Imaging Plates as detectors[23] was carried out at Photon Fa
The wavelength o
data for the hollo
ence under the sa
pattern of Y@C
sponds to 2.9 Å
whether the Y at
ous X-ray single-
space group of t
preliminary struc
model. The prese
good agreement
of Y@C_{82} is also

M.Takata *et al.*,
Nature(1995)

Atom in a cage

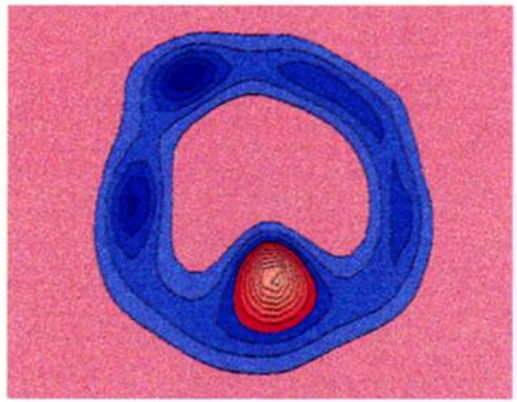

NOT abstract art, but concrete evidence of something that fullerene specialists had hoped and suspected to be the case, the figure shown here demonstrates that a metal atom can indeed be trapped within a cage of carbon. The contours map the electron density across a section through the metallofullerene Y@C_{82}, the shorthand notation for yttrium in an 82-carbon cage. The pink and swollen bulge inside the circle's lower rim shows the high electron density expected to be associated with the yttrium atom — here clearly ensconced within the blue carbon framework. Theory and experiment had both suggested that this was so; but the new structure, derived from X-ray powder diffraction experiments, may finally allay any doubts. Details of the experiment, carried out by Japanese researchers M. Takata *et al.* at Mie and Nagoya Universities, can be found on page 46 of this issue. L. N.

2次元MEM電子密度分布図

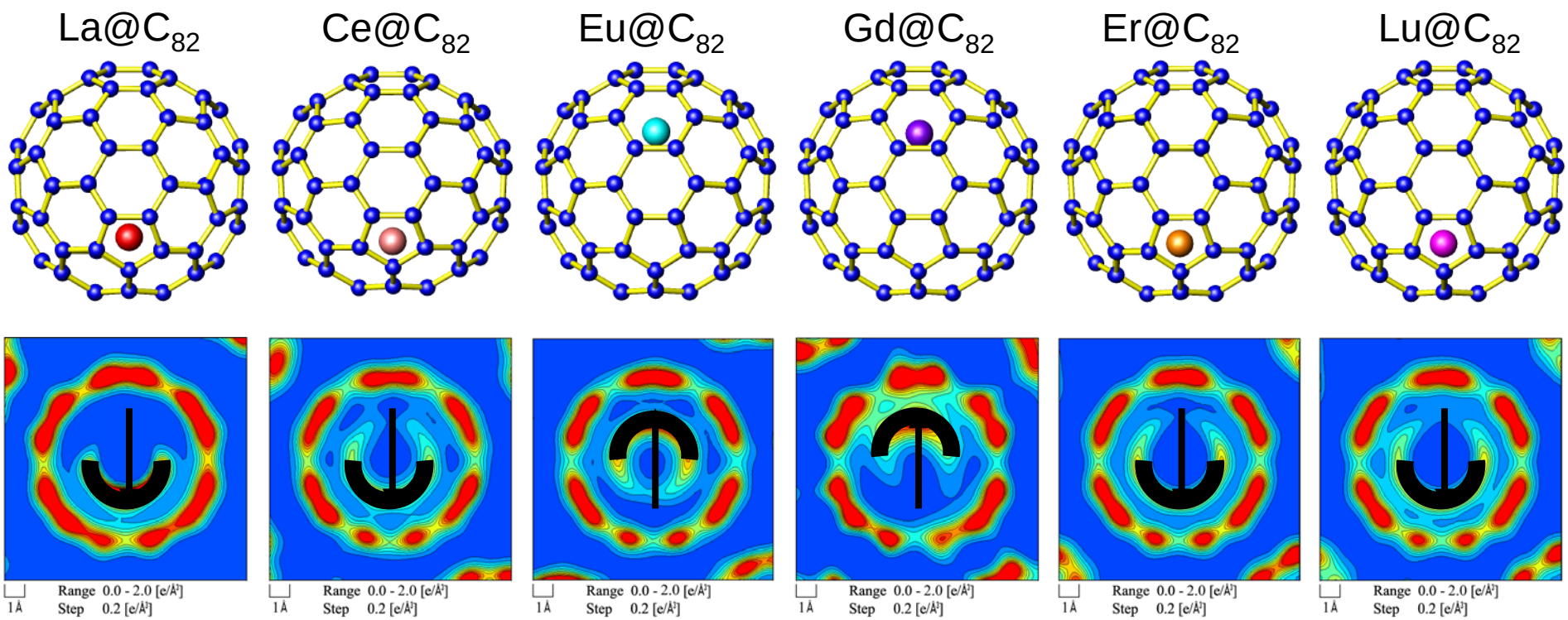

1） 内包金属原子は、ケージ内部で半球殻状に熱運動している

2） 内包金属原子はC_{2V}対称性の2回軸方向に主に位置する

IPR-Violated Metallofullerene, $Sc_2@C_{66}$

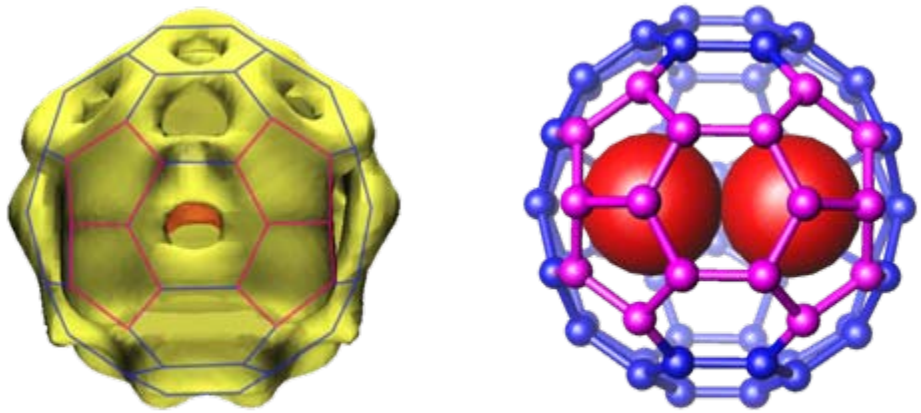

Top View

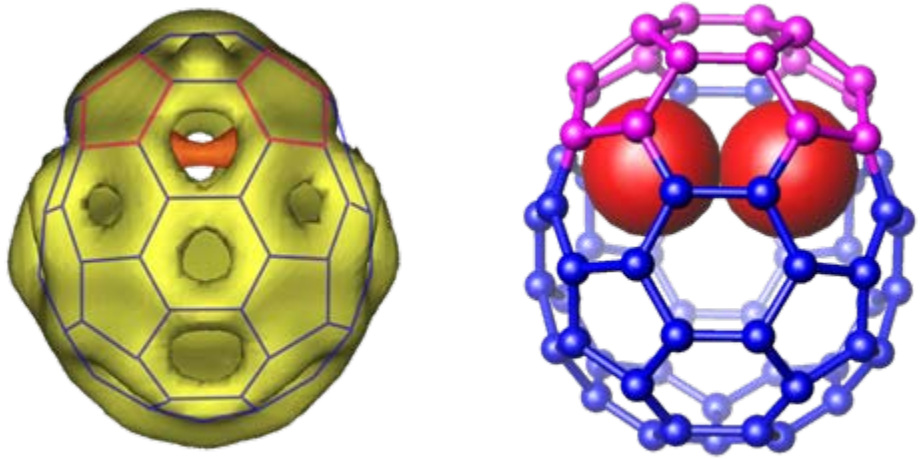

R_F=5.4%

Side View

Nature **408**(2000)426-427

The MEM Charge Density of $Sc_2C_2@C_{84}$

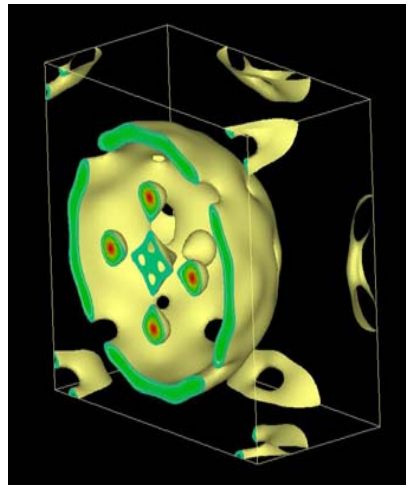

R=1.7%

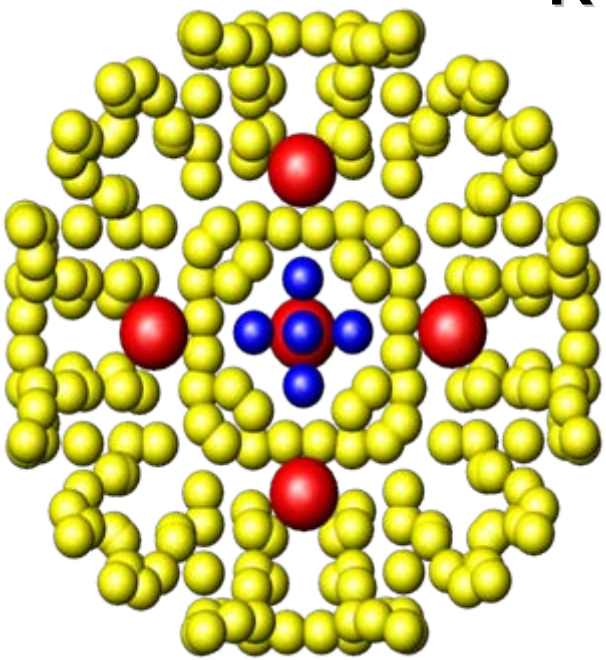

Structure Model

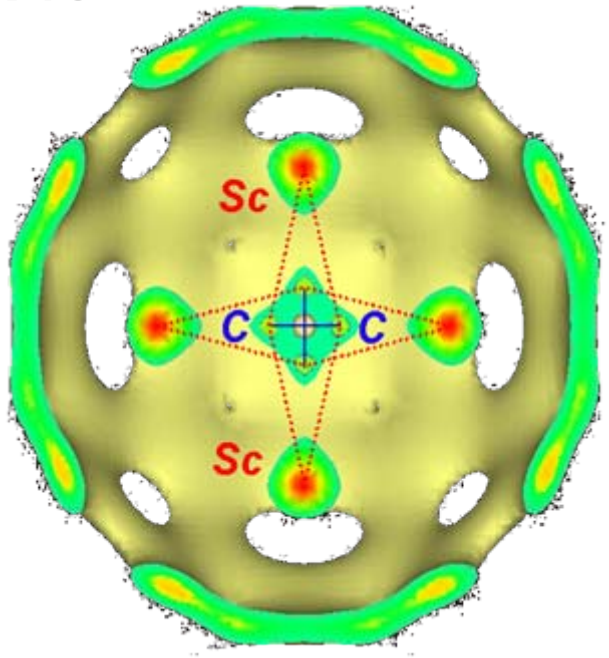

Half Section of
MEM Charge Density

Sc_2C_2 *Imprisoned in* C_{84}

$(Sc_2C_2)^{2+}@C_{84}^{2-}$

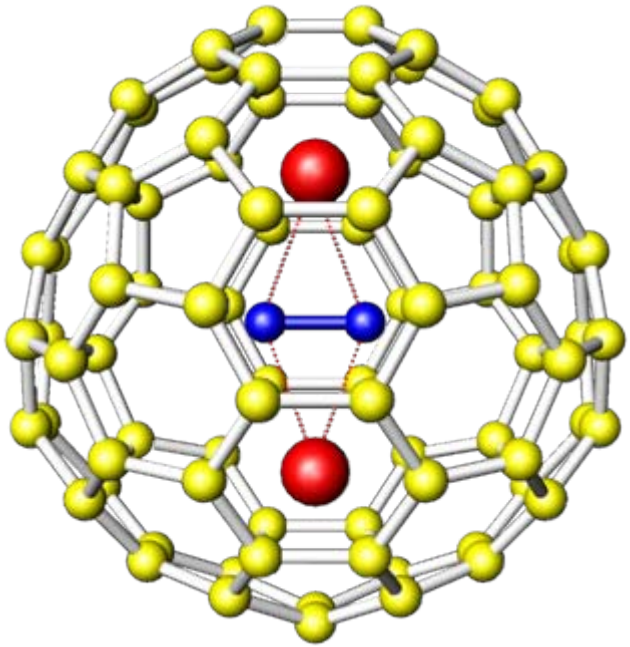

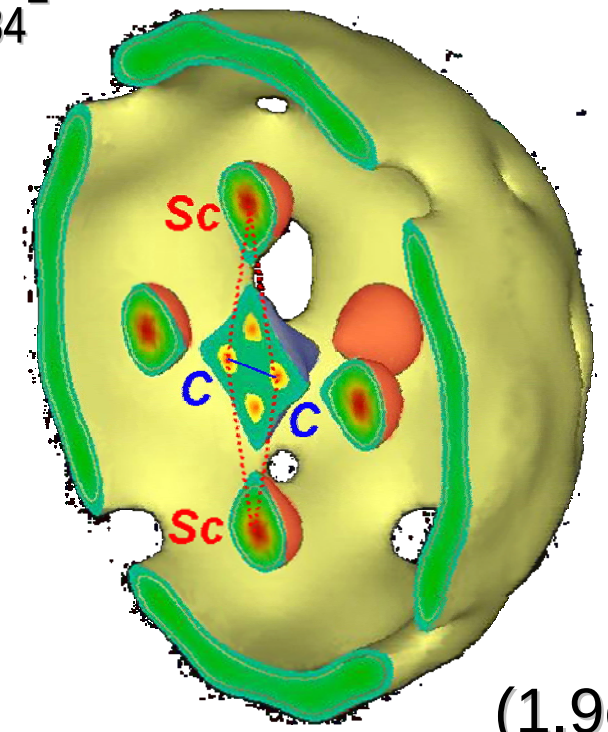

(1.9eÅ^{-3})

Angew.Chem.Int.Ed. **40**(2001)397

MEM Charge Density of $La_2@C_{80}$

$(La^{3+})_2@C_{80}^{6+}$

$\otimes S_{10}$

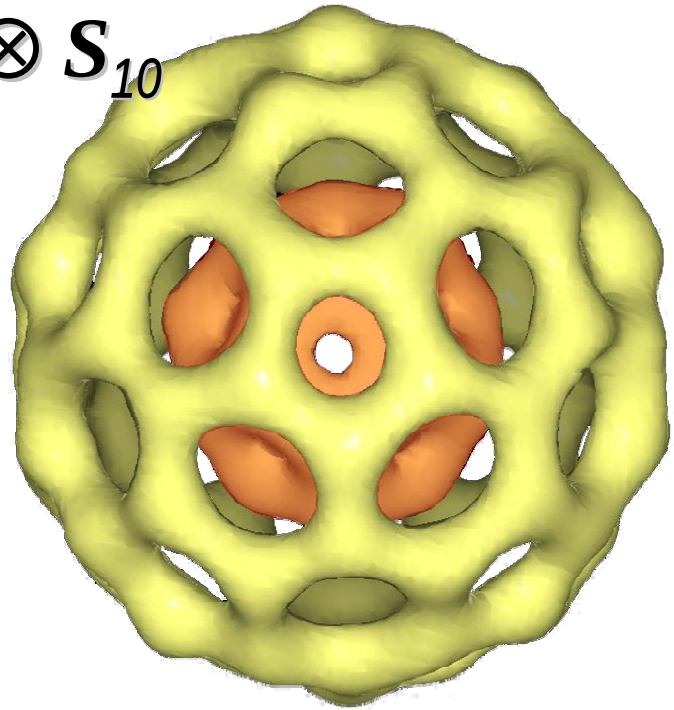

$\otimes C_2$

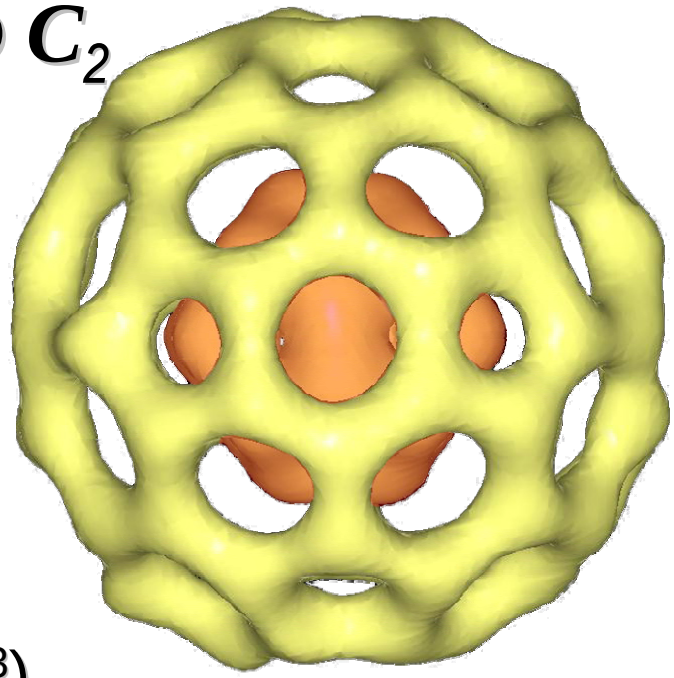

(1.7eÅ^{-3})

The section of Charge Density of $La_2@C_{80}$

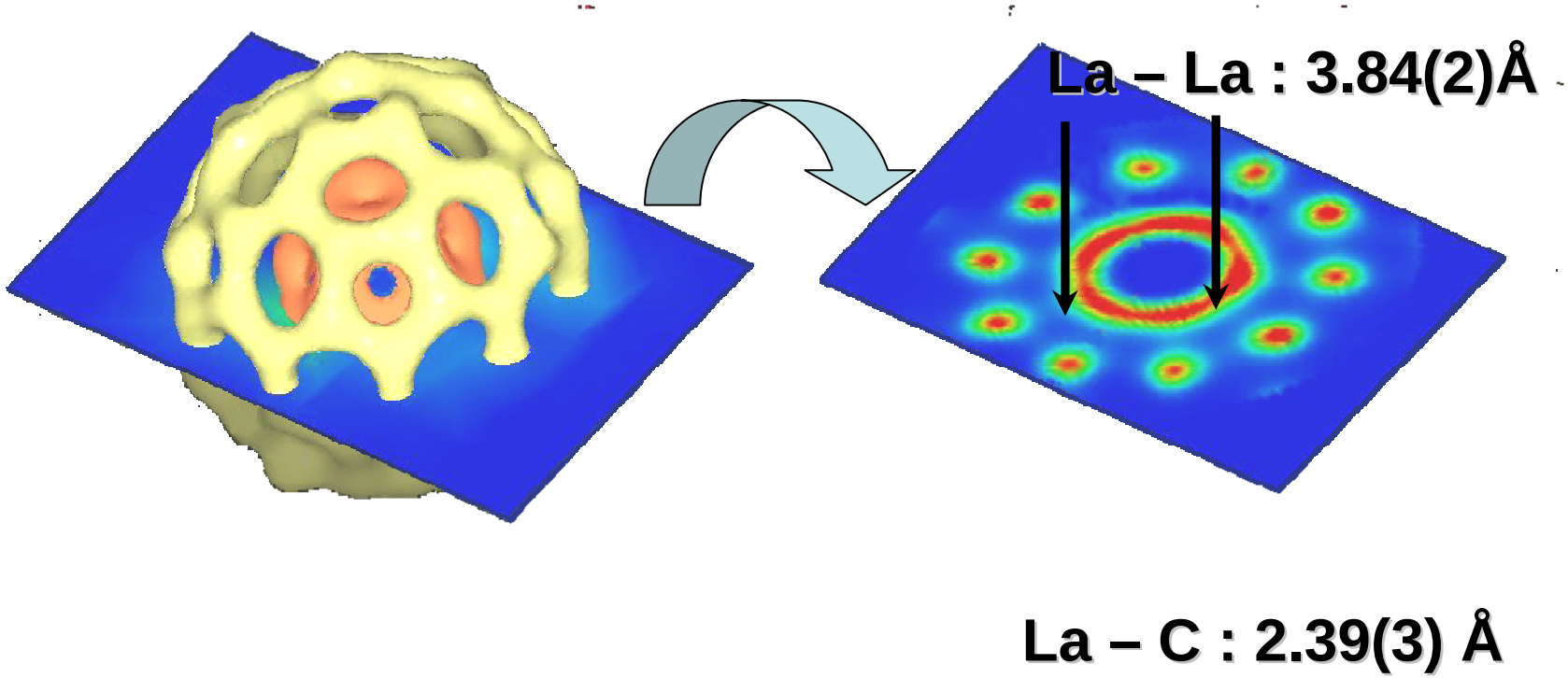

Pentagonal Dodecahedral La_2 Charge Density in Icosahedral C_{80} Fullerene

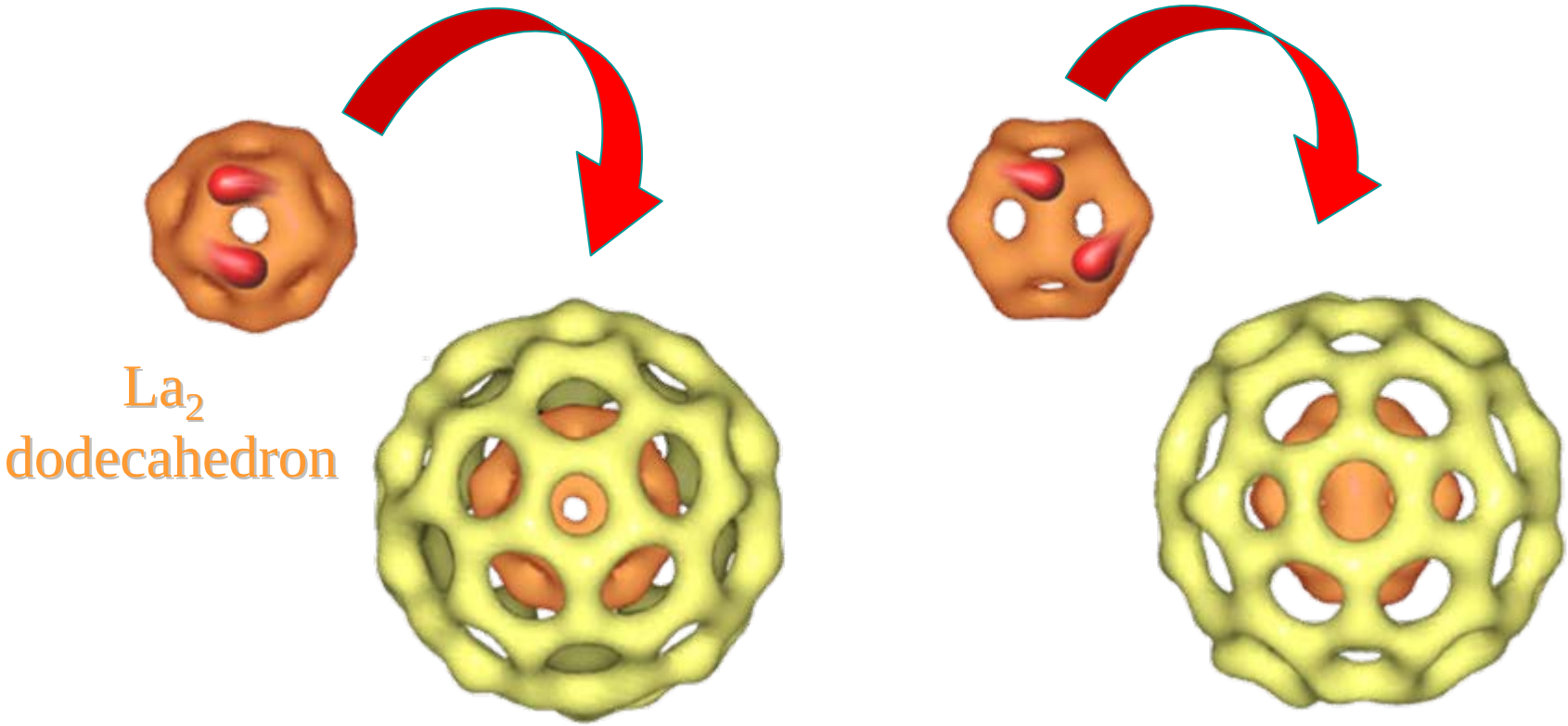

I_h - $La_2@C_{80}$

Orbital order in perovskite manganite.

Magnetic Structure of Perovskite-type Manganite

A-type

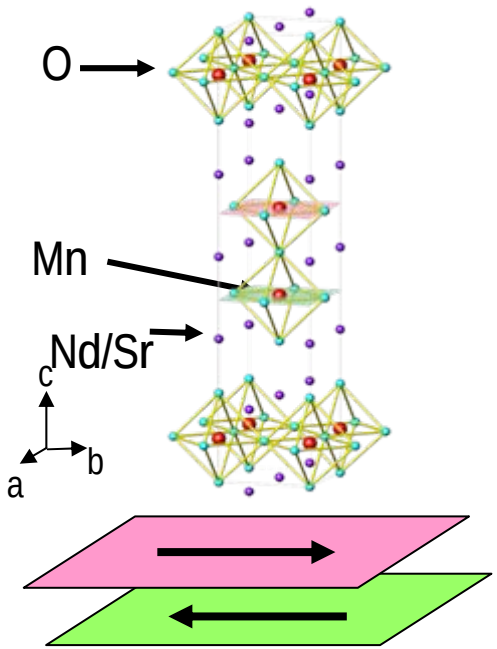

$NdSr_2Mn_2O_7$

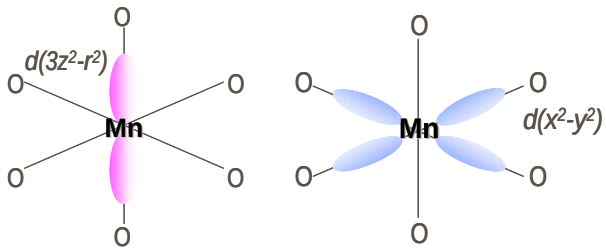

C-type

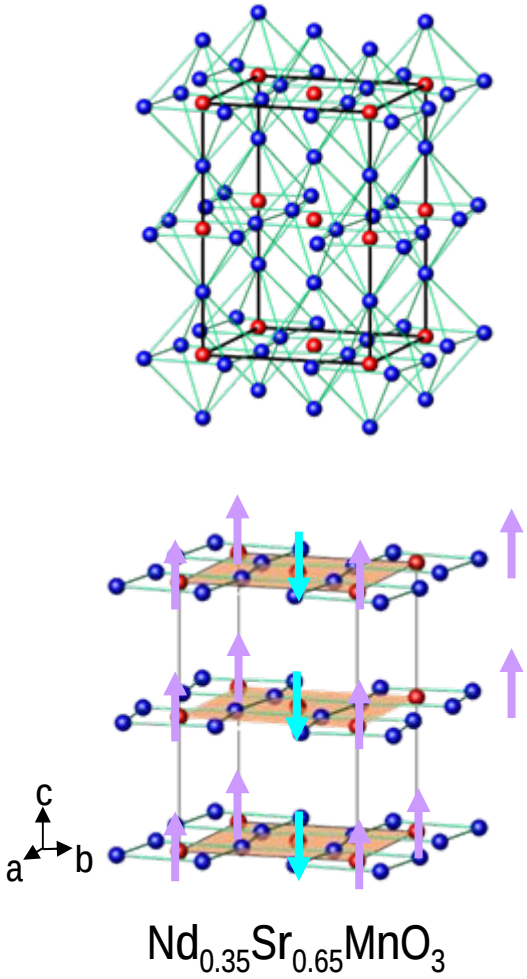

$Nd_{0.35}Sr_{0.65}MnO_3$

CE-type

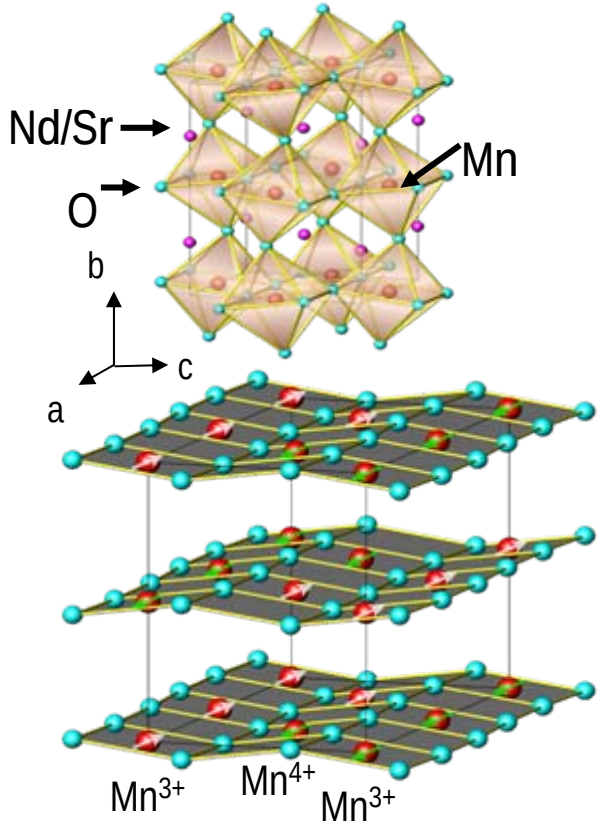

$Nd_{0.5}Sr_{0.5}MnO_3$

Structure Parameters of $NdSr_2Mn_2O_7$ from Rietveld Analysis

I4/mmm		*R.T.*	*19K*
Lattice Parameters(Å)	*a*	3.85029(6)	3.85015(7)
	c	19.9540(3)	19.8867(4)
Bond Lengths(Å)	*Mn-O1*	1.934(1)	1.928(1)
	Mn-O2	2.009(4)	1.968(4)
	Mn-O3	1.925181(7)	1.925086(5)

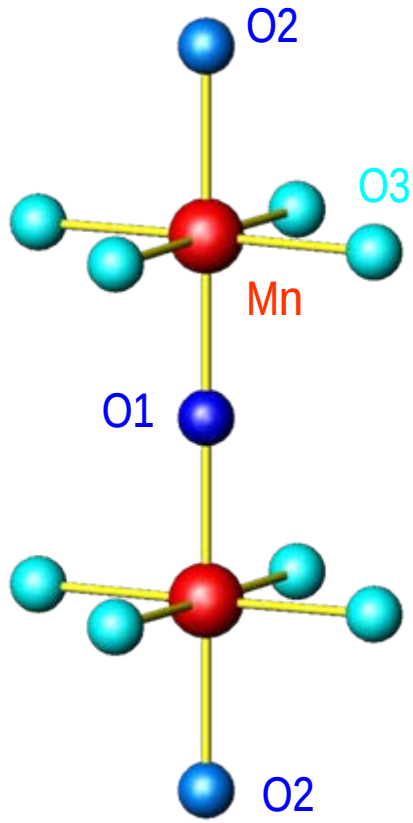

The MEM Charge Densities of $NdSr_2Mn_2O_7$ for (200) Plane

0.0~4.0[e Å^{-3}],step:0.2 [e Å^{-3}]

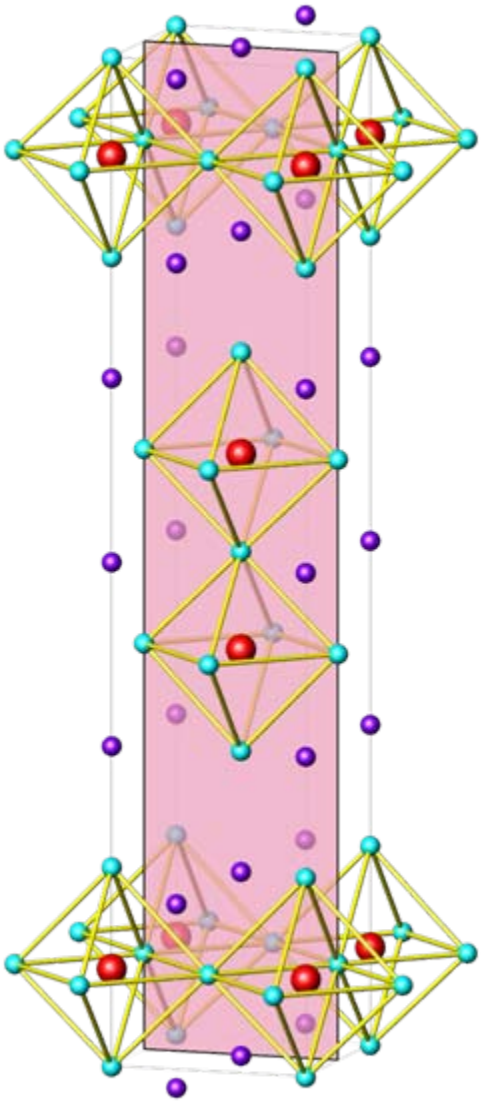

[R.T.]

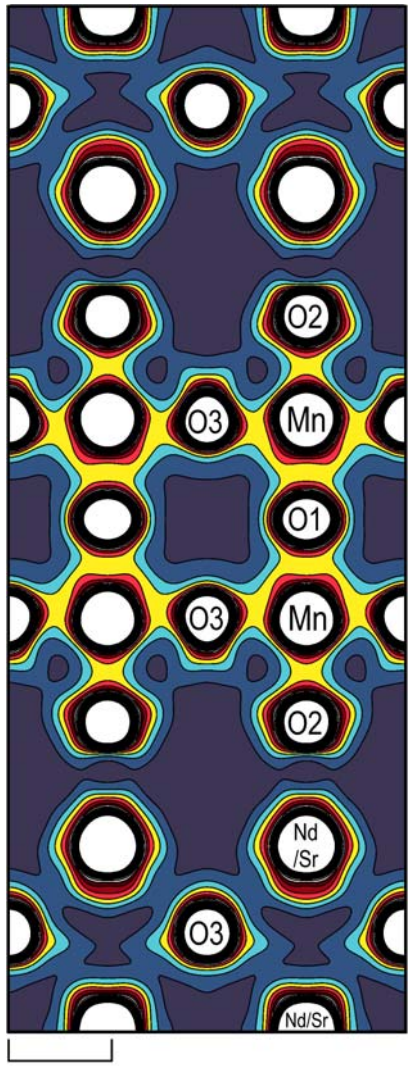

2 Å

[001]Axis

[19K]

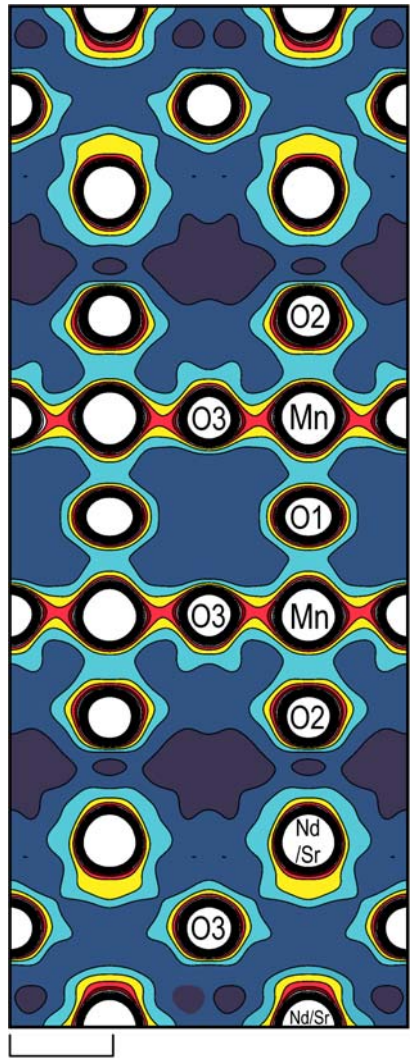

2 Å

The Equi-contour(*0.6eÅ*$^{-3}$) Density Map of the MEM Charge Densities of $NdSr_2Mn_2O_7$ at R.T.

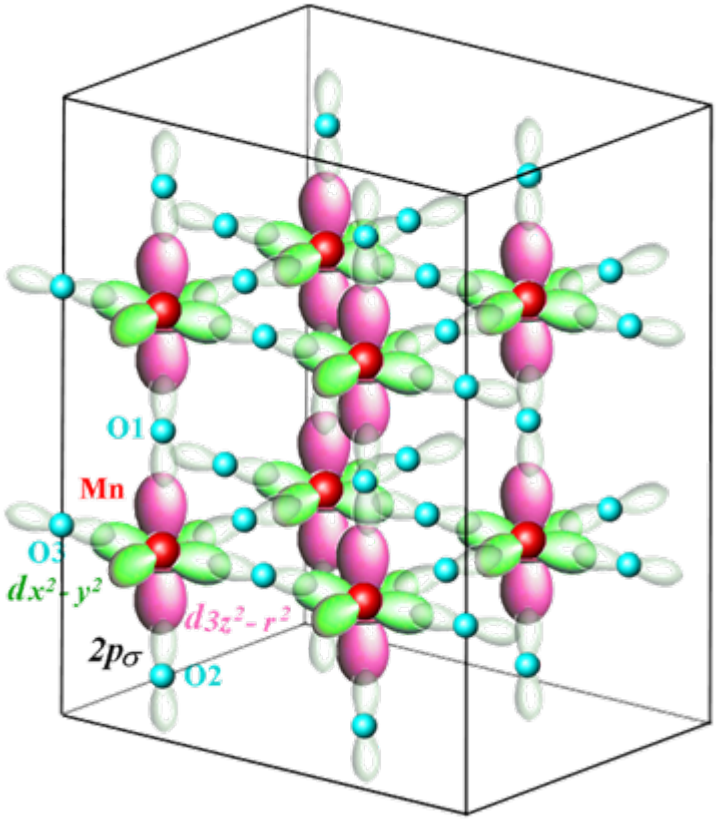

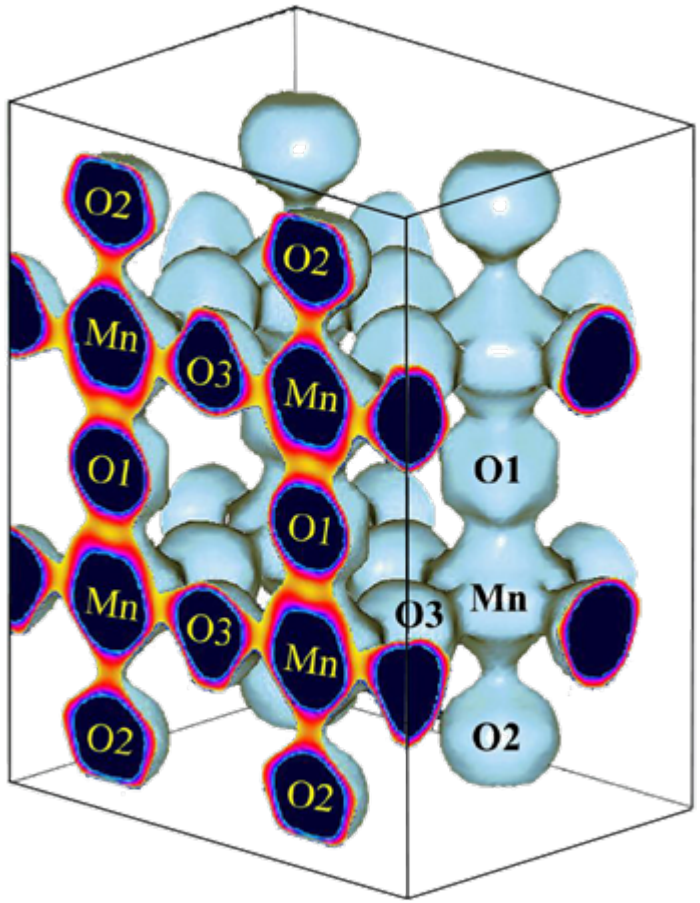

The Equi-contour(*0.6e Å*$^{-3}$) Density Map of the MEM Charge Densities of $NdSr_2Mn_2O_7$ at 19K

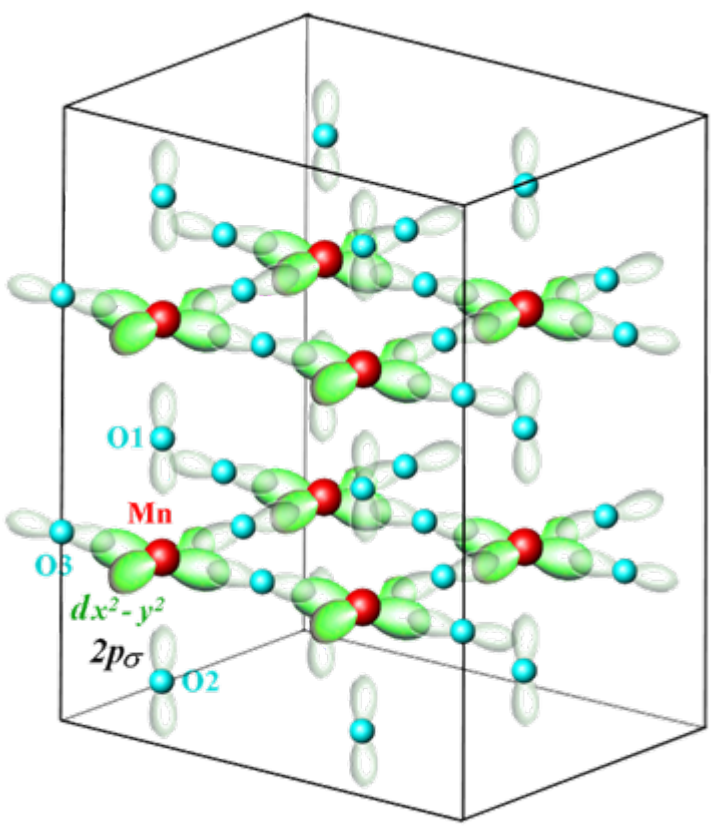

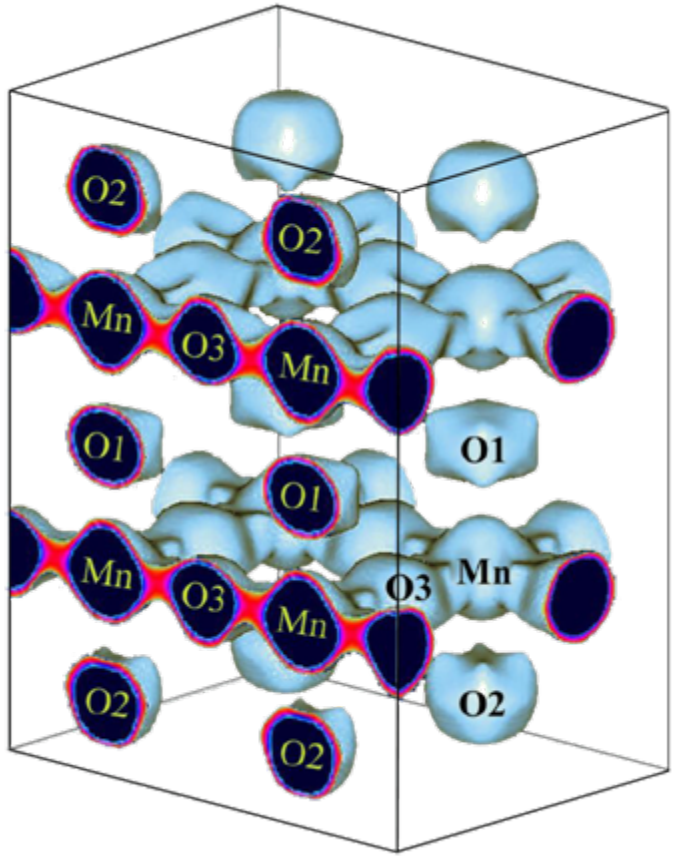

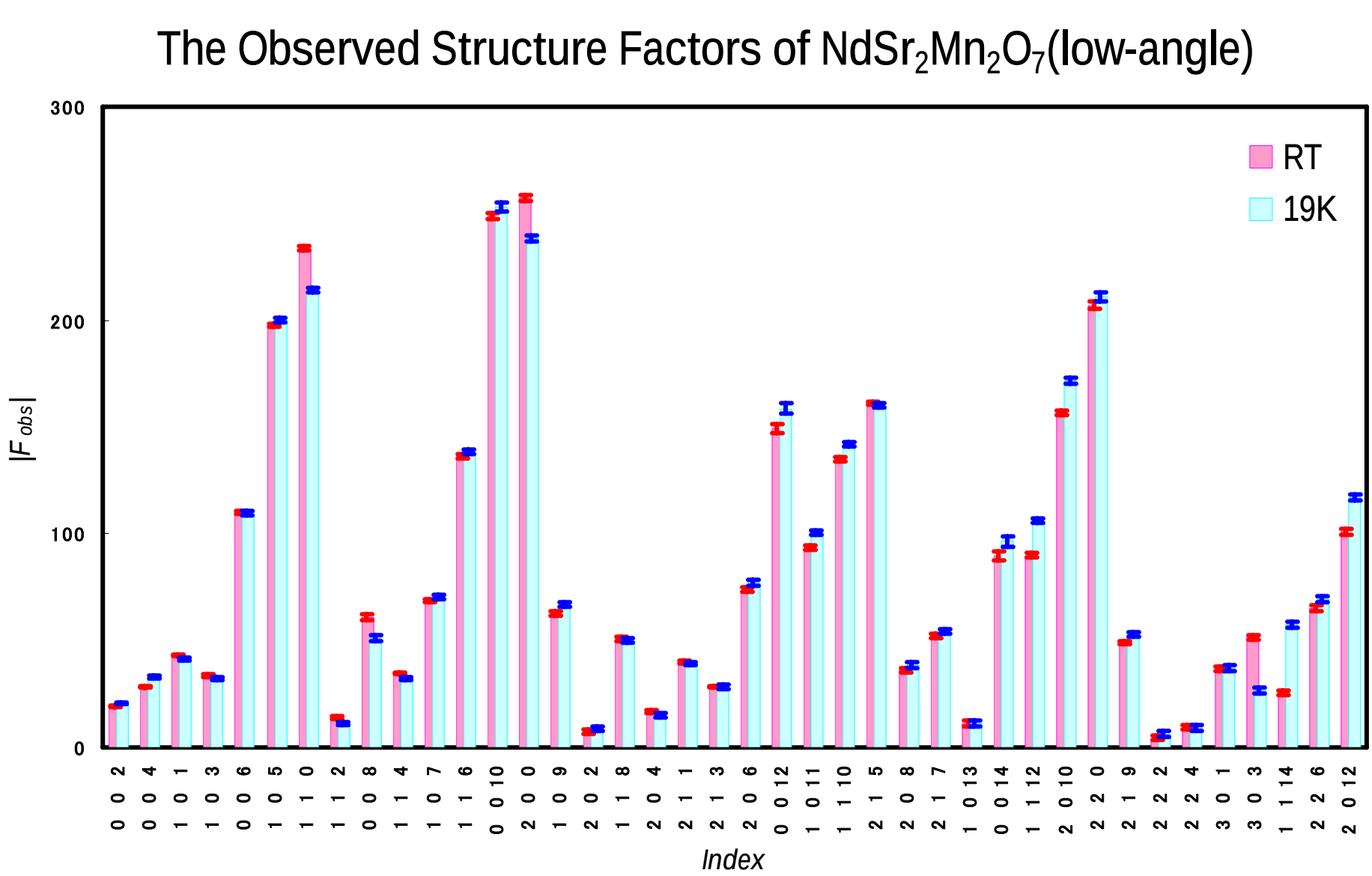
The Observed Structure Factors of NdSr2Mn2O7(low-angle)
300
200
100
0
|F obs|
RT
19K
0 0 2
0 0 4
1 0 1
1 0 3
0 0 6
1 0 5
1 1 0
1 1 2
0 0 8
1 1 4
1 0 7
1 1 6
0 0 10
2 0 0
1 0 9
2 0 2
1 1 8
2 0 4
2 1 1
2 1 3
2 0 6
0 0 12
1 0 11
1 1 10
2 1 5
2 0 8
2 1 7
1 0 13
0 0 14
1 1 12
2 0 10
2 2 0
2 1 9
2 2 2
2 2 4
3 0 1
3 0 3
1 1 14
2 2 6
2 0 12
Index

The MEM Charge Densities of $Nd_{0.5}Sr_{0.5}MnO_3$ at 18K

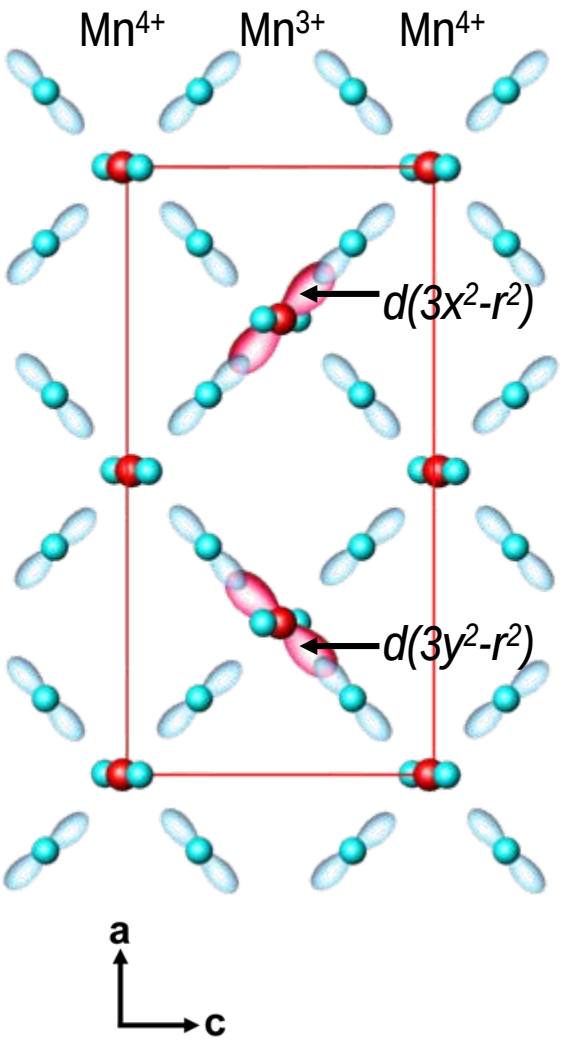

(020) Plane

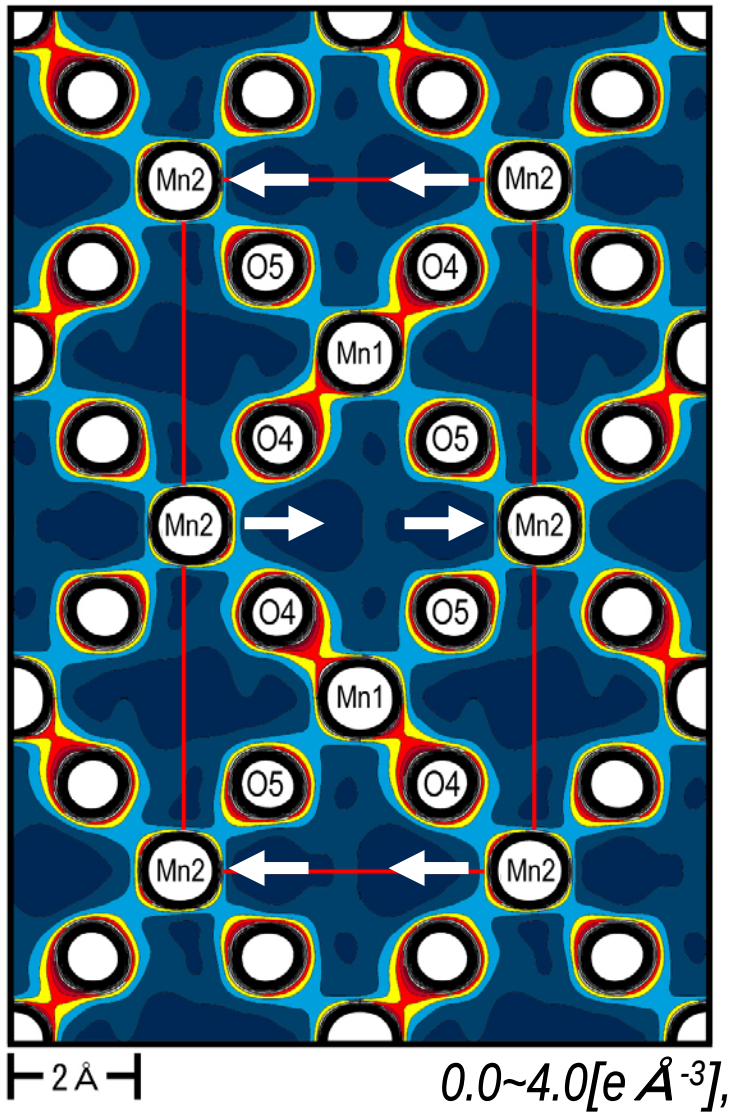

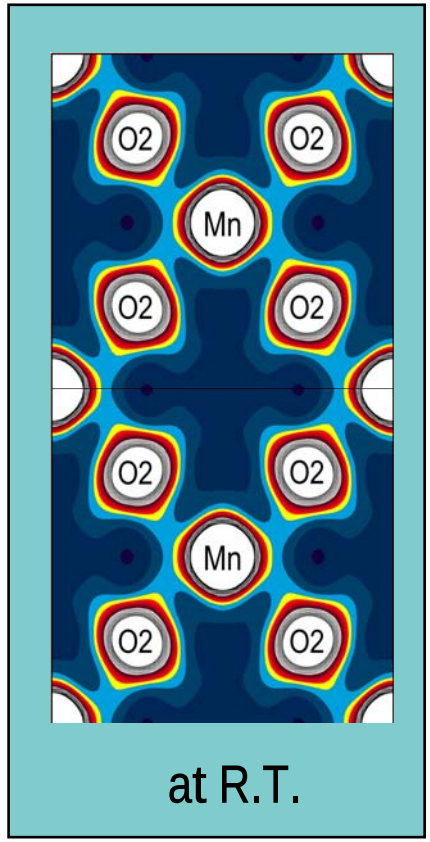

0.0~4.0[e Å^{-3}],step:0.2 [e Å^{-3}]

Equi-charge ($0.8 e Å^{-3}$) MEM density map of $Nd_{0.35}Sr_{0.65}MnO_3$ at R.T. and 30K for the MnO_6 octahedron

R.T.

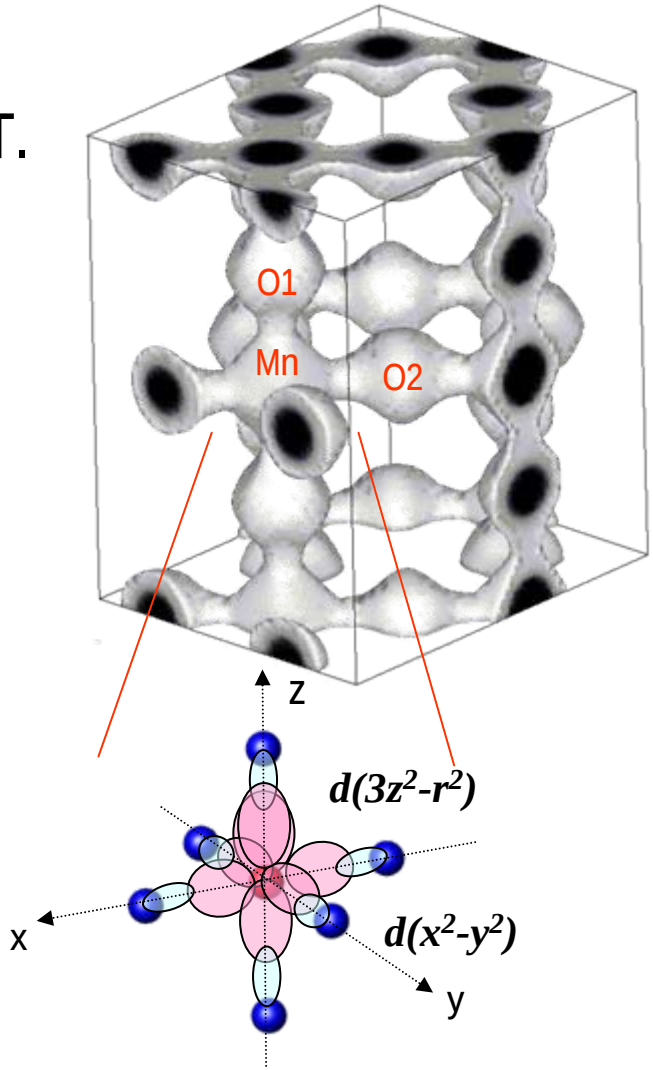

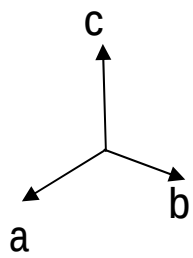

30K

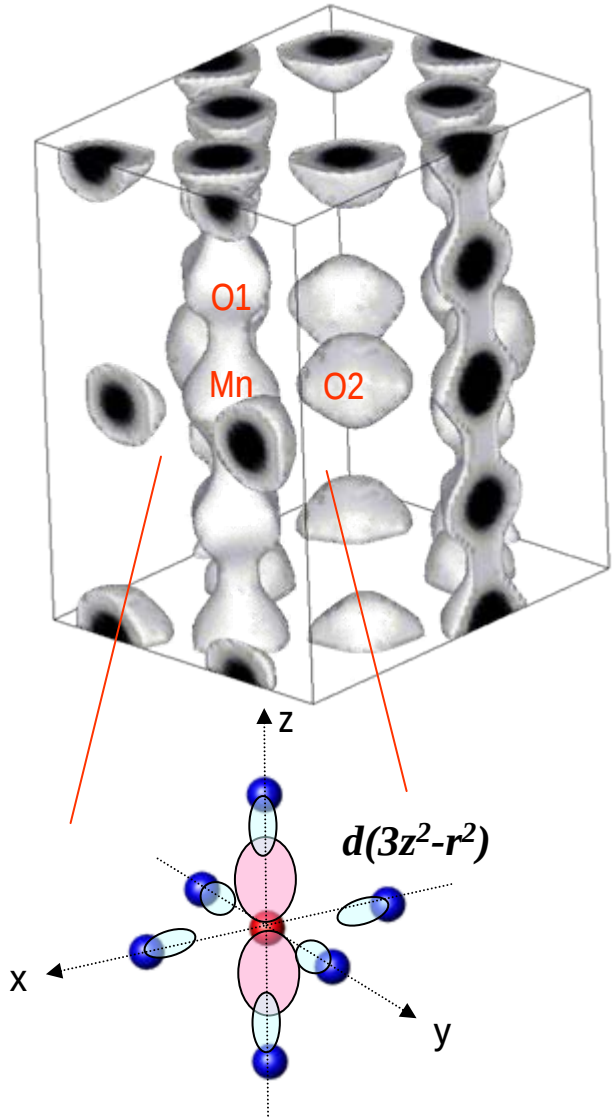

Direct Observation of Orbital Ordering

Synchrotron Radiation Powder Data

MEM / Rietveld

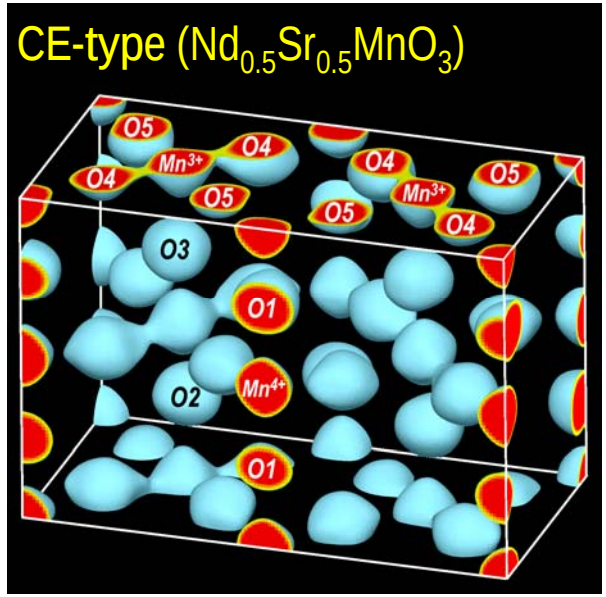

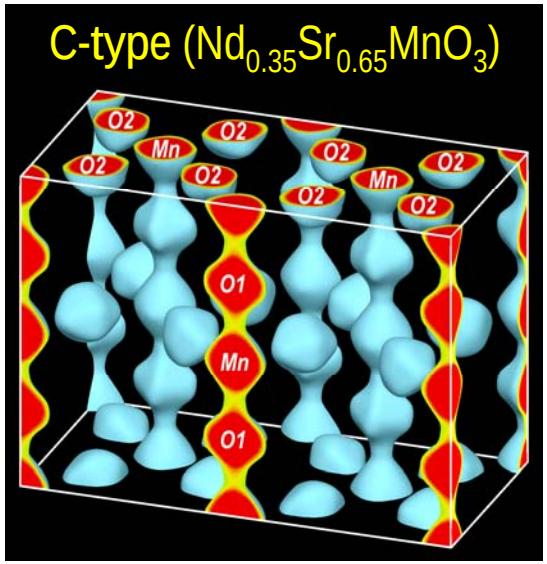

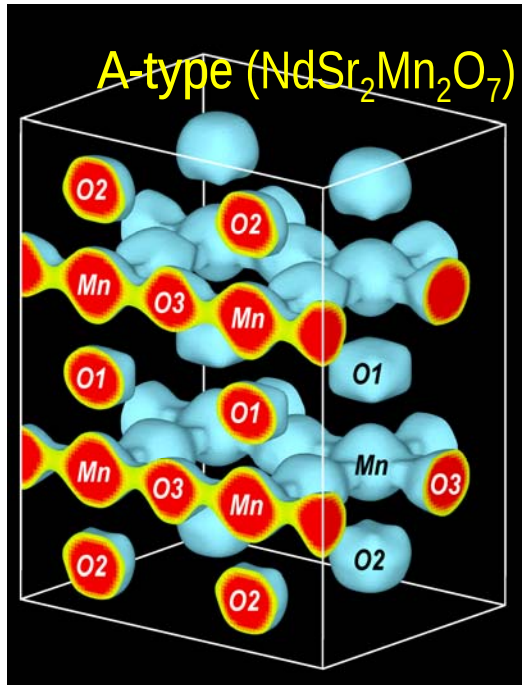

国内の主要なMEM研究者

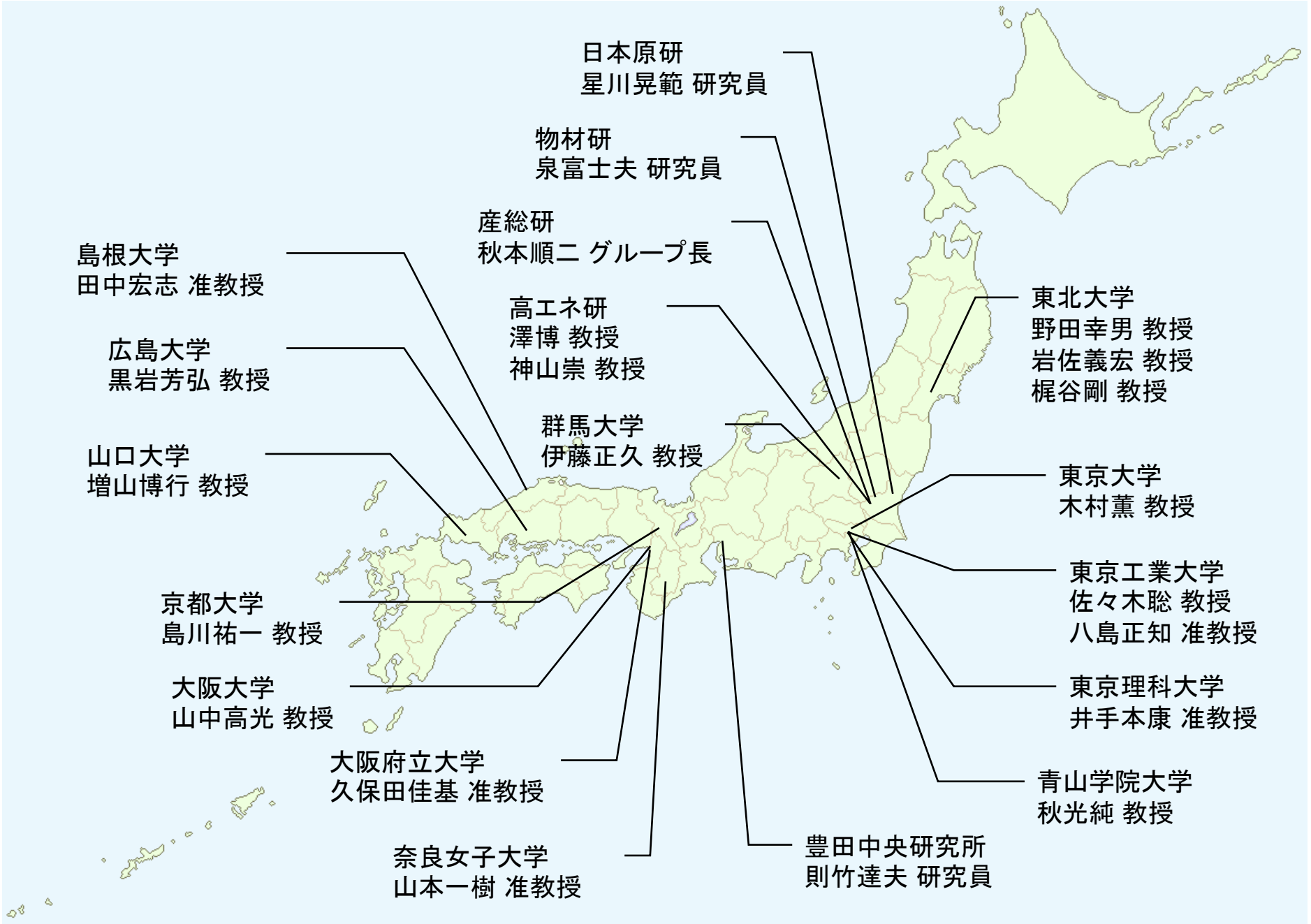

A 281 Tflops Calculation for X-ray Protein Structure Analysis with Special-Purpose Computers MDGRAPE-3

Yousuke Ohno[1], Eiji Nishibori[2], Tetsu Narumi[3], Takahiro Koishi[4], Tahir H. Tahirov[5], Hideo Ago[6],

Masashi Miyano[7], Ryutaro Himeno[8], Toshikazu Ebisuzaki[9],

Makoto Sakata[10] and Makoto Taiji[11]

RIKEN (Institute of Physical and Chemical Research), Nagoya University, Keio University and University of Fukui

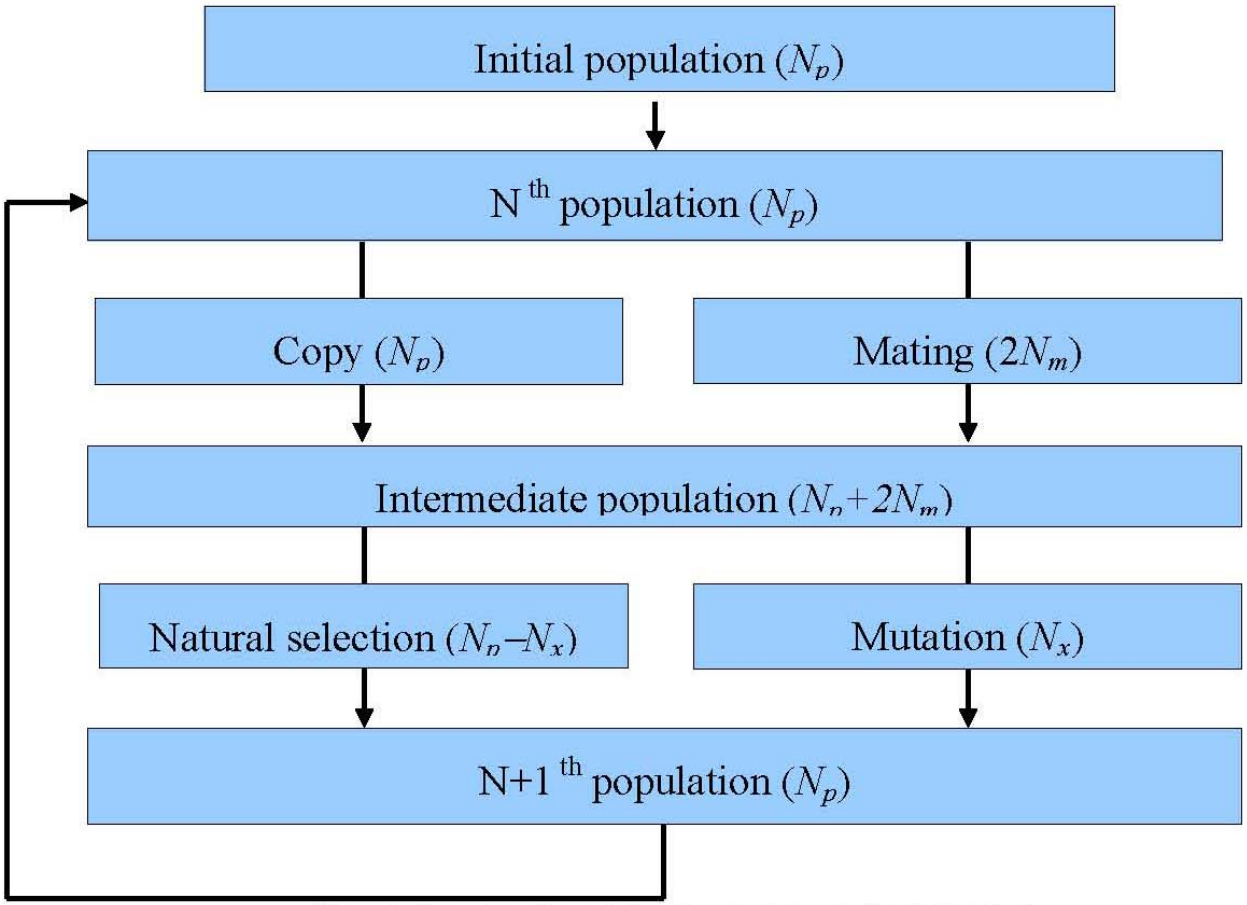

Figure 1: Procedure for updating the population in GA-DS method.

Acta Crystallographica Section D
Biological Crystallography
ISSN 0907-4449

Application of maximum-entropy maps in the accurate refinement of a putative acylphosphatase using 1.3 Å X-ray diffraction data

Eiji Nishibori,[a]* Takahiro Nakamura,[a] Masanori Arimoto,[a] Shinobu Aoyagi,[a] Hideo Ago,[b] Masashi Miyano,[b] Toshikazu Ebisuzaki[c] and Makoto Sakata[a]

[a]Deparment of Applied Physics, Nagoya University, Nagoya 464-8603, Japan, [b]Structural Biophysics Laboratory, RIKEN SPring-8 Center, Harima Institute, 1-1-1 Kouto, Sayo, Hyogo 679-5148, Japan, and [c]Computational Astrophysics Laboratory, RIKEN Discovery Research Institute, 2-1 Hirosawa, Wako, Saitama 351-0198, Japan

本研究で検討した項目

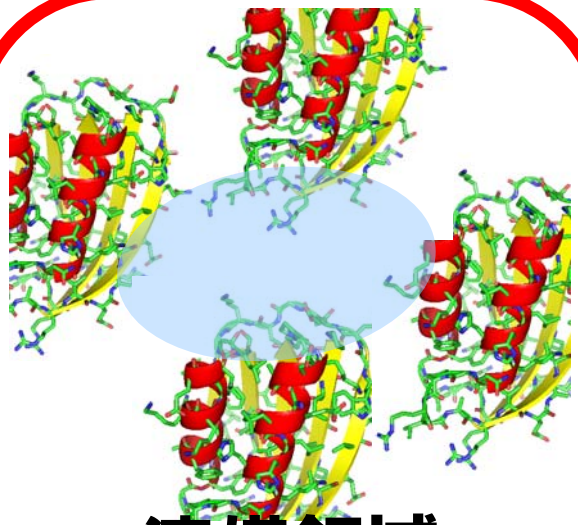

溶媒領域

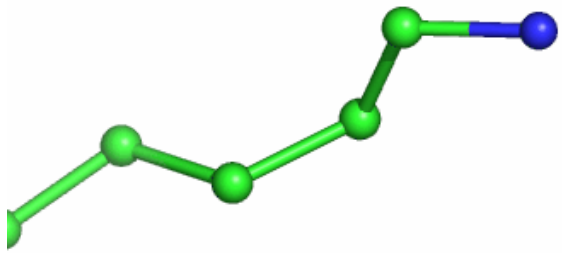

Disorder

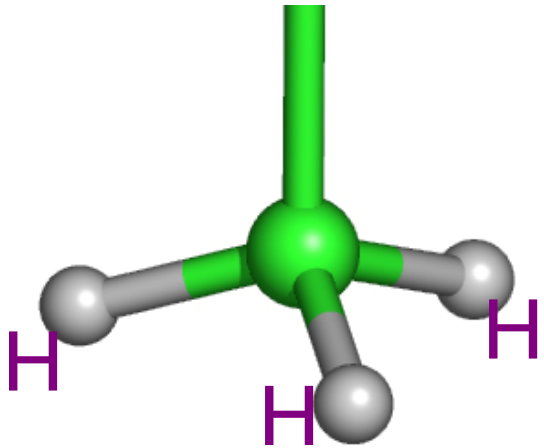

水素原子

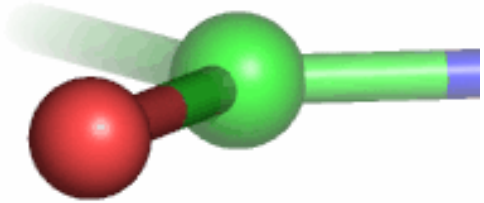

原子の異方性熱振動

溶媒領域のモデル構築

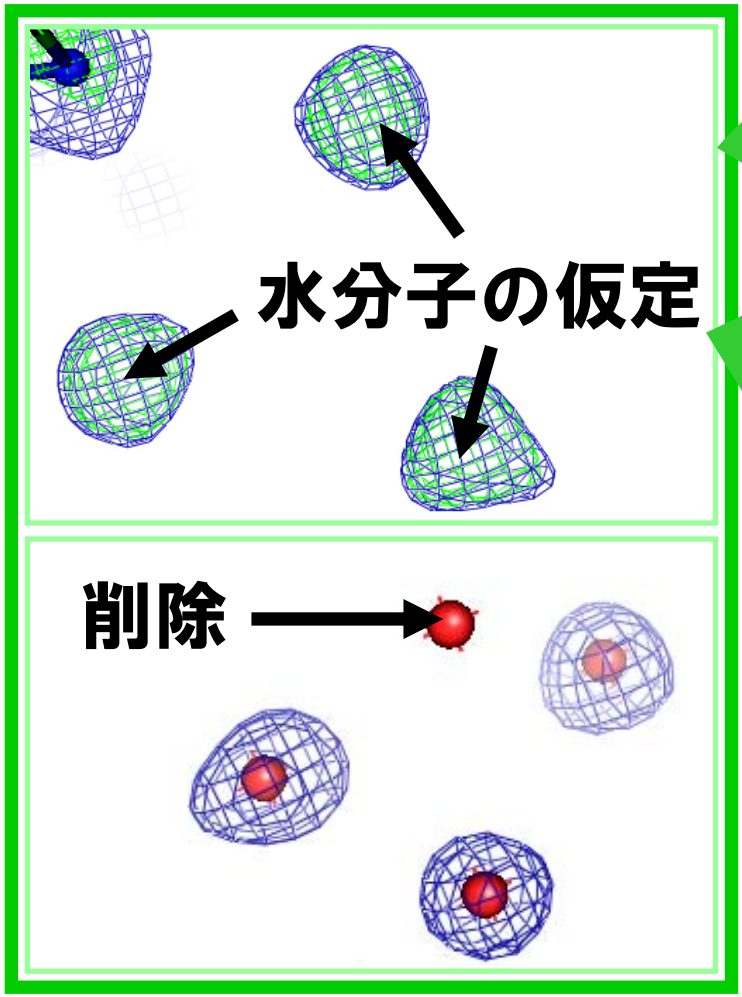

SHELXL-97

ENIGMA

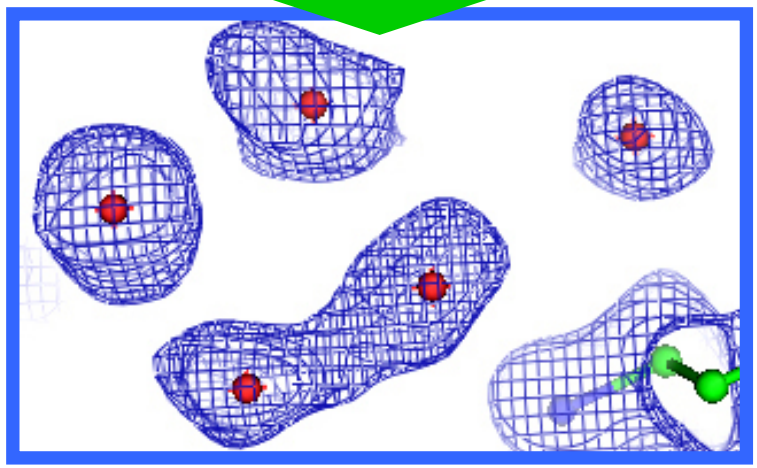

R1 : 17.54%

R1 : 14.73%

本研究で検討した項目

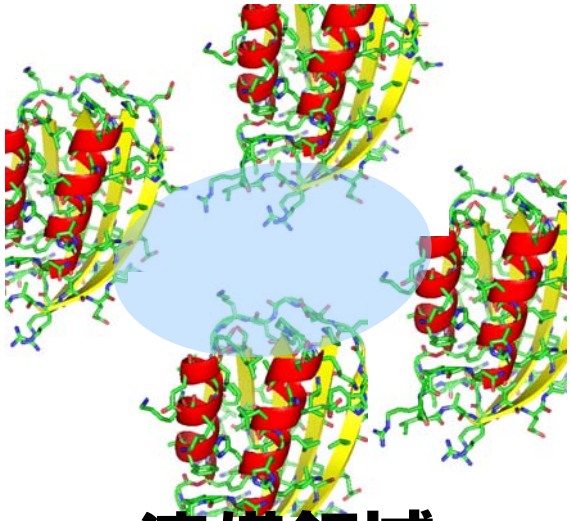

溶媒領域

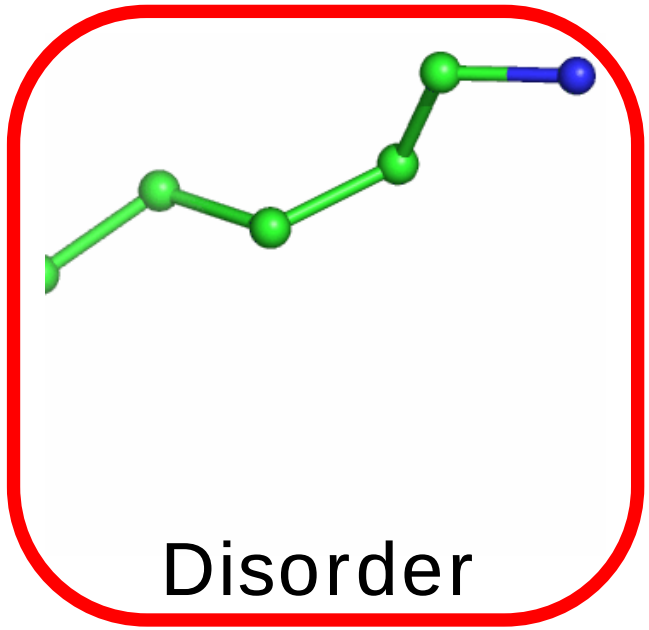

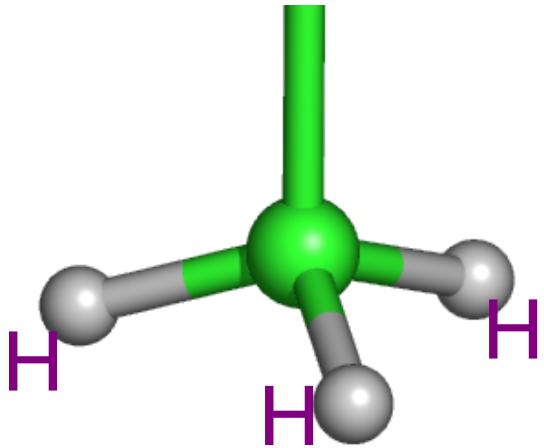

水素原子

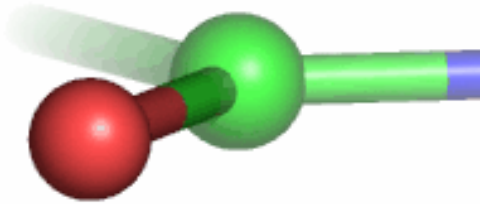

原子の異方性熱振動

Disorderモデルの構築

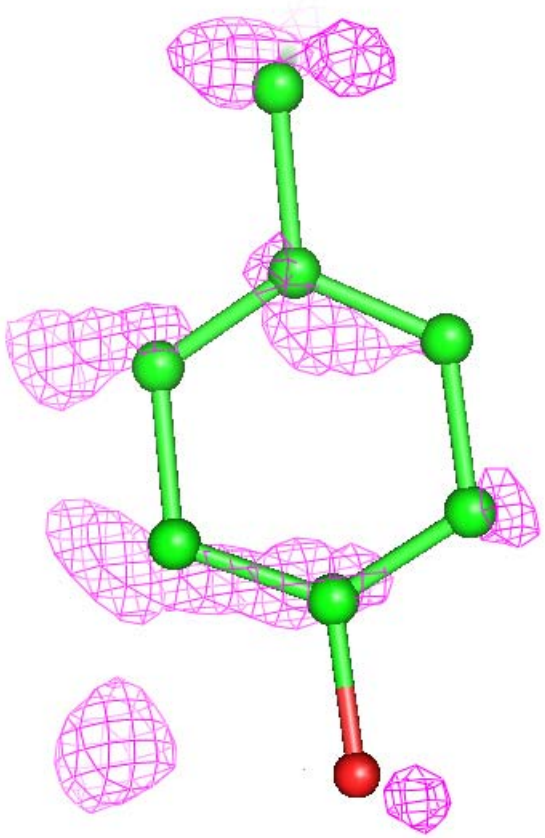

ー：差MEM Density 0.4[e/Å^3]

R1＝14.41 %

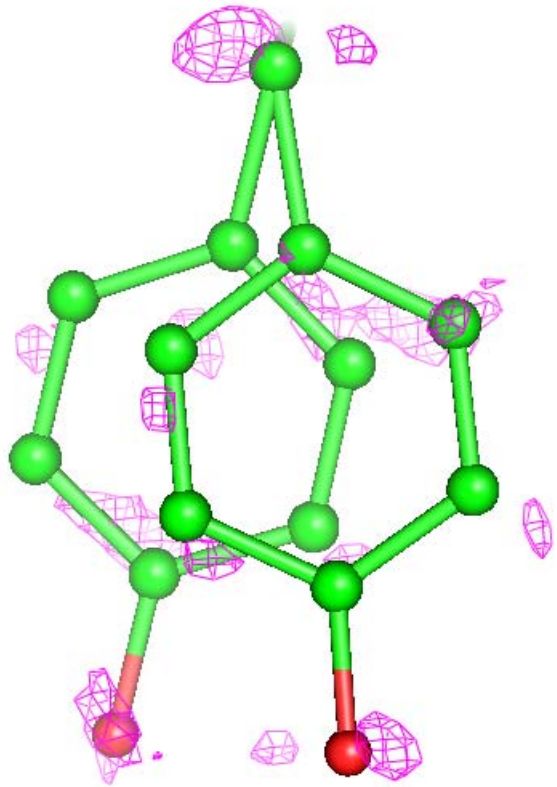

ー：差MEM Density 0.4[e/Å^3]

R1＝14.29 %

本研究で検討した項目

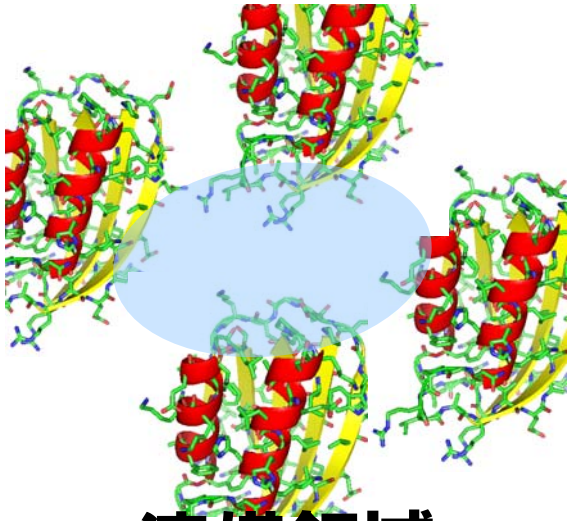

溶媒領域

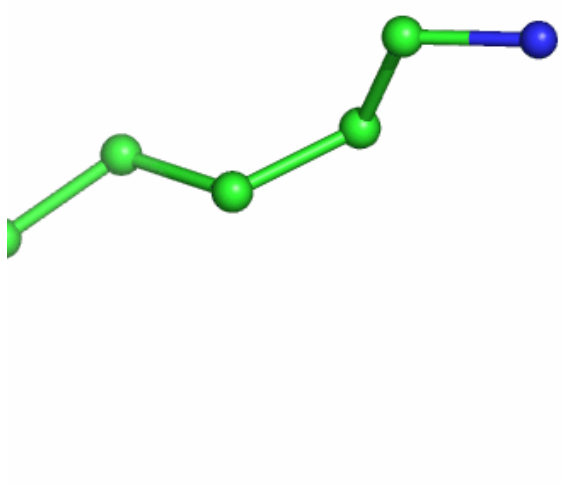

Disorder

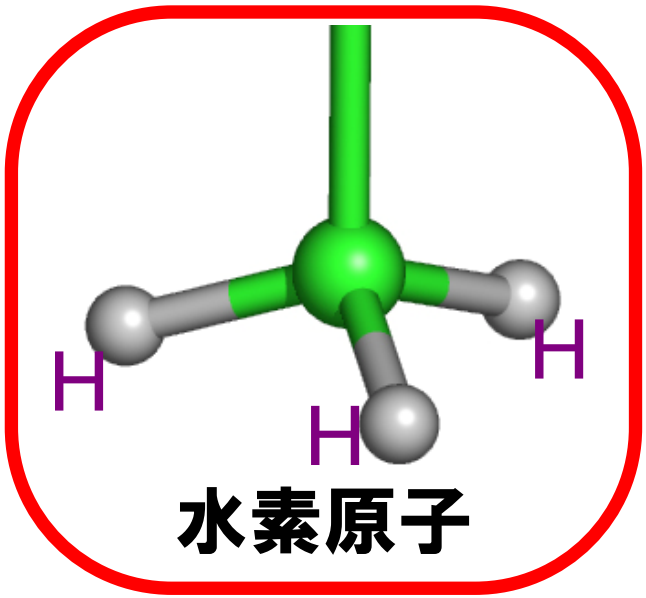

水素原子

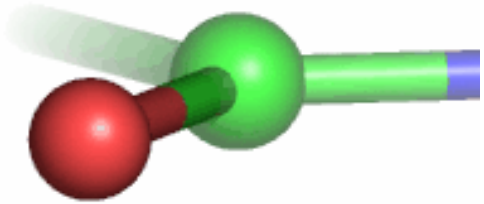

原子の異方性熱振動

水素原子

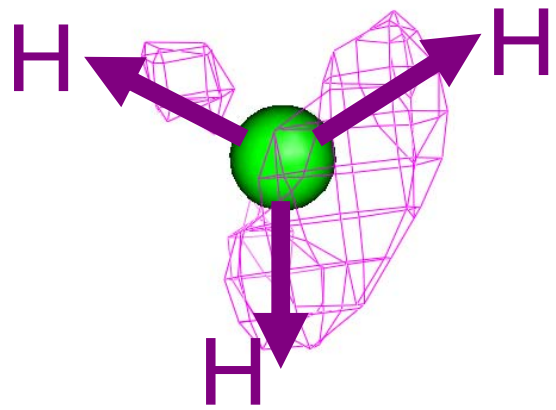

メチル基

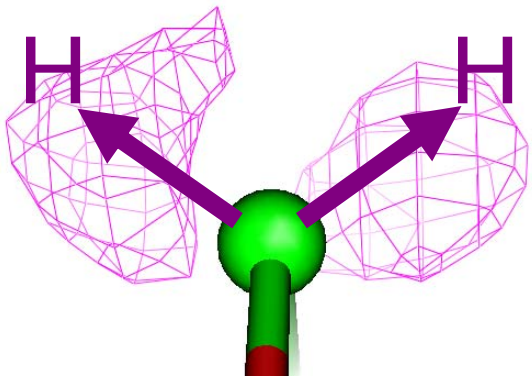

炭素鎖

ー：差MEM Density 0.4[e/Å^3]

R1＝14.73％

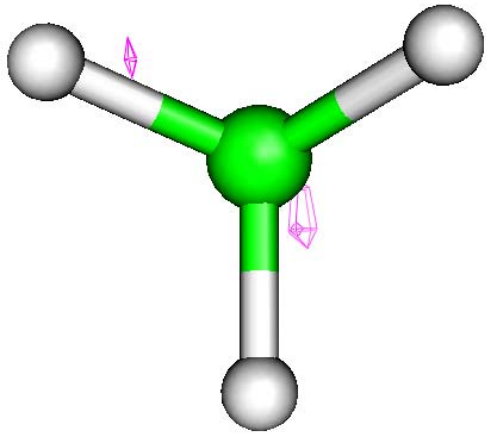

メチル基

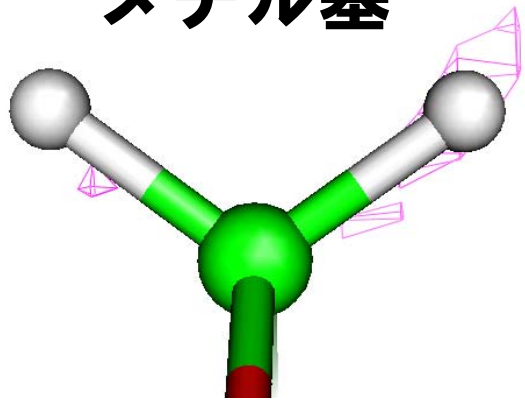

炭素鎖

ー：差MEM Density 0.4[e/Å^3]

R1＝13.92％

本研究で検討した項目

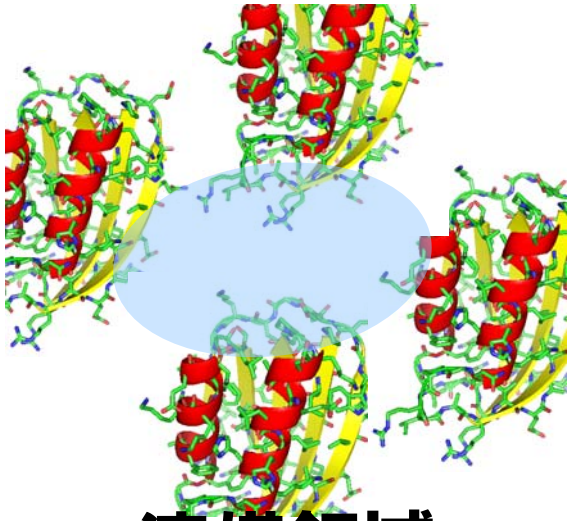

溶媒領域

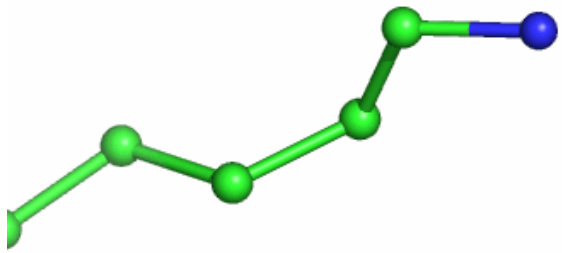

Disorder

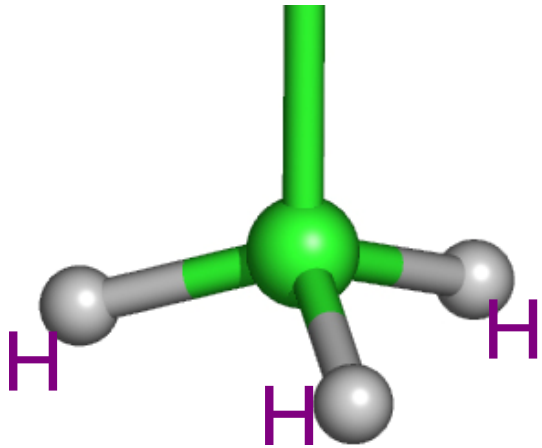

水素原子

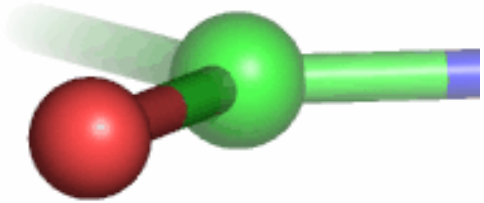

原子の異方性熱振動

原子の異方性

原子の異方性の確認

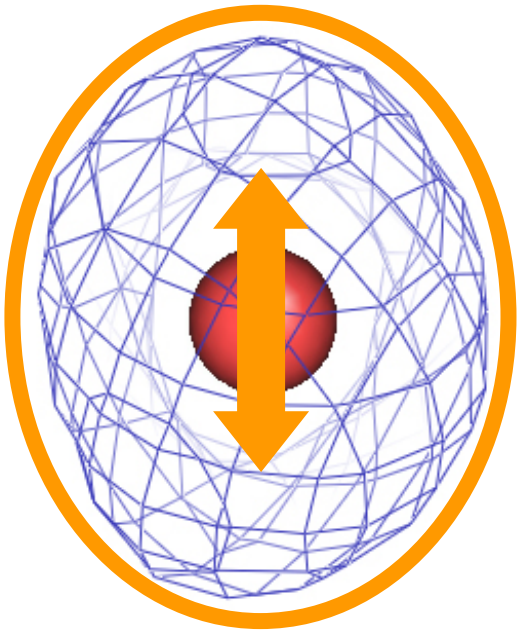

ー：MEM Density 2.0[e/Å^3]

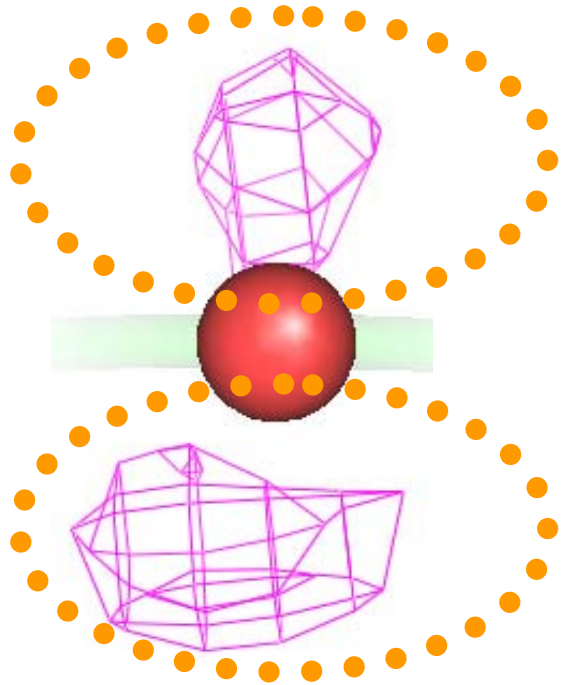

ー：差MEM Density 0.4[e/Å^3]

楕円体状のMEM電子密度

■ ■ ■

・XFEL（X-ray Free Electron Laser)

X線自由電子レーザー

2010年度の完成を目指し、2006年から施設の建設が始まりました。

・J－PARC(Japan Proton Accelerator Research Complex) MLF

大強度陽子加速器施設

2001年度に建設に着手, 2008年度中には、ビームを供給の予定です。

・ERL(Energy Recovery Linac)

エネルギー回収型ライナック

Thanks to:

三宅泰男
松尾貞士
原田仁平　（リガク）
加藤範夫
星埜貞男
藤井保彦　（JAEA）
新村信雄　（茨城大学）
M. J. Cooper　（AERE, Harwell）
K. D. Rouse　（AERE, Harwell）
N. W. Cowlam　（Sheffield Univ. ）
H. A. Davies　（Sheffield Univ. ）
岩崎博　（東北大学）
橋本真也　（いわき明星大学）
高田昌樹　（理化学研究所）
西堀英治　（名古屋大学）
久保田佳基　（大阪府立大学）
山村滋　（北里大学）

Thanks to:

加藤健一	(理化学研究所)
黒岩芳弘	(広島大学)
青柳忍	(名古屋大学)
田中宏志	(島根大学)
中川敦史	(大阪大学蛋白研)
篠原久典	(名古屋大学)
佐藤正俊	(名古屋大学)
谷垣勝己	(東北大学)
岩佐義宏	(東北大学)
真庭　豊	(首都大学東京)
守友　浩	(筑波大学)
秋光　純	(青山学院大学)
木村　薫	(東京大学)
大石泰生	(JASRI)
下村　理	(物質構造科学研究所)
Dave E. Cox,	(BNL U.S.A.)

Thanks to:

小林昭子　（日本大学）
小林達生　（分子研）
北浦良　（名古屋大学）
Finn Larsen　（Ahus Univ.）
Bo Iversen　（Ahus Univ.）
B. T. M. Willis　（AERE, Harwell）
堀顕子　（北里大学）
・西原寛　（東京大学）
北川進　（京都大学）
宮野雅司　（理化学研究所）
吾郷日出夫　（理化学研究所）
泰地真弘　（理化学研究所）
R. Laude　（AERE, Harwell）
S. Wilkins　（CSIRO）
A. Stevenson　（CSIRO）
藤井保彦　（JAEA）

Thanks to:

- 後藤　　（北海道大学）
- 郷原一壽　（北海道大学）
- 折原 宏　　（北海道大学）
- 町田 晃彦　（JAEA）
- 高野
- 佐々木聡　（東京工業大学）
- 鹿児島誠一　（東京大学）
- 池田直　　（岡山大学）
- 伊藤正久　（群馬大学）‥‥
- ‥‥‥
- ‥‥‥
- ‥‥‥
- ‥‥‥
- ‥‥‥
- ‥‥‥
- ‥‥‥